MAY 2021 | HydrocarbonProcessing.com

HYDROCARBON PROCESSING®

HYDROCARBON PROCESSING®

MAY 2021 | Volume 100 Number 5
HydrocarbonProcessing.com

SPECIAL FOCUS: MAINTENANCE AND RELIABILITY

VALVES, PUMPS AND TURBOMACHINERY

HEAT TRANSFER

PROCESS CONTROLS, INSTRUMENTATION AND AUTOMATION

ENVIRONMENT AND SAFETY

DEPARTMENTS

COLUMNS

WEB EXCLUSIVE

Cover Image: Operators at a Saudi Aramco facility. Photo courtesy of Saudi Aramco.

99TH ANNIVERSARY | 1922–2021 |

HP Industry Perspectives

Will capital investments increase in 2021 and beyond?

Over the past several years, the world witnessed a significant increase in downstream capacity growth in all sectors of the hydrocarbon processing industry (HPI). However, the COVID-19 pandemic caused a significant decline in demand for transportation fuels and certain petrochemical value chains.

As governments start to ease lockdown measures, how has the global capital expenditure market been affected and what are the major trends for the rest of 2021 and beyond? These topics will be tackled during *Hydrocarbon Processing's* Market Outlook: 2021 Update webcast. On June 17, the webcast will take a deep dive into capital projects around the world and how spending has been affected by COVID-19 restrictions, as well as how major economic, environmental and political trends are shaping and influencing the HPI in the near term.

At present, Gulf Energy Information's Global Energy Infrastructure database is tracking nearly 1,300 projects around the world in the refining, petrochemicals and gas processing/LNG sectors. These projects represent total capital expenditures of nearly $1.8 T. However, after a tumultuous year, many capital projects have been deferred, delayed or even abandoned.

New project numbers also suffered in 2020. According to the Construction Boxscore Database, new project announcements declined from 358 in 2019 to 238 in 2020, representing a decrease of approximately 34% year-over-year. However, capital freezes due to safety measures taken during COVID-19 restrictions are being pushed into this year and beyond. New project announcements have increased every month since November 2020, reaching a 5-mos high of 24 in March (FIG. 1).

Where are these projects and how are governments, organizations and companies investing in new capital projects? These questions will be answered during a deeper look into capital markets in the June webcast. To register for the Market Outlook: 2021 Update webcast, visit HydrocarbonProcessing.com. HP

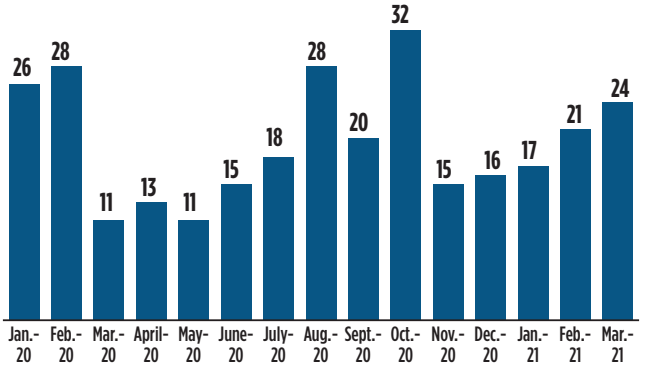

FIG. 1. New project announcements, January 2020–March 2021.

HYDROCARBON PROCESSING®
www.HydrocarbonProcessing.com

P. O. Box 2608
Houston, Texas 77252-2608, USA
Phone: +1 (713) 529-4301
Fax: +1 (713) 520-4433
Editors@HydrocarbonProcessing.com

PUBLISHER Catherine Watkins

EDITOR-IN-CHIEF/ ASSOCIATE PUBLISHER Lee Nichols

EDITORIAL

Executive Editor	Adrienne Blume
Managing Editor	Mike Rhodes
Digital Editor	Stephanie Bartels
Technical Editor	Sumedha Sharma
Reliability/Equipment Editor	Heinz P. Bloch
Contributing Editor	Alissa Leeton
Contributing Editor	ARC Advisory Group
Contributing Editor	Anthony Sofronas

MAGAZINE PRODUCTION / +1 (713) 525-4633

Vice President, Production	Sheryl Stone
Manager, Advertising Production	Cheryl Willis
Manager, Editorial Production	Angela Bathe Dietrich
Assistant Manager, Editorial Production	Melissa DeLucca
Graphic Designer	Krista Norman
Artist/Illustrator	David Weeks

ADVERTISING SALES
See Sales Offices, page 89.

CIRCULATION / +1 (713) 520-4498 / Circulation@GulfEnergyInfo.com
Director, Circulation Suzanne McGehee

SUBSCRIPTIONS
Subscription price (includes both print and digital versions): One year $399, two years $679, three years $897. Airmail rate outside North America $175 additional a year. Single copies $35, prepaid.

Hydrocarbon Processing's Full Data Access subscription plan is priced at $1,995. This plan provides full access to all information and data *Hydrocarbon Processing* has to offer. It includes a print or digital version of the magazine, as well as full access to all posted articles (current and archived), process handbooks, the *HPI Market Data* book, Construction Boxscore Database project updates and more.

Because *Hydrocarbon Processing* is edited specifically to be of greatest value to people working in this specialized business, subscriptions are restricted to those engaged in the hydrocarbon processing industry, or service and supply company personnel connected thereto.

Hydrocarbon Processing is indexed by Applied Science & Technology Index, by Chemical Abstracts and by Engineering Index Inc. Microfilm copies available through University Microfilms, International, Ann Arbor, Mich. The full text of *Hydrocarbon Processing* is also available in electronic versions of the Business Periodicals Index.

DISTRIBUTION OF ARTICLES
Published articles are available for distribution in a PDF format or as professionally printed handouts. Contact Foster Printing at Mossberg & Co. for a price quote and details about how you can customize with company logo and contact information.

For more information, contact Jill Kaletha with Foster Printing at Mossberg & Co. at +1 (800) 428-3340 x 149 or jkaletha@mossbergco.com.

Hydrocarbon Processing (ISSN 0018-8190) is published monthly by Gulf Energy Information, 2 Greenway Plaza, Suite 1020, Houston, Texas 77046. Periodicals postage paid at Houston, Texas, and at additional mailing office. POSTMASTER: Send address changes to Hydrocarbon Processing, P.O. Box 2608, Houston, Texas 77252.

Gulf Energy Information

BPA WORLDWIDE

President/CEO	John Royall
CFO	Alan Millis
Vice President, Upstream and Midstream	Andy McDowell
Vice President, Finance and Operations	Pamela Harvey
Vice President, Production	Sheryl Stone
Vice President, Downstream	Catherine Watkins

Publication Agreement Number 40034765 Printed in USA

Other Gulf Energy Information titles include: *Gas Processing™, Petroleum Economist®, World Oil®, Pipeline & Gas Journal* and *Underground Construction.*

LEE NICHOLS, EDITOR-IN-CHIEF/ASSOCIATE PUBLISHER
Lee.Nichols@HydrocarbonProcessing.com

Maintenance and reliability: A cornerstone of safe and efficient plant operation

Refineries and petrochemical plants are comprised of a series of crucial processes to produce transportation fuels, products and chemicals demanded by the global market. These processes consist of capital-intensive units that must be maintained to provide reliable performance. Failure to adequately maintain these assets can have a detrimental effect to not only operations and profit, but also to worker safety.

It is imperative to maintain a robust maintenance strategy to ensure these units are operating effectively. Equipment failures can lead to unit downtime, severely affecting the plant's profitability. Therefore, maintenance should not be considered an expense, but rather a value-added operation to ensure unit reliability and uptime.

Maintenance and reliability special focus. *Hydrocarbon Processing* has dedicated an entire Special Focus section of this issue to this topic—the publication also highlights this topic in more than 60% of the editorial lineup.

Within this issue, the editors of *Hydrocarbon Processing* have assembled seven technical articles focusing on how maintenance can lead to equipment and plant reliability:

- SK Energy provides a detailed study on hot spots that occurred in the catalysts of the reactors of its residue hydrodesulfurization process. This phenomenon happened during the unit's end-of-run in early 2019. The company's study modeled the hot spots occurrences to analyze the temperature effects of the catalysts, reactor shells and internal parts. The purpose of the study was to assess structural stability by estimating the exposed temperature of reactor internals and the shell in the event of similar hot spot phenomena in the future, as well as to predict corrosivity and devise measures during operation.
- Tüpraş details a new method for the maintenance of the preflash distillation column to prevent flooding problems.
- Wood Plc. provides a description of fundamental concepts, practices, challenges and process checklists involved in the process of rerating/restaging centrifugal compressors. This practice is necessary to ensure the equipment meets any new operating requirements, such as increased or decreased flow, increased or decreased head or a combination of both.
- Engineers at Kuwait Oil Co. and The Welding Institute present the detrimental effect of a tack weld in a pressure vessel fabrication, leading to fatigue cracking and the eventual breach of containment. Welding best practices are also showcased in Central Mechanical Research Institute's article.
- Servomex describes how maintenance and reliability in gas analysis equipment increases industrial plants' efficiency and safety.
- Finally, an investigation into issues with high-velocity gases in piping systems—known as isentropic or kinetic effects—details several case studies to help identify the characteristics of isentropic effects and how to physically address them, thus leading to more reliable and safer operations.

A life-long legacy. The topic of maintenance and reliability has been a staple in the pages of *Hydrocarbon Processing* since its founding more than 99 yr ago. Due to its crucial nature of ensuring reliable, efficient and safe processing, maintenance and reliability will continue to be a primary focus of this publication for another 100 yr. HP

INSIDE THIS ISSUE

J. KRIMMEL, Pinnacle, Houston, Texas

The economics of reliability: An interim report on the global refining industry

What is reliability? Most people think reliability is simply a measure of failure, or lack of failure. If something runs for a longer period without failing, then it is more reliable than something that runs for less time. However, reliability is a measure of how often something performs *when you want it to.*

The basis for the author's company's annual and interim quarterly reports are to explore the connection between reliability and economics so that we can understand how these key components of modern society intertwine. In doing so, we begin to see some striking trends and key indicators of opportunity. The goal of these reports is to challenge key industries in ways never seen before.

Most of the world's industrial facilities buy and sell commodities. Therefore, they have little impact on the price they pay for their feedstocks or the price they receive for their products. The nature of every commodity is that producers will fill the market with enough product until the margins—or profits—for producing that product decrease to a level that no one will produce more. Inevitably, the balance of supply and demand will separate organizations that are very good at running their facilities from those that are not. One of the biggest differences between these two groups is reliability.

Whether discussing jet transportation, power generation, water processing and treatment, chemicals, mining, oil and gas production, refining, automotive manufacturing or agriculture, reliability can mean the difference between excellence and mediocrity, and even profitability vs. bankruptcy.

The author's company's analysts estimate operators of complex facilities around the world spend more than $500 B/yr on reliability. The author's goal is to view several of these segments in detail and better characterize the role reliability plays in the broader economy.

For decades, lean manufacturing has driven companies and operators to improve runtimes, lower costs and minimize risk for their facilities. While this push has affected multiple sectors, no area has produced as much public data as the refining sector, especially in the U.S. The U.S. Energy Information Administration (EIA) has collected and reported refining data for decades and, when combined with international reports from the Organization of the Petroleum Exporting Countries (OPEC) and the International Energy Agency (IEA), among others, the level of information is unparalleled to other reporting sectors.

Refining reliability overview: Crack spreads as health indicators. A refiner's financial performance is largely driven by two variables: the price of raw feedstock (e.g., crude oil) and the price of finished products (e.g., gasoline, diesel and jet fuel). As a result, crack spreads—the difference in price between refined products and chosen inputs—are the most useful indicators of the health of the refining sector.

Crack spreads do not account for the cost of running the plant. Crack spreads ignore costs for items such as the energy to heat and process the feedstock, the people to operate the plant and all repair, maintenance and ongoing reliability work.

If we are mostly interested in reliability, then why do we care about crack spreads? More than 80% of the costs for a refinery are its feedstock. Crack spreads help us understand what is left over when we remove a refiner's single largest cost from its theoretical revenue. This leftover amount is what the refiner uses to cover its remaining costs, with ideally some profit remaining at the end. As crack spreads widen, the refiner has more capital available to invest in its operation or return to its owners. As crack spreads narrow, refiners have less flexibility and must make difficult decisions about how to deploy their limited capital. Crack spreads inform about the resources available to invest in best-in-class reliability programs, which is the primary area of interest.

Refining financial landscape. One measure of crack spreads is shown in **FIG. 1.** The blue line shows the spot price for Brent—the international benchmark for light, sweet crude oil. The green lines show the crack spread between reformulated blendstock for oxygenate blending (RBOB)—the primary component of gasoline—and Brent. The solid green line shows the monthly average crack spread. The dashed green line shows the crack spread's trailing 1-yr average.

FIG. 1. shows the volatility through which refiners have learned to manage their business. Since the beginning of 2006, the smallest monthly average crack spread was $0.01/gal, while the largest spread was $1.32/gal. In this 16-yr analysis, the crack spread has averaged $0.40/gal. In comparison, the 2020 year-to-date average is $0.30/gal, a 25% decline from the historical norm. If we use consumer price index data to account for the time value of money, the average crack spread from 2006 to the present increased to $0.46/gal. In constant dollar terms, the 2020 year-to-date spread is then at a 35% discount to the historical average, which explains a large fraction of the prevailing distress across the global refining sector.

Interesting patterns are apparent in this dataset. Starting around 2010, aggressive development of U.S. conventional oil and gas plays brought excess supply to the market. This sup-

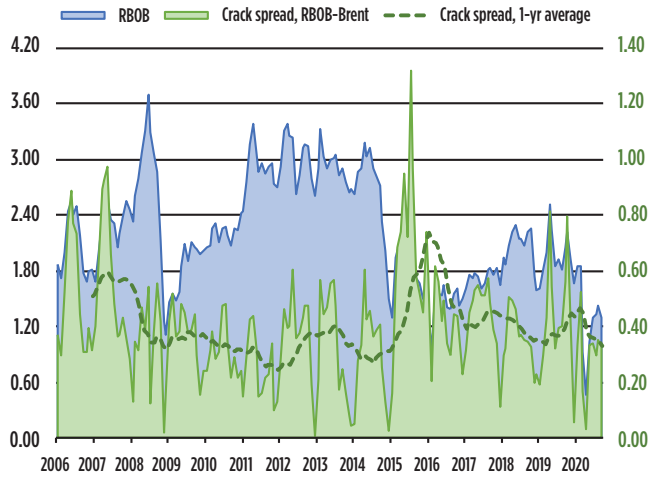

FIG. 1. RBOB and crack spreads, January 2006–September 2020. Source: U.S. EIA.

ply glut eventually caused the crude oil price collapse of 2014. Conversely, demand did not experience a similar shock, which kept product prices from collapsing as aggressively as crude oil prices. As a result, crack spreads increased through 2015. Over the course of a year, refined product prices reset to the lower oil price regime, which caused crack spreads to return to their normalized level of around $0.40/gal, where they remained from 2017 through 2019.

As noted previously, the 2020 year-to-date crack spread average is approximately 35% below historical levels when measured in constant dollar terms. The initial decline was triggered by a rapid deterioration in refined product consumption, driven by government lockdowns as a result to the COVID-19 pandemic. Refined product consumption has only weakly recovered as government restrictions persist, combined with (at least temporarily) changed travel preferences among the general population. As a result, crack spreads have witnessed continuous pressure throughout the year, with the most vulnerable refineries experiencing negative margins.

However, the news is not all bad for refiners. Capacity reductions will accelerate the pace with which the market normalizes. As of December 2020, the author's company's analysts estimate that 2 MMbpd of refining capacity is out of the market vs. the beginning of 2019. Therefore, the market should reach a healthy balance of consumption and production this year. Assuming this to be the case, analysts are forecasting an upward trend in refining margins through 2025.

Anticipated trends in the refining industry. Looking at global reliability spending patterns, the refining market will improve but will still face challenges. Regulatory pressures will keep growing, placing a lid on potential future margin expansion, and slowing upstream production growth will buoy feedstock prices and compress margins. In the U.S., natural gas prices are edging higher, which may reduce one of the U.S. refining sector's largest structural advantages—the cost of energy. These pressures may be offset by announcements by companies like BP and Shell that say they are exiting refining, but this is not anticipated to have an impact for several years.

Operational improvements are coming. In the face of adverse market forces, companies are pushing harder than they have in decades to make operational improvements, while simultaneously cutting costs. At the same time, virtually every major oil and gas company is investing heavily in strategic improvements, especially digital transformation. The author's company estimates that the energy industry—including exploration and production, midstream operations and downstream facilities—plans to spend $20 B over the next 5 yr on these projects alone. While several challenges exist in achieving operating improvement, especially in digital infrastructure, there is substantial potential for this improvement and cost optimization.

The pace of change is accelerating. For the first time in modern history, oil and gas majors began to diverge dramatically in their forecast of energy markets in 2020. Environmental, social and governance (ESG) pressures have been a dominant topic for the past few years. Within the refining industry, ESG pressures continue to mount. A difficult economic environment in 2020 forced virtually every refiner to make massive cuts in spending and sparked questions as to the stability of some of the facilities. In an industry with a tradition of very slow changes, the future leaders will most likely achieve that position due to the pace at which they evolve and focus, in part, on improved reliability.

Takeaways. The author's company estimates that global refiners spend more than $50 B/yr on reliability-focused activities, primarily on routine maintenance efforts and turnaround programs. It is also estimated that between 10% and 30% of this investment is wasted, meaning it does not improve reliability. In some instances, this spending may have a detrimental impact on performance, weighing even further against profitability. In this sense, suboptimal approaches to reliability costs refiners around the world between $5 B/yr–$15 B/yr.

To optimize reliability, spending and reliable performance to minimize risks and maximize profits, a refinery can do four things. These include:

1. Develop consistent, quantitative systems for evaluating system performance
2. Integrate reliability data from a range of sources and assets into single-system models to ensure critical inputs and influences are identified
3. Ensure personnel are adopting their work processes and utilizing these systems effectively to leverage their capabilities
4. Push past traditional decision processes or practices to uncover new opportunities and solutions.

While these suggestions sound simple, they have proven challenging for many refiners. Across the board, those that are doing all four of these appear to have both a lower risk profile and a higher profitability result, validating the premise that reliability is one of the leading indicators of profitable operations. HP

JEFF KRIMMEL is Director of Market and Data Analysis at Pinnacle. He has extensive analytical experience in the commercial and market intelligence domains. Before joining Pinnacle, Dr. Krimmel was the Director of Pricing and Market Research at Key Energy Services. He has also held various data-driven positions in pricing and profitability, strategic marketing and new product research and development at Baker Hughes. He earned his PhD in mechanical engineering from Caltech, where he used computational approaches to study the use of shockwaves in biomedical applications.

HEINZ P. BLOCH, RELIABILITY/EQUIPMENT EDITOR
Heinz.Bloch@HydrocarbonProcessing.com

Pushing the limit can have unexpected consequences

A prominent manufacturer rediscovered the old axiom, "pushing the limit can have unexpected consequences," after experiencing many bearing failures in its 40-hp air blowers. These lifetime-lubricated (sealed) bearings had been properly installed on 20-mm shafts, and it can be assumed that premium greases were being used. However, the blower rotors spin at 22,000 rpm, and the radial ball bearings did not last very long. As one engineer noted, these bearings failures became a costly repeat-warranty problem.

The manufacturer had selected these bearings based on load-related information, and the operating loads were well below the rated or permissible values. Chances are, however, that the manufacturer had not consulted **FIG. 1,** which is related to re-lubrication intervals.

One of the characteristics of mechanical components is their designed-in range of application. SKF America published the recommended re-greasing intervals in **FIG. 1;** they are a function of bearing bore diameter, shaft speed (rpm) and bearing type. The highest rpm for a 20-mm bearing is shown as 16,000 rpm. According to **FIG. 1,** this bearing would need to be re-lubricated every 10 hr. Since it is lifetime lubricated and sealed, it cannot be re-greased, although it will probably survive a few months of operation on a sealed-in charge of premium grease. The curve for the same 20-mm bearing operating at 22,000 rpm is off the chart. It is reasonable to believe that its L-10 life (the number of operating hours at which 10% of the bearings will have failed) may be only a few weeks.

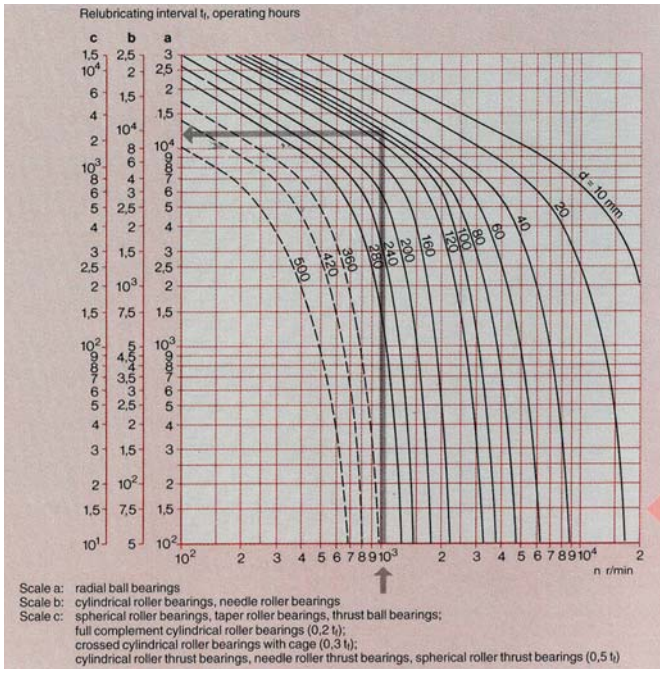

FIG. 1. Recommended re-lubrication intervals. Source: SKF.[1]

SKF recommends a "speed factor limit" of 500,000 mm/min for either of the angular contact bearings in **FIG. 2.**[1] The unsatisfactory blower bearings had similar contact angles, as depicted on the left side of **FIG. 2.** Bearings with a variation in contact angles are shown on the right side of **FIG. 2;** these probably would have given marginally better service. The contention that grease lubrication will disappoint is based on the fact that the actual speed factor for the bearings at issue is ([20 mm] × [3.14]) mm/revolution × [22,000] revolutions/min = 1,381,600 mm/min.

Considerable research by bearing experts at FAG/Kugelfischer Georg Schäfer in the early 1970s argues against lifetime-lubricated sealed bearings long before speeds approach 22,000 rpm.[2] Its authors concluded that re-lubrication, even for open bearings and well below 22,000 rpm, would need to be scheduled in intervals measured in weeks, not months. A small, dedicated, closed-circuit oil mist module would be well suited for this blower and its 1,381,600 speed factor. HP

LITERATURE CITED

[1] SKF, SKF General Catalogue, "5,000 E," June 2003.
[2] Eschmann, P., L. Hasbargen and K. Weigand, *Ball and Roller Bearings—Theory, Design, and Application,* 1st Ed., John Wiley & Sons, Hoboken, New Jersey, January 1985.

HEINZ P. BLOCH resides in Montgomery, Texas. He retired as Exxon Chemical's Regional Machinery Specialist for the U.S. and has authored or co-written more than 780 publications, among them 23 comprehensive books on practical machinery management, failure analysis, failure avoidance, compressors, steam turbines, pumps, oil mist lubrication and optimized lubrication for industry. Mr. Bloch holds BS and MS degrees (cum laude) in mechanical engineering from the Newark College of Engineering (NCE). He is one of 10 inaugural inductees into NCE's Hall of Fame, which honors its most distinguished alumni.

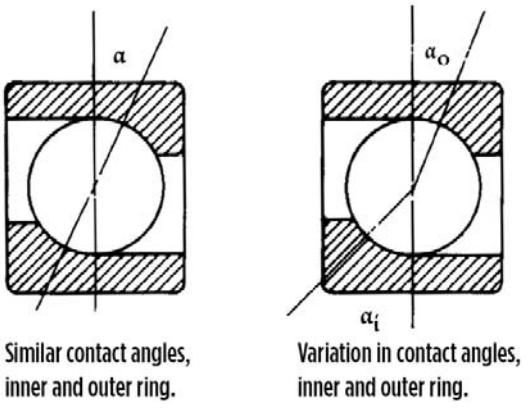

FIG. 2. Competent bearing manufacturers design contact angles to ascertain favorable rolling motion and minimize skidding. Source: SKF.[1]

Case 112: Remote failure analysis consulting

An article on "Remote training of personnel"[1] is interesting and appropriate at this time of COVID-19. It outlines the difficulties in presenting remote training courses and suggests methods that can help.

Challenges of remote consulting. As an independent consultant, I can relate to the ideas presented in this article. I formerly presented worldwide engineering failure analysis seminars to industry onsite as part of my consulting work. The satisfaction came in talking to the participants and recognizing when they had questions. These seminars lasted a full day and included a PowerPoint presentation, whiteboard explanations, group problem-solving, demonstrations and frequent breaks. This type of approach does not work as well in a remote presentation.

While I do not present at seminars any more, I still perform failure analysis consulting of machinery and fixed equipment. No matter how far technology advances, equipment still experiences failures. I had conducted my failure analysis consulting onsite, like my seminars, until recently when this type of work transitioned to remote. It is difficult working this way for many of the same reasons that remote training is less than optimum.

Remote consulting is just that. The consultant is not present to personally interface with the failure investigation team members, analyze the field failure data, review drawings in detail, talk with onsite personnel, perform testing, follow the progress of repairs and other items that are usually necessary. Instead, these functions must be performed by onsite plant personnel and the appropriate information must be relayed to the consultant. The consultant has only this information to work with, and any recommendations are limited to the data received. It is difficult to obtain the desired details over the telephone or internet. In the case of erroneous or missing data, the consultant's conclusions can be incomplete.

Benefits of remote consulting. On the other hand, some benefits do exist for remote failure analysis using a consultant:[2]

- Consultants analyze a variety of failures as their major activity, and have probably seen a similar failure and its solution already. The consultant can explain this failure to the team without being onsite.
- The consultant might have a different toolkit than the client company, such as finite element, structural, gear analysis, fracture analysis and torsional analysis programs or material evaluation.
- The consultant might be able to remotely direct the team to items not previously considered.
- The work can be limited to simply answering questions from the investigation team. In this respect, consulting can be more like mentoring.
- The cost of travel, time onsite, errors and omissions liability insurance, and personal insurance may not be included in the billing rate when consulting remotely.

Independent consultants are often used when the client company has personal knowledge of their capabilities. This type of consultant is a person with a high level of problem-solving experience who may be very familiar with the equipment and process at the client's location. The consultant may have even retired from the company or a similar industry.

With an initial telephone or internet contact, the potential client outlines the problem and may present data to show the extent. The consultant may be asked to perform specific tasks outlined by the failure investigation team or suggested by the consultant.

The consultant will then explain what can be done, the expected timing and the maximum billing expected for the agreed-upon proposal. In cases where an agreement is made, work will proceed on receipt of a job contract and purchase order.

When the job is outside the scope of the independent consultant's capabilities, a larger, established consulting firm may be recommended. For example, as an individual consultant I will not usually accept jobs where severe injuries have occurred and the cause needed to be determined. Those types of investigations can quickly expand outside the scope of the agreed-upon proposal.

Larger consulting firms with specialists covering several specific fields are usually selected on jobs that require onsite personnel and liability insurance or jobs that require onsite evaluation, testing or possibly court appearances as an expert trial consultant.

While remote failure analysis might not be right for every company, it is worth discussing with a consultant on the next failure that requires assistance. The consultant may be able to provide the team with additional help. HP

NOTE

Case 111 was published in *HP* March 2021. For past cases, please visit www.HydrocarbonProcessing.com.

REFERENCES CITED

[1] Munson, P., "Five lessons to get the most out of remote training and tools," *Hydrocarbon Processing*, December 2020.
[2] Sofronas, A., *Survival Techniques for the Practicing Engineer,* "Ch. 6: How a consultant can help," John Wiley & Sons, Hoboken, New Jersey, 2016.
[3] Sofronas, A., *Unique Engineering Methods for Analyzing Failures and Catastrophic Events: A Practical Guide for Engineers,* John Wiley & Sons, Hoboken, New Jersey, to be published in 2021.

TONY SOFRONAS, D. Eng, was the worldwide Lead Mechanical Engineer for ExxonMobil Chemicals before retiring. He now owns Engineered Products, which provides consulting and engineering seminars on machinery and pressure vessels. Dr. Sofronas has authored several engineering books and numerous technical articles on analytical methods.

Andy Howell, Chief Executive Officer, KBC, a Yokogawa Company, London, UK; and Russell Byfield, Global Simulation Business Leader, KBC, a Yokogawa Company, Singapore

It was the best of times

"It was the best of times, it was the worst of times, it was the age of wisdom, it was the age of foolishness…". Fortunately, this opening line from *A Tale of Two Cities* does not often present itself as an appropriate analogy to the oil and gas industry. Yet, here we are.

The industry is experiencing a perfect storm of events, and they are all moving in different directions. Within all these conflicting circumstances, there is both opportunity and risk—the best of times for some and the worst of times for others.

Enabled by fracking, horizontal drilling and many other, lesser-known technologies, a shift in global oil and gas supply chains has taken place in recent, pre-COVID times in the U.S. It has elevated the country to a world leader in oil and gas production and has provided sovereign certainty regarding the domestic, hydrocarbon supply chain. However, powerful lobbying groups have vowed to ban fracking, putting the industry at risk. The shale boom started the slow but steady transition of petrochemical industry manufacturing to the U.S.—with its 'lower for longer' gas prices—and away from manufacturing locations with cheaper labor.

COVID lock downs caused a drastic decline in global jet fuel consumption, while travel bans devastated many domestic and global airline companies. Those have led to refiners fighting for survival, some unsuccessfully.

Capital for upstream projects will most likely favor the lower-risk expansion of existing fields over the development of new exploration plays. Some small- to medium-cap companies focusing purely on new plays will invariably go out of business.

A combination of COVID and the U.S.-China trade war is leading many companies to reassess their global supply chain risks. For bulk-manufactured commodities, this will likely lead to an increased flight of capital from China to alternative, low-cost countries such as India and Vietnam. For high-tech manufactured goods, this flight of capital will likely favor Japan, Korea and Taiwan.

The re-evaluation of sovereign risk by all countries will also likely lead to a resurgence in several domestic manufacturing sectors that globalization had been eroding for some time.

Energy security will continue to be a focus with an increasing understanding by the population of the duck curve nature of renewable energy and that the ultimate enabler of renewables is natural gas. That is slowly shifting to hydrogen; however, while hydrogen is clean, it is expensive.

This global oil and gas realignment could also result in a global supply chain shift as petrochemical and polymer manufacturing migrates. No matter how much we consume hydrogen, we still need hydrocarbons to produce the polymers that are used in everything from clothing and cars to building materials, not to mention flying planeloads of people around the world.

Add digitalization to the mix. The industry has at its disposal an unprecedented array of disruptive technologies and it is exploiting their value more quickly than ever before. The pursuit and adoption of these technologies exists in the context of a digitalization journey that is driven by both internal and external factors. Ultimately, it supports the quest for superior results in a sustained manner.

The drive toward semi- and fully-autonomous operations in the oil and gas and petrochemicals industries is forcing operating companies to seek digital platforms and fully adopt disruptive, digital technologies as the normal way of doing business. The technologies allow them to bring together capabilities in real-time data capture and processing, information flows and integrated execution with process simulation capabilities, technical savvy and a deep knowledge of business value drivers.

Many companies in the oil and gas, petrochemical and associated service industries have been implementing workflow best practices and slowly progressing towards more flexible operating procedures. This has been a work in process for years. Who would have thought we could suddenly all do it in 6 mos? The impossible a year ago is, today, practically *fait accompli.* Of course, this is still a bit of an overstatement. Many wrinkles remain to be ironed out regarding efficiencies, who best works remotely and who should work onsite.

Due to the COVID pandemic, the oil and gas and petrochemicals industries will digitalize much more quickly. The path from manual to automatic to autonomous is now the path for all as we aim to survive and ready ourselves to thrive in a post-COVID world.

A post-COVID world will consume fewer hydrocarbons per capita than it did before. More people will continue working from home or will travel to an office or site less frequently. Business air travel will not cease but will surely decrease as we are now far more tolerant of meeting online. This is not a bad thing. The use of hydrocarbons is here to stay for a long time, but their consumption has permanently changed and will continue to change.

How will the oil and gas industry take advantage of these opportunities and manage the risks? By now, the industry should be very good at all this; however, dealing with the entire perfect storm of new circumstances, simultaneously, will test us all. HP

ANDY HOWELL is the Chief Executive Officer of KBC, a Yokogawa Company. He has held senior positions with bp, AspenTech and Schlumberger. Mr. Howell earned an MS degree in chemical engineering from the University of Cambridge, UK, and holds several patents in integrated asset modeling, process simulation and digitalization.

RUSSELL BYFIELD is the Global Simulation Business Leader for KBC, a Yokogawa Company. He has international experience in the oil and gas, petroleum and process industries.

L. ÖZKAN, İ. AYDIN and G. ÖZTÜRK, Tüpraş, İzmit, Turkey

Cleaning distillation column and heat exchangers through cutter stock circulation

The Tüpraş İzmit refinery's largest crude distillation unit (CDU) is designed with a preflash column prior to the atmospheric distillation column. The preflash column regularly suffers flooding problems, followed by high pressure drop that results in the discoloration of light straight-run naphtha product. The problem occurs due to organic fouling and choking of column trays, which causes a shutdown due to off-specification products. The unit shutdown includes all the required precautions (steam-out phase, blinding, etc.) for the safe entry to the preflash column. These precautions, along with mechanical cleaning of the column, extend shutdown time to nearly 10 d, which significantly impacts refinery margins.

In December 2019, the CDU was again forced to shut down due to severe fouling of trays. A new method was applied, instead of mechanical cleaning, to eliminate foulants. The maintenance of the column lasted nearly 3 d, with promising results. Not only were shutdown time and production cuts significantly reduced, but also the fouling-prone heat exchangers and preflash column heater tubes were cleaned within this time frame. This article describes the details of the new method for the maintenance of the preflash distillation column.

Operational background. The CDU is the largest, by capacity, and has a more energy efficient design than other CDUs in the refinery. The CDU has a preflash column upstream of the crude preheat furnace that removes light fractions of crude oil to reduce duty required by the furnace and to minimize the pressure of the main distillation column.

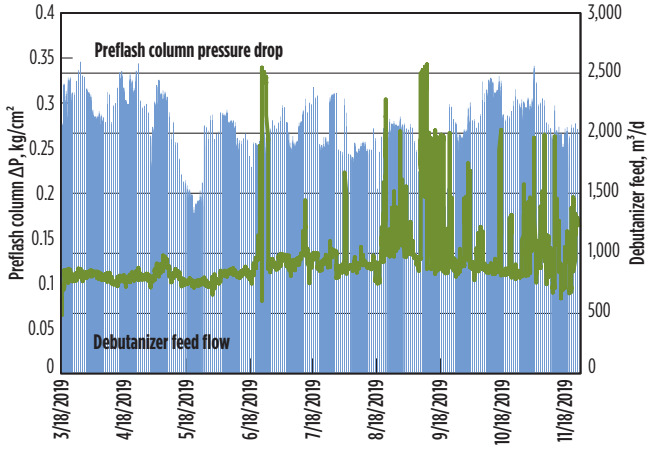

FIG. 1. The debutanizer feed vs. the preflash column *ΔP*.

However, the CDU's preflash column trays are known to have poor resistance against fouling problems. The column has a history of shutdowns—around once every 2 yr, on average—because of high pressure drop resulting from severe fouling on the trays. During the refinery's 2018 turnaround, the floating valve trays in the preflash column were replaced with fouling-resistant, fixed-valve trays with wider openings. However the problem appeared again a few months after startup.

Problem definition. The CDU had faced tray contamination problems three times during the period between two turnarounds in 2014 and 2018, therefore it had to experience two breakdown maintenances within this time frame. Although there was a fouling problem followed by a high pressure drop through the column prior to the 2018 turnaround, it did not require downtime since maintenance was scheduled to be performed. The unit suffered similar fouling problems in the preflash column before 2014, which was resolved by mechanical cleaning that took 10 d of downtime.

During the 2018 turnaround, the floating valve trays of preflash column were replaced with fouling-resistant trays, which are not prone to contamination because they have wider tray openings that create lower pressure difference. These trays help avoid downtime from tray contamination in the preflash column. The new trays reduced the ΔP value from 0.15 kg/cm² to 0.1 kg/cm², which led to a decrease in pressure drop along the column. After replacing the column trays, even light crudes with

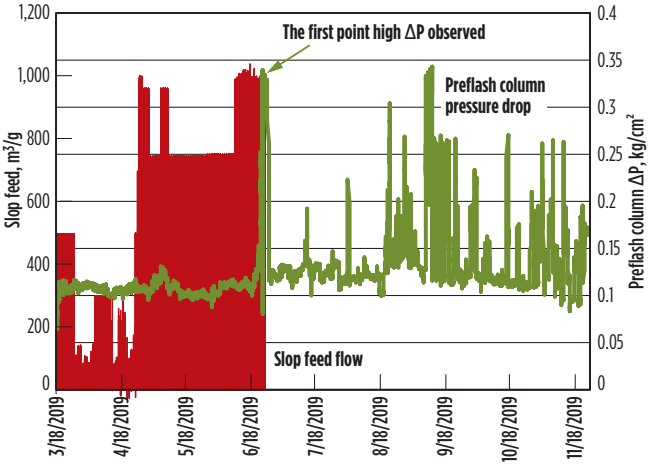

FIG. 2. The slop feed amount vs. preflash column pressure drop.

high amounts of naphtha did not cause a high pressure drop in the column, contrary to what had been experienced before. FIG. 1 represents the relation between pressure drop along the column and debutaniser feed volume.

In June 2019, when the incident occurred for the first time, a high amount of slop (6% of the feed rate) was processed, including cracked products formed during the startup of the cracking units, which had undergone a turnaround the previous month. The slop included coker products, especially coker naphtha, which may have been responsible for the rapid fouling in the preflash column due to its molecular structure. The amount of slop processed and the change in pressure drop through the preflash column are shown in FIG. 2.

In a similar way, the increase in the pressure drop through the column had been observed after processing the slop products formed by the cracking units in 2015 and 2017. All these findings are indications that slop products produced from the cracking units may have caused foulants on the trays and, therefore, an increase in the pressure drop. Another reason for the fouling might be asphaltene precipitation. Light opportunity crudes are blended with heavy opportunity crudes, making the processed blend prone to asphaltene precipitation, which can lead to fouling on trays.

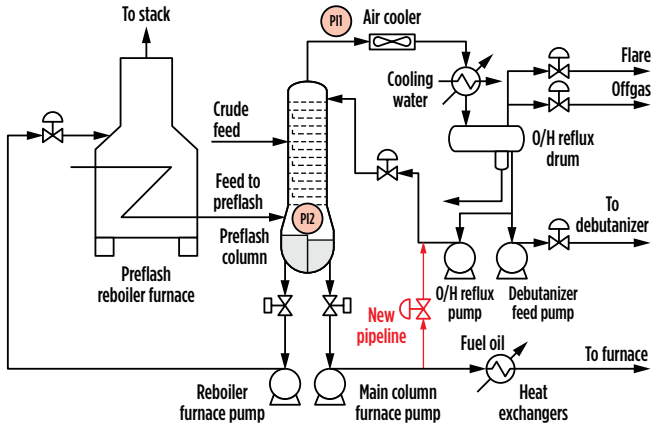

FIG. 3. Preflash column process flow diagram.

FIG. 4. Clean and dirty cutter stock samples after four circulations.

Preparation and application. The aim was to minimize downtime for the CDU with the highest crude processing. The maintenance history of the preflash column shows that the mechanical cleaning takes at least 10 d, with many hours needed for blinding, access opening, cleaning, steam-out, etc. The heated cutter stock circulation was considered for removing and dissolving foulants on the tray and for minimizing the downtime of the unit. Light-cycle gasoil, a product of fluid catalytic cracking unit (FCCU), was used as cutter stock because of its solvent properties.

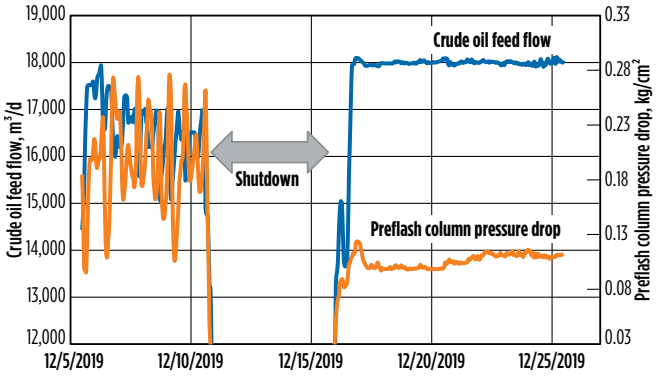

FIG. 5. Pressure drop of preflash column vs. crude oil feed flow before and after cleaning.

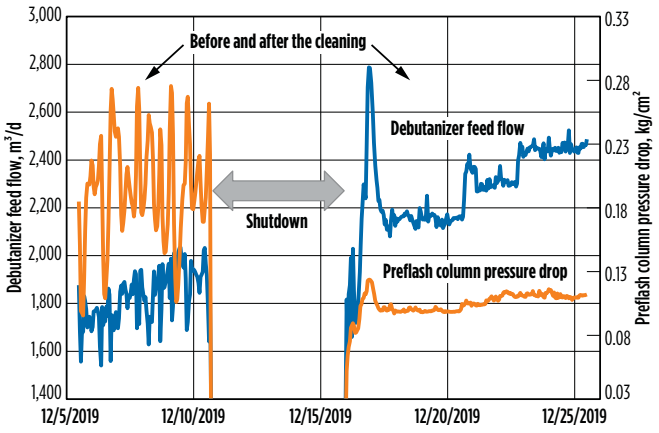

FIG. 6. Pressure drop of preflash column vs. debutanizer feed flow before and after cleaning.

TABLE 1. Cutter stock sample results

Tests	Clean cutter ctock	First circulation	Second circulation	Third circulation	Fourth circulation
Asphaltenes, % m/m	0	0.12	0.041	0.033	0.01
Carbon residue, % m/m	0	0.42	0.12	0.48	0.02
API	24.4	25.5	24.8	28.1	32.9
Viscosity, mm²/s	1.597	1.785	1.627	1.697	1.822

To minimize downtime, preparations were made prior to reducing the feed rate. The outlet of the spare main column furnace pump was connected to the outlet of the preflash column overhead reflux pump to create a closed loop (FIG. 3), while the other two pumps—the main column furnace pump and overhead reflux pump, both with electric motors—were in operation. Only the spool connection was completed after the shutdown for the sake of operational safety, since leakage through the gate valve would be too risky.

After the unit shutdown, the cutter stock pumps were started, and the column was flushed with cutter stock to the slop tank. The flushing was followed by column loading with cutter stock. The column was filled to the top (approximately 80%–90%) with cutter stock while the spool connection was completed, making the closed loop. The loading of the entire column took 5 hr–6 hr.

The cutter stock circulation between the preflash column and the reboiler furnace started through the reboiler furnace pump after 80% of the column bottom level was reached. The cutter stock flow was heated to 180°C to increase the solvency of the cutter stock. The level of the column was indicated through a calculation making use of pressure transmitters located at the top and bottom of the column according to the formula in Eq. 1, where pressure values are given in kg/cm^2 and 0.8 is approximately the specific gravity of the heated cutter stock:

$$1\ (\text{kg} / \text{cm}^2) = 10{,}000\ \text{mm}\ H_2O = 10\ \text{m}\ H_2O$$
$$\text{Level} = (P_2 - P_1) / (0.8\ \text{S.G.} \times 0.1) \quad (1)$$

After the spool connection was completed and the level was increased in the preflash column, the main column furnace pump was started to make the cutter stock fluid circulate through the overhead line and upper trays of the column. The cutter stock temperature was observed by the temperature indicator at the flash zone. To prohibit the fluid from boiling, the cutter stock temperature was not allowed to exceed 180°C. The circulation at 180°C lasted around 10 hr, followed by column draining. The column was drained with the main column furnace pump to the slop tank in nearly 2 hr.

After column draining, an entire cycle is fulfilled in a 16 hr–20 hr time range. The same phases (loading, circulating and draining) were repeated for the second, third and fourth circulation. After draining of the fourth circulation, the unit was ready for startup. The last drain was made through the heat exchangers to eradicate organic foulants in the heat exchanger tubes.

Takeaway. In total, four circulations were carried out. After each circulation, a sample from the dirty cutter stock was analyzed for asphaltene, carbon residue, API gravity and viscosity. The results are shown in **TABLE 1.**

According to the sample results, asphaltene values decreased after the fourth circulation and then became negligible. In the third and fourth circulations, light diesel and kerosene were used as cutter stock instead of LCGO since LCGO product volume was inadequate. The low LCGO volume was the reason for the increase in API and viscosity values after the third circulation. Carbon residue declined, as well, except for the third circulation sample. As shown in **FIG. 4,** the color of the fourth sample was detected to be lighter than prior samples, indicating the cleaning of column and heater tubes.

Before this application, feed to the CDU was reduced due to high pressure drop at the preflash column, especially when the crude oil blend contained a greater quantity of lighter products. However, the problem was eliminated after the successful application. The unit was shut down for 3 d of maintenance (**FIG. 5** and **FIG. 6**) instead of reducing feed.

In addition to this solution, the use of cutter stock as a solvent during these circulations had a cleaning effect on not just the preflash column but the heat exchangers, reboiler furnace and pipelines. The cutter stock was drained after the fourth circulation through the heat exchangers to clean them. After startup, the heat exchanger's heat transfer performance was improved—the heat transfer duty was improved by 0.35 Gcal/hr.

The downtime of the unit was reduced by a total of 5 d. The maintanence required less labor, with a better method in terms of health and safety. Additionally, energy gain was achieved due to the cleaning of heater tubes and heat exchangers with cutter stock. This application is promising in terms of production and energy savings. HP

LEVENT ÖZKAN is a Process Supervisor at the Tüpraş İzmit refinery. He holds a BSc degree in chemical engineering from Bosphorus University.

İLKE AYDIN is a Process Supervisor at the Tüpraş İzmit refinery. She is responsible for crude and vacuum distillation units. She holds a BSc degree in chemical engineering from Bosphorus University.

GÖZDE ÖZTÜRK is a Process Engineer at the Tüpraş İzmit refinery. She holds a BSc degree in chemical engineering from Middle East Technical University and an MSc degree from Bosphorus University.

S. M. LEE, S. H. BAE and D. S. LEE,
SK Energy, Seoul, South Korea

Stability evaluation of hot spots in the RDS process reactor

During the end-of-run (EOR) period of the authors' company's residue hydrodesulfurization (RDS) process in early February 2019, some hot spots occurred in the catalysts of the reactors. The normal operating temperatures of the catalytic bed of the reactors are about 370°C–400°C, and the temperature gradually rises as the severity of the process increases during the EOR period. However, the temperatures at that time reached 600°C–1,100°C. Fortunately, the planned shutdown of the process was in March, so personnel were able to adjust the operational conditions for the remaining month.

Impurities such as metal, sulfur and asphaltene accumulate in the catalysts, resulting in uneven feedstock flow. Areas that are not in contact with the feedstock undergo a rapid exothermic reaction inside, which is called a "hot spot" phenomenon. It occurs occasionally during the EOR period because a lot of impurities accumulate in the catalysts and the operational severity of the process is increased to fully use the remaining catalyst life. In addition, if the catalyst loading quality is poor, it rarely appears, even during normal operation.

When a hot spot occurs, the bed temperature rises rapidly in a short time due to a rapid heat reaction, and the range is expanded and continuously deteriorated. The inside of a hot spot mass comprises a solid chunk of coke and is made worse by not penetrating the feedstock coolant.

In this study, the authors modeled hot spot phenomena experienced to analyze the temperature effects of the catalysts, reactor shells and internal parts. This was completed through computational fluid dynamics (CFD) analysis and, with finite element analysis (FEA) techniques, these results were used to evaluate structural reliability. Also reviewed was the corrosion mechanism of internal structures exposed at high temperatures during this time.

Ultimately, the purpose of this study was to assess structural stability by estimating the exposed temperature of reactor internals and the shell in the event of similar hot spot phenomena in the future—and to predict corrosivity and devise measures during operation. In other words, if an abnormal temperature zone occurs due to a hot spot, then an operational guide could be provided to determine whether the process can be operated continuously or if feedstock supply must be halted and measures taken (such as nitrogen cooling).

Hot spots. Hot spot cases are very diverse, and their characteristics may differ depending on shape, temperature and location of occurrence. Hot spot sizing is not easy, but it can be estimated using thermocouples for temperature sensing of catalysts. It could be easier if thermocouples for multi-point sensing were installed. The actual size can be checked during the catalyst replacement work during a shutdown. The hot spot area rises rapidly in a short time and is observed as a hard coke mass.

The analysis was done in three stages. These include:

1. The temperature profile—in axial and radial directions—was analyzed through CFD after modeling hot spots. The authors compared several items to find

TABLE 1. Variable for CFD analysis

Condition	Description/properties
Hot spot location	Axial direction: 500 mm above the interbeam
	Axial direction: 900 mm above the outlet collector
	Radial direction: 50 mm away from the wall
Hot spot shape	Spherical, having diameters of 500 mm, 1,000 mm and 1,500 mm
Hot spot temperature	800°C–1,100°C
Feed phase	Single phase
Feed velocity	0.0031 m/sec
Viscosity	0.000023 Pascal second (Pa-sec)
Catalyst thermal conductivity	0.25 watts/m Kelvin (W/mk)* vs. 12 W/mK vs. 25 W/mK**
Specific heat	1,886.7 J/K/kg
Feedstock temperature	400°C
Ambient temperature	21°C
Shell outside	Adiabatic condition

*Thermal conductivity for coke in literature
**Thermal conductivity reflecting the temperature change (10°/cm) in the radial direction experienced by SK Energy

the best model, since there were a wide variety of cases.

2. It was possible to know the exposure temperature of the surrounding structures through CFD of hot spot modeling. The mechanical stability of the structure was evaluated by reflecting this exposure temperature through the FEA method. It was the structure affected by the shell, interbed beam and outlet collector.
3. The important item was the corrosion review. In general, Tp347 is a corrosion-resistant stainless steel in the typical operating envelope of a hydroprocessing reactor. However, at elevated temperatures above the design condition, Tp347 is known to be susceptible to high-temperature corrosion and/or metallurgical change associated with chromium carbide precipitation.

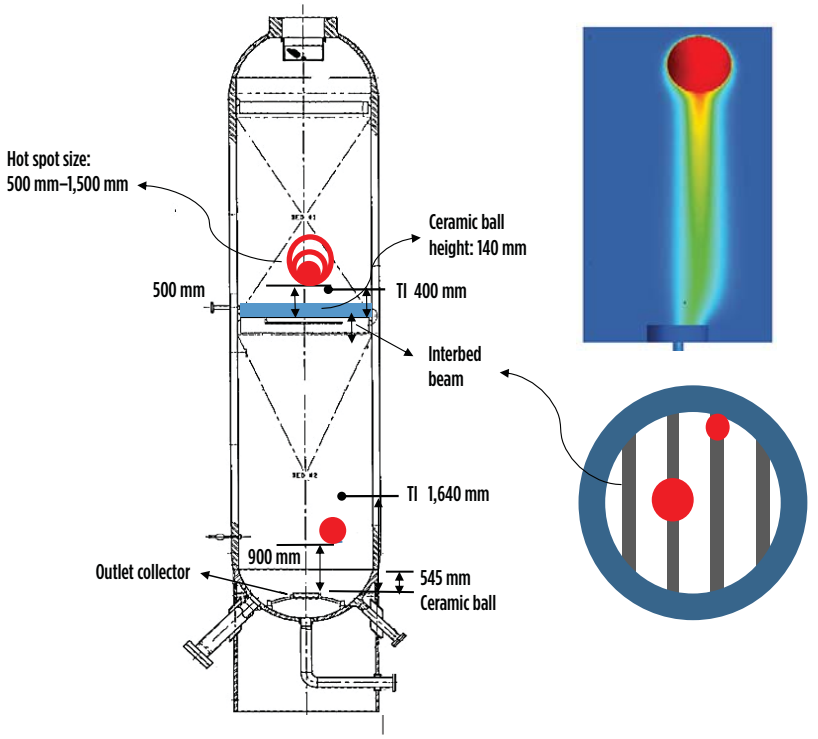

FIG. 1. CFD modeling.

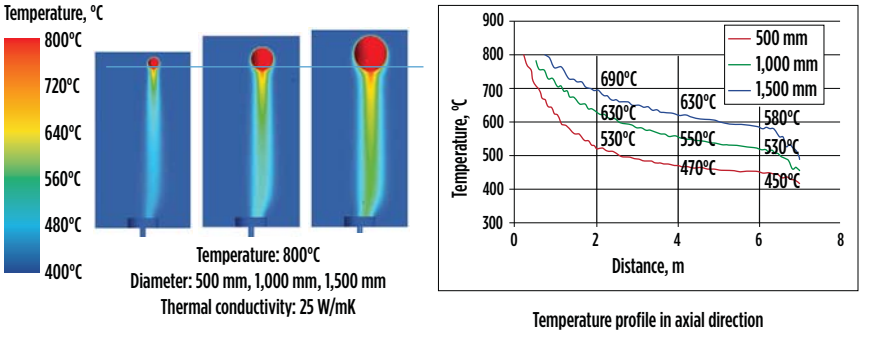

FIG. 2. Temperature profile for sizing hot spots.

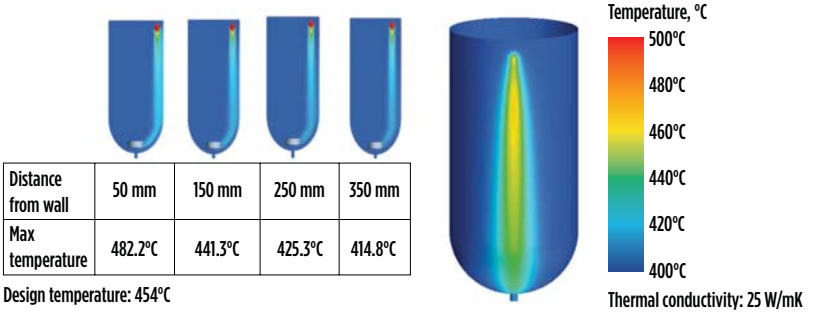

FIG. 3. Inside wall temperature.

Temperature profile analysis of catalysts and structures by CFD modeling.

The purpose of this test is to check the temperature profile in the downward and radial directions, according to the hot spot conditions. The modeling selected a reactor having an interbed beam. The assumed conditions for CFD modeling are shown in **TABLE 1.**

The structure of the reactor, the hot spot size and location are shown in **FIG. 1.** It consists of two catalyst beds and an interbed in the middle of the reactor. The bottom head has an outlet collector installed. The shell is made of 2.25 Cr-1 Mo steel with a Tp347 weld deposit, and the internal structure is made of Tp347 material.

The following are the results of the CFD modeling:

- **Temperature profile of the axial direction:** The lower direction of the hot spot showed a long tail-type temperature profile (**FIG. 2**). Three models were found to be affected by temperatures up to about 7,000 mm in the lower direction. Higher temperatures will result in longer temperature distances, and larger sizes will also result in longer lengths. When a hot spot occurs, the lower structure (i.e., the interbed beam and outlet collector) is directly affected by the temperature. It is seen that this is related to the directional flow of the feedstock, and it can be estimated that a long tail-shaped temperature profile can be seen in the lower direction. However, it was only possible to

confirm how far the influence would be through this modeling.

- **Temperature profile of the radial direction:** Conversely, the temperature effect in the radial direction was very limited. If the hot spot was only 150 mm away from the reactor wall, the wall temperature could be reduced below the design temperature (FIG. 3). This is closely related to the directional flow of the feedstock, which seems to rapidly reduce the range of high-temperature areas as feedstock flows from the top to bottom. This means that, even if the hot spot location is close to the wall, the temperature increase of the wall does not have to be a concern. In fact, in the authors' experience, an increase in wall temperature was not detected.

In the structural analysis of the reactor wall, the hot spot case at 50 mm was considered. A peculiar item is that the point where the maximum temperature appears is not the area of the hot spot occurrence. Since the maximum temperature area appeared below approximately 1.8 m, it is necessary to take this into account when checking the actual shell temperature. This can be confirmed in the CFD temperature profile on the right side of FIG. 3.

To summarize the CFD results, the temperature effect is much larger in the direction below the hot spot, while the effect is very small in the radial direction. This seems to be closely related to the directional flow of the feedstock.

Based on this, the master curve—which can be used for various hot spot sizes—is prepared to estimate the exposure temperature of the lower structure, by distance, according to the hot spot size and temperature (FIG. 4). The exposure temperature of the lower structure is 50°C–160°C lower than the hot spot indicator temperature. For example, with a hot spot of 900°C, the exposure temperature of the lower structure can be predicted to be as high as 750°C–840°C.

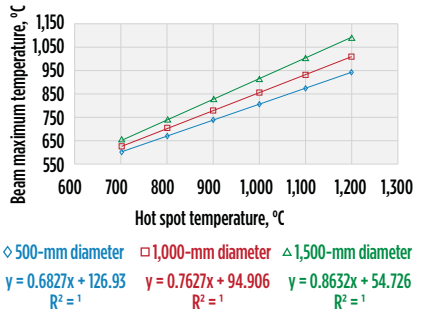

FIG. 4. Maximum surface temperature of the internal structure according to hot spot size and temperature.

Evaluation of the shell and interior structure stability through FEA.

A structural stability evaluation was performed on the reactor wall, interbed beam and outlet collector. Only 800°C and 500-mm diameters were considered for the shell and outlet collector, while 500 mm, 1,000 mm and 1,500 mm were considered for the interbed beam. The standard ASME VIII, Div. 2 Part 5 specification was applied to the analysis.

The shell's material comprises 2.25Cr-Mo steel with thermal conductivity of 35 W/mK, and the internal structures are composed of Tp347 steel with thermal conductivity of 25 W/mK.

Evaluation results. The following are the results of the evaluation:

- **Reactor wall:** Consider when a hot spot mass with a temperature of 800°C and a 500-mm diameter exists 50 mm away from the wall. As a result of the analysis, the maximum stress caused by the hot spot was 322 MPa—and there were no problems, as it was below the acceptance criteria of 331 MPa. It was analyzed that the maximum stress was applied inside of SCL-A-2-L1; whereas, it was found that lower stress was applied at the maximum temperature point (SCL-A-2-L2). The previous CFD analysis indicated that the maximum surface temperature of the wall was located at the lower part of a certain distance, not at the point of the hot spot occurrence. The stress analysis results were similar (FIG. 5).
- **Interbed beam:** The top of the interbeam's center showed the highest temperature (750°C), with a stress of 48.6 MPa (less than the allowable stress of 230 MPa). Conversely, the maximum stress at the bottom of the beam's center was 172 MPa (less than the allowable stress of 315 MPa), and the temperature was 638°C. The maximum temperature was at the top, but the maximum stress was at the bottom. Although the surface temperature of the upper part of the beam was at its maximum due to the hot spot, it was in line with the expectation that the maximum bending stress would be the

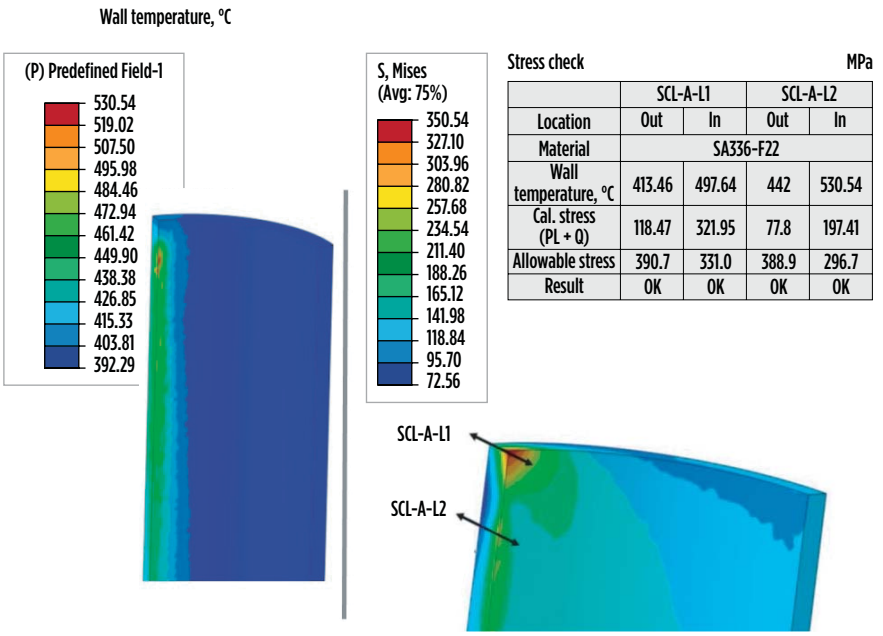

Stress check MPa

	SCL-A-L1		SCL-A-L2	
Location	Out	In	Out	In
Material	SA336-F22			
Wall temperature, °C	413.46	497.64	442	530.54
Cal. stress (PL + Q)	118.47	321.95	77.8	197.41
Allowable stress	390.7	331.0	388.9	296.7
Result	OK	OK	OK	OK

FIG. 5. Stress at the reactor wall.

bottom point of the beam (FIG. 6).

- **Outlet collector:** As a result of the evaluation of the outlet collector, the maximum temperature area was 551.6°C with the structure's top, but the calculated stress value was 82 MPa (less than the allowable stress of 354 MPa), which was enough (FIG. 7). Conversely, the bottom area had a maximum calculated stress of 337.2 MPa (less than the allowable stress of 396 MPa). This area was where the maximum bending stress was applied, as shown in the inter-beam analysis. In other words, the surface temperature at the top of the structure exceeded the design conditions due to the hot spot, but it was not the area where the maximum stress was applied, so it could be assessed that there was no significant impact on the stability of the structure.

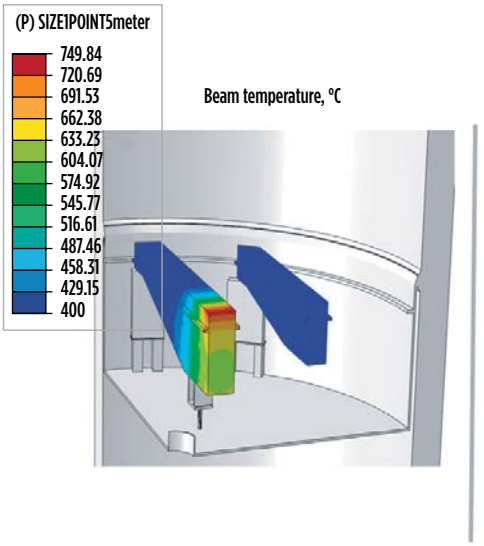

Stress check MPa

Material	SA182 F347			
Point	A	B	C	D
Metal temperature, °C	635.5	638.4	749.8	400.08
Cal. stress	163.8	172.6	48.6	146.7
Allowable stress	326.9	315	230	397.5
Result	OK	OK	OK	OK

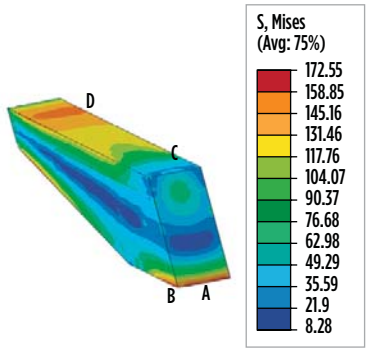

FIG. 6. Stress at the interbed beam.

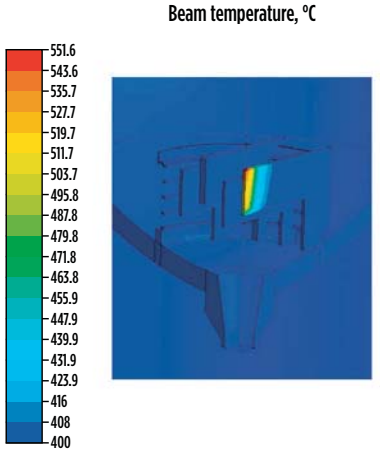

Stress check MPa

Material	SA182 F347		
Point	A	B	C
Metal temperature, °C	445.5	551.6	425.8
Cal. stress	337.2	82	127.5
Allowable stress	396	354	396
Result	OK	OK	OK

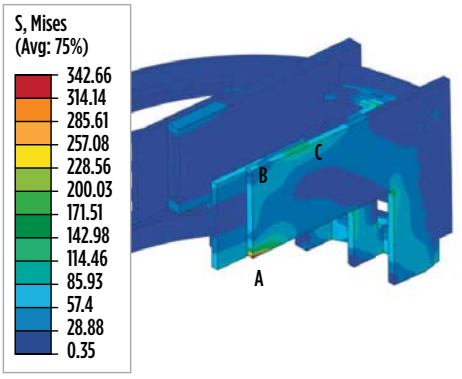

FIG. 7. Stress at the outlet collector.

Summarizing the structural stability evaluation results, the surface temperature of the shell wall, interbed beam and outlet collector structure exceeded the design temperature by the hot spot. It was decided that there were no structural stability problems, even if the temperature of some of the shell and internal structures exceeded the design standard due to the hot spot effect. The cause seemed to be that the maximum temperature point and the maximum stress point did not coincide in the structure. In other words, due to the hot spot, the temperature exceeded the design conditions locally, but there was no problem with the stability of the structure.

Corrosion analysis. A review of the corrosion environment is essential, even if structural stability assessment results are satisfied. The internal structure is composed of a part supporting the load, a beam, a supporting bar and a mesh screen that simply prevents catalysts from passing through. A thermowell pipe is installed to measure the temperature. If these parts are severely damaged by corrosion or cracks, then catalyst leaks or structure collapse may occur during operation, and repair or replacement may be long and expensive. In particular, the thin mesh screen is susceptible to damage and, if the gap is widened and the catalyst escapes, normal operation is not possible.

In normal operating conditions, corrosion of the internal parts (Tp347 steel) rarely occurs, so no special care is taken. However, the problem changes at high temperatures above 500°C. If this temperature is exceeded, high-temperature sulfidation (HTS) corrosion and/or polythionic acid stress corrosion cracking (PASCC), induced by sensitization,

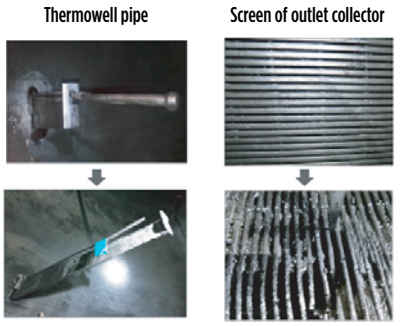

FIG. 8. Corrosion at the internal parts.

may occur. While HTS is a well-known corrosion phenomenon within the typical operating range of a hydroprocessing unit, corrosion data above the design temperature of the reactor (454°C) is limited, especially for austenitic stainless steel. The corrosion rate of Tp347 stainless steel at 500°C–600°C has a maximum of 60 mils/yr. However, this value has a low confidence level because it is calculated by extrapolation.

In the authors' case, the process ran for about a month after the hot spot occurred. As a result of the inspection of the internal structure during shutdown, a severe corrosion phenomenon was found on part of the mesh screen of the outlet collector and on several thermowell pipes on the wall. Even with the austenitic stainless-steel material, it was found that corrosion may occur within a short period of time under hot spot conditions where the temperature rises rapidly. As shown in **FIG. 8,** the mesh screen had a wider gap, and some of the mesh was completely corroded. If exposed for a longer period, the catalyst above may have been lost. Although the thermowell pipe was 3-mm thick, it was completely corroded within a short period of time, and high-temperature corrosion was accelerated by carburization and metal dusting phenomena. Based on the authors' inspection data, the amount of corrosion was acceptable when the exposed metal temperatures were below 700°C, and the duration of high-temperature exposure was less than 1 mos.

In the case of PASCC, it is known that sensitization occurs first and contact with polythionic acid is required. Sensitization occurs more frequently with higher temperatures. According to literature, austenitic 347 stainless steel can be exposed at 495°C for 10,000 hr, but at 530°C for only 1,700 hr. In the authors' case, the microstructure of the bolting bar—which is a part of the bottom collector assembly—was inspected using the filed replication technique. It was found that there were no signs of sensitization, even though corrosion was spotted at the nearby mesh. **Note:** The microstructural review was conducted after replacing corroded/damaged internal parts. Therefore, the authors believe that the remaining part of the reactor internal, which was not replaced, still maintains enough PASCC resistance because the temperature and duration of the hot spot were not enough to cause sensitization.

In summary, the possibility of HTS corrosion should be kept in mind, even if the hot spot period is a short duration. Furthermore, high-temperature exposure may cause sensitization of austenitic stainless steel, but the level of damage should be carefully reviewed by metallography.

Considering the exposure temperature, time and area, the authors decided to maintain a temperature of 650°C. Corrosion testing under the same conditions—high temperatures with high sulfur—was not easy. Only a hardness comparison was made through simple heat treatment experiments, and some of the 650°C limit was reflected.

Takeaway. CFD modeling of hot spot cases in the RDS reactor catalysts was performed to analyze temperature profiles for catalysts, reactor walls and internal structures. Accordingly, structural stability was evaluated through FEA for structures where temperature increases locally. Corrosion under this condition was also identified, and the following conclusions were drawn:

- The larger the hot spot size or the higher the internal temperature, the larger the temperature area of the axial direction—and the temperature of the lower internal structure increases locally. In the downward direction, the influence of temperature was confirmed to about 7,000 mm, as it was affected by the directional flow of feedstock.
- Conversely, the effect of temperature in the radial direction was relatively small. Even if it is only about 150 mm away, it has been cooled rapidly below the design temperature. This means that, even if an internal hot spot occurs, the temperature of the reactor wall does not rise significantly.
- It was analyzed that the temperature of the internal structure increased locally due to the hot spot. Compared to the 500-mm distance, the structure was evaluated to be 50°C–150°C lower than the hot spot temperature.
- As a result of evaluating the structural stability of the wall and internal structure of the reactor reflecting CFD, there was no indication that the structural stability was unsatisfactory, even if the design temperature was exceeded locally.
- Two types of corrosion must be considered: HTS and PASCC. In this case, corrosion by HTS was observed on the mesh screen and thermowell pipe. For HTS, the exposure temperature is important, and the authors suggested a short-term allowable excursion temperature of 650°C. No PASCC was found on the remaining internal parts by field metallography because the temperature and duration were not enough to cause sensitization.

This study is the result of reviewing the hot spot case of the RDS reactor. It is difficult to apply these results to all hot spots; however, when similar hot spots occur, it is believed that reasonable decisions can be made by referring to them. HP

SANG-MO LEE has more than 26 yr of experience as a Fixed-Equipment Engineer at SK Energy. His main tasks include root cause analysis (RCA), troubleshooting, fitness-for-service (FFS) evaluation, maintenance procedures and technical support for the refining and petrochemical business. He earned a BS degree in mechanical engineering, and is qualified as a professional engineer for welding and metallurgy by the South Korean government.

SUN HYUK BAE is a Chief Researcher for SK Innovation. His background is in transport phenomena and reaction engineering. He has designed over 30 commercial and pilot reactors. Prior to joining SK Innovation, Dr. Bae was a senior researcher at LG Chemical. After joining SK Innovation, he was the leader of the computational engineering group from 2009–2016. Dr. Bae earned a BS degree in chemical engineering, along with his PhD, from the Korea Advanced Institute of Science and Technology (KAIST).

DONG-SIK LEE is a Senior Engineer and a Non-Destructive Examination (NDE) Specialist at SK Energy. He has more than 21 yr of experience in the inspection department, and supports the technologies of NDE, corrosion control and failure analysis in refineries, especially hydroprocessing and residual fluid catalytic cracking units. He earned a BS degree in mechanical engineering from Yonsei University in South Korea.

A. GUPTA and M. AL-MUWAIL, Kuwait Oil Co., Kuwait;
and R. DONNELLY and J. NICHOLAS, The Welding Institute, Cambridge, UK

An investigation into pressure vessel fatigue cracking caused by a tack weld

Pressure vessels and piping constitute the maximum percentage of static equipment in any oil and gas facility. Separators, drums, desalters, columns, reactors and heat exchangers are only a few examples of the numerous types of pressure vessels used in the hydrocarbon industry. The design of welds is critical to any pressure vessel fabrication process. As part of weld joint fit-up and proper alignment prior to welding, tack welding is done between the pressure vessel components (such as the shell, dish ends and nozzles) prior to the initiation of the actual welding process. This is a common practice during pressure vessel fabrication and repair. During the fabrication process and any repair during service, the significance of tack welds to join metallic parts cannot be ignored. However, from a practical perspective, tack welds are not always explicitly addressed in fabrication drawings or quality control plans. In this article, the authors present the detrimental effect of a tack weld in a pressure vessel fabrication, leading to fatigue cracking and the eventual breach of containment.

Background. A pressure vessel leak happened in an oil and gas surface production facility. The subject vessel (a degassing boot) was constructed as per the ASME Sec VIII Div. 1 code. The vessel separates out/disengages the gases from liquid streams before they enter the downstream storage tank. Separation of gases in the degassing boot (**FIG. 1**) helps to maintain a stable interface level in the tank, along with proper separation of produced water from crude in the tank.

The operating pressure was 0.361 psig (maximum), with an operating temperature of 15.5°C–60°C. The process fluid was hydrocarbon gas, with crude oil and water. During operation, crude oil seepage was observed at the reinforcement pad of the 8-in. NB riser nozzle.

The subject vessel was isolated from service to assess the cause of the leak and to carry out necessary repair work. During internal inspection, a crack—approximately 70 mm in length—was observed on the shell (10-mm-thick ASME SA516 Grade 60 carbon steel) at a peripheral distance of approximately 16 mm from the N1B nozzle internal bore. A region measuring 1.4 m x 1 m was removed from the shell to facilitate a failure investigation of the cracked region.

Objectives of the failure investigation. The following were the objectives of the failure investigation:

- Identify the mode or mechanism of cracking
- Identify the possible causes of cracking, and comment on their likelihood
- Provide short-term and long-term actions for an immediate remedial response and for future avoidance of reoccurrence, as appropriate.

Approach. To achieve these objectives, the following work items were carried out:

1. Upon receipt of the sample, the appearance of the crack and the surrounding area were subjected to visual examination. Photographs were taken to record the observations.
2. The extent of cracking was evaluated using phased array ultrasonic examination.
3. The cracked region was cut down and chilled in liquid nitrogen.

FIG. 1. Typical degassing boot.

Approximately half of the crack was broken open to reveal the crack surfaces, and these were examined visually before and after appropriate cleaning. The cleaned fracture surface was examined using scanning electron microscopy. Photographs were taken to record the observations.

4. A metallographic section through the nozzle, shell and reinforcement pad was taken to characterize the crack's location and morphology. This section was mounted in Bakelite and polished to a 0.25-μm diamond finish, using standard metallographic preparation techniques. The section was then etched in 2% nitric acid in alcohol (nital) to reveal the microstructure and then examined using high-power light microscopy. Photographs were taken to record the observations.
5. A Vickers hardness survey was carried out on Weld 1, Weld 2, the sampling weld regions, the heat-affected zones (HAZs) and other regions of interest by using a 5-kg load. A microhardness survey was

undertaken of the region adjacent to the gouge, using a load of 100 g.

6. Duplicate tensile tests were carried out on the shell's material away from the crack to ensure conformance with the requirements of the ASME SA516 Grade 60 specification.
7. Chemical analysis of the shell, nozzle, reinforcement pad materials and both weld metals were carried out, using direct-spark optical emissions spectrometry, and the results were compared to the requirements of the ASTM 516-17 Grade 60 specification.

FIG. 2. Photographs of the nozzle and location of the crack.

FIG. 3. Photographs of part of the fracture faces: (A) nozzle side of the fracture, and (B) the fracture face from the opposite side of the nozzle, showing a macroscopically flat surface and the presence of ratchet marks. Note: This is in mm scale.

Results. An initial examination revealed two crack-like features on the inner surface of the shell. The larger of these was around 70 mm. Ultrasonic testing inspection revealed that the two features were part of a larger crack around 180 mm in length (**FIG. 2**). At this stage in the investigation, the outer surface of the shell could not be inspected due to the presence of the reinforcement pad.

Approximately half of the crack was examined after breaking it open. This revealed that the fracture face had multiple flat, smooth regions, which are consistent with fatigue cracking. **FIG. 3** shows both halves of the part of the fracture (before cleaning) that was broken open.

Scanning electron microscopy (SEM) confirmed the failure mode to be multi-initiation fatigue from the outer surface of the shell. The fracture surface was characteristically smooth and flat (**FIG. 4**).

A photo macrograph of the metallographic section is shown in **FIG. 5.** The crack had initiated from the root of Weld 1. An examination of this section revealed that the reinforcement pad had been attached to the shell plate and then the main weld had been performed, both from the inside of the shell. A 2-mm gap existed between the reinforcement pad and the shell parent materials. The crack was initiated at the corner where the shell parent material side of this initial weld bead met at a stress concentrating feature.

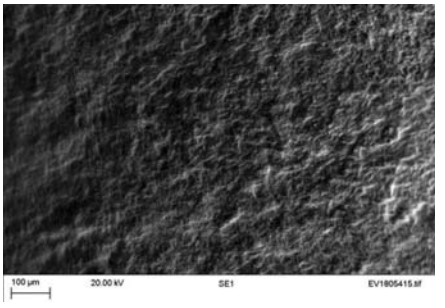

FIG. 4. SEM of the fracture surface, showing the absence of cleavage fracture or microvoid coalescence. The flat featureless surface is consistent with fatigue. Magnification is indicated by the micron marker.

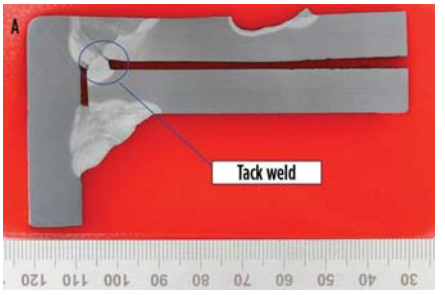

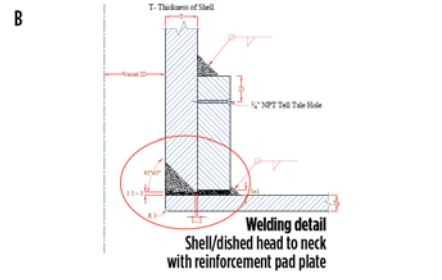

FIG. 5. (A) Metallographic section through the reassembled fracture. The nozzle parent metal is on the left, the upper plate is the shell, and the lower plate is the reinforcement pad; (B) as-built drawing schematic representing the joint details for comparison with the metallographic section.

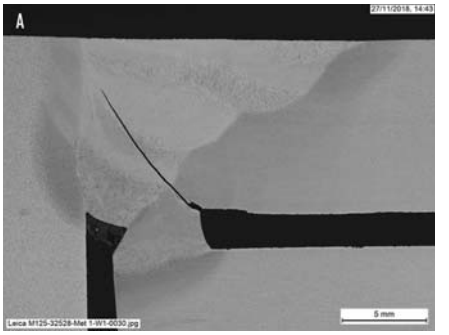

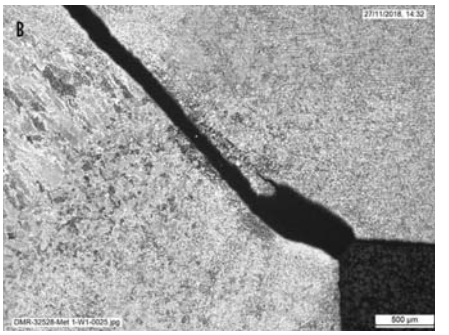

FIG. 6. (A) Microscopic image of Weld 1 (between the shell and the nozzle), showing the connection to the reinforcing plate and the location of the crack; (B) detail of the crack mouth region with magnification indicated by the micron marker.

The crack then propagated through the weld metal of Weld 1 toward the inner surface of the shell.

In FIG. 5, a second weld can be seen between the reinforcement pad and the nozzle. There is also a gouge in the shell. Material has been removed from this location and a small quantity deposited adjacent to the gouge. Both this gouge and another parallel gouge can be seen in FIG. 2 running across the entire width of the material.

A microscopical examination of this section revealed that all three parent materials were ferrite-pearlite microstructure. Weld 1 had been carried out from the inside of the shell (FIG. 6A). It appears that an initial tack weld was performed to attach the reinforcement pad, and that the cap was ground flush to the inside of the shell. This weld has HAZ regions on all three parent materials. The crack has propagated through the main part of the weld. FIG. 6B shows detail of the crack and microstructure at the mouth of the crack.

Weld 2 is between the nozzle and the reinforcement pad (FIG. 7A). There is a feature that is likely to be lack of fusion associated with the root pass on the reinforcement pad side of the weld (FIG. 7B).

Hardness results for Weld 1 found a peak hardness of 258 HV5, which was associated with the HAZ of the tack weld on the reinforcement pad parent material. Peak hardness in the HAZ associated with the nozzle and shell parent materials were 179 and 206 HV5, respectively. The peak weld metal hardness measured 202 HV5 in the tack weld, 207 HV5 in the subsequent root pass, and 194 HV5 in the cap. The hardness results for Weld 1 are detailed in TABLE 1.

The peak hardness associated with Weld 2 was 280 HV5 in the HAZ adjacent to the cap in the reinforcement pad parent material. The HAZ associated with the root pass of this weld had a peak hardness of 232 HV5 in the reinforcement pad parent material. The HAZ associated with the nozzle parent material had a lower peak hardness of 203 HV5. The peak hardness measured in the weld metal was 225 HV5 in the cap and 202 HV5 near to the root. The hardness results for Weld 2 are detailed in TABLE 2.

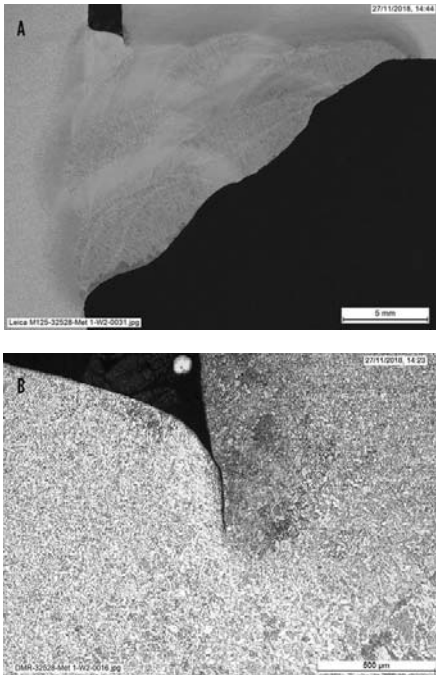

FIG. 7. (A) Overview of Weld 2, which was located between the nozzle and the reinforcement pad; and (B) detail of the lack of fusion at the reinforcement pad side of the weld.

Tensile test results are provided in TABLE 3. These conform to the ASTM 516M-17 Grade 60 specification. The chemical composition of all three parent materials and both welds are given in TABLE 4. This is compared to the ASTM 516M-17 Grade 60 specification. Both the shell and reinforcement pad materials fall within this specification. The nozzle material falls within the limits of the ASTM A106-18 Grade B specification.

Discussion. This component has suffered cracking through the thickness of the shell due to a fatigue mechanism. This cracking was initiated from the root of the weld in multiple locations. Nearly all fatigue failures are multi-initiation failures. In this case, initiation has occurred at several locations along the length of the weld due to the poor root profile. These have then coalesced to form a single crack front. This is the usual progression for fatigue failures. Evidence of the multiple initiations is shown by ratchet marks on the fracture surface. The flat, featureless fracture surface is typical of high-cycle fatigue. This fracture face is not typical of low-cycle fatigue failures, as there would need to be more evidence of plastic deformation.

Considering the geometry of the weld, it would be classified as a butt weld on a backing bar. The full-penetration weld between the shell and the nozzle is functioning as the butt weld, and, since

TABLE 1. Vickers hardness data for Weld 1 (taken as per BS EN ISO 6507-1:2005)

Indent no.	Ocular 1	Ocular 2	HV	Comments Cap	Indent no.	Ocular 1	Ocular 2	HV	Comments Root	Location of indentations
1	233	237	168	Parent metal	18	245	241	157	Parent metal	
2	241	242	159	Parent metal	19	252	243	151	Parent metal	
3	245	244	155	Parent metal	20	240	235	164	Parent metal/HAZ	
4	243	242	158	Parent metal/HAZ	21	228	227	179	HAZ	
5	237	239	164	HAZ	22	220	221	191	Fusion boundary	
6	232	234	171	Fusion boundary	23	214	214	202	Weld metal	
7	219	229	185	Weld metal	24	212	211	207	Weld metal	
8	217	220	194	Weld metal	25	216	213	202	Weld metal	
9	223	225	185	Weld metal	26	187	192	258	Fusion boundary	
10	224	230	180	Weld metal	27	217	218	196	HAZ	
11	214	210	206	Fusion boundary/HAZ	28	241	241	160	Parent metal	
12	225	225	183	HAZ	29	234	238	166	Parent metal	
13	227	228	179	HAZ	30	234	232	171	Parent metal	
14	234	238	166	HAZ/parent metal						
15	235	231	171	Parent metal						
16	228	228	178	Parent metal						
17	234	233	170	Parent metal						

TABLE 2. Vickers hardness data for Weld 2 (taken as per BS EN ISO 6507-1:2005)

Indent no.	Ocular 1	Ocular 2	HV	Comments Cap	Indent no.	Ocular 1	Ocular 2	HV	Comments Root	Location of indentations
1	234	240	165	Parent metal	13	235	237	166	Parent metal	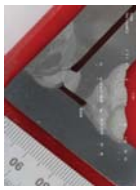
2	239	244	159	Parent metal	14	238	239	163	Parent metal	
3	233	239	166	Parent metal	15	218	223	191	HAZ	
4	209	211	210	HAZ	16	221	220	191	HAZ	
5	185	179	280	Fusion boundary	17	201	203	227	HAZ	
6	209	206	215	Weld metal	18	199	201	232	Fusion boundary	
7	220	220	190	Weld metal	19	217	221	193	Weld metal	
8	203	203	225	Weld metal	20	223	218	191	Weld metal	
9	209	218	203	Fusion boundary	21	208	221	202	Weld metal	
10	235	242	163	HAZ/parent metal	22	221	220	191	Fusion boundary	
11	250	243	153	Parent metal	23	229	234	173	HAZ	
12	258	253	142	Parent metal	24	235	237	166	HAZ/parent metal	
					25	240	237	163	Parent metal	
					26	241	245	157	Parent metal	

the tack weld—which joins the weld root to the reinforcement pad—is present, the pad is functioning as the backing bar. The root of the weld comprises this tack weld. This section (FIG. 5) shows that there is a sharp corner between the reinforcement pad and the tack weld.

When a backing bar is used to assist with the manufacture of a single-sided butt weld, the resulting weld root often has a poor profile and a relatively poor fatigue performance. This weld detail has a Class F fatigue performance. The fillet weld around the edge of the reinforcement pad (joining it to the shell) would be expected to also have Class F fatigue performance.

In this case, cracking has occurred in the expected location for a butt weld on a backing bar, which is at the stress concentration associated with this sharp corner at the weld root. A large gap exists between the reinforcement pad and the shell, at the interface with the nozzle. The tack weld (which functions as the root of the full-penetration butt weld) has extended a few millimeters beyond the shell to fuse to the reinforcement pad, producing a particularly unfavorable weld root profile. The applied stresses and actual fatigue life are not known, but a poor weld root profile results in a more severe stress concentration and, therefore, produces a lower fatigue life than would be expected in the absence of the stress-concentrating feature. This corroborates with the service condition of the degassing boot, which is susceptible to flow-induced vibration and fatigue.

Recommended practices for tack welds. API 577 (Recommended Practice—Welding Inspection and Metallurgy) defines a tack weld as "… a weld made to hold the parts of a weldment in proper alignment until the final welds are made." Clause 4.3.3.1 mentions quality control items to assess if "tack welds to be incorporated in the weld are of acceptable quality."

To improve the fatigue life of a joint with this fit-up, the welder should not tack the reinforcement pad to the shell before welding the shell to the nozzle. This will avoid fusing the root of the full-penetration butt weld to the reinforcement pad and will allow a more uniform root profile to be produced at the shell-to-nozzle weld. The welder should take care to ensure that the shell-to-nozzle weld is full penetration, but that the root bead does not protrude very far from the shell plate. This should allow the weld's Class F fatigue weld to be achieved.

An inlet riser deflector was previously welded to the inner side of the shell. After this failure had occurred, the deflector plate was removed to be reused during repair work. This deflector plate was removed by gouging, which explains the two parallel gouge marks. As this was removed after the failure, it has not had any effect on the failure.

Conclusion and recommendations. The following conclusions can be drawn from this investigation:

- The component has failed due to fatigue crack propagation through the full thickness of the shell.
- Cracking had initiated at a poor weld root profile, caused by the presence of the tack weld.

The investigation ultimately yielded these recommendations:

- It may not be possible to avoid tack welds during manufacturing or repair activities. To improve the fatigue life of this component, the reinforcement pad should not be tacked to the shell during the manufacture of the nozzle weld. This would allow a Class F fatigue weld to be achieved.
- Attention should be provided to the detrimental effects arising out of tack welds, particularly where fatigue loading is envisaged.
- Welders and inspectors must be more cautious and vigilant regarding tack welds, fit-ups and weld quality to improve the fatigue life of the components.
- Welds should be considered as a checkpoint in the inspection checklist during manufacturing/repair activities. HP

ACKNOWLEDGMENTS

The authors thankfully acknowledge the support of Kuwait Oil Co. and the management of The Welding Institute in the publication of this article.

TABLE 3. Summary of tensile properties

	Proof stress Rp 0.2%, MPa	Tensile strength, MPa
Shell material, Specimen 1	300	535
Shell material, Specimen 2	317	530
ASTM A516M-17 Grade 60	220	415–550

TABLE 4. Summary of chemical compositions compared to ASTM A516M-17 Grade 60 and ASTM A106-18 Grade B specifications

	Element, wt%																
Material	**C**	**Mn**	**P**	**S**	**Si**	**Cr**	**Mo**	**Ni**	**Al**	**As**	**Co**	**Cu**	**Nb**	**Sn**	**Ti**	**V**	**Ca**
ASTM A516M-17 Grade 60*	0.21 (max.)	0.79–1.3	0.025 (max.)	0.025 (max.)	0.025 (min.)	–	–	–	–	–	–	–	–	–	–	–	–
ASTM A106-18 Grade B*	0.3 (max.)	0.29–1.06	0.035 (max.)	0.035 (max.)	0.1 (min.)	0.4 (max.)	0.15 (max.)	0.4 (max.)	–	–	–	0.4 (max.)	–	–	–	–	–
Shell parent	0.16	1.18	0.011	0.002	0.32	0.034	0.004	0.19	0.036	< 0.004	0.005	0.03	0.012	0.012	0.003	0.002	0.0017
Nozzle parent	0.18	0.66	0.012	0.011	0.18	0.058	0.008	0.036	0.022	< 0.004	0.005	0.067	< 0.002	0.006	0.001	0.004	0.0023
Reinforcement pad parent	0.16	1.16	0.017	0.003	0.35	0.036	0.006	0.19	0.044	< 0.004	0.006	0.025	0.015	0.017	0.006	0.003	0.0022
Weld 1	0.06	1.05	0.016	0.008	0.62	0.049	0.009	0.034	< 0.003	0.005	0.006	0.05	0.003	0.005	0.011	0.008	0.0003
Weld 2	0.07	1.16	0.017	0.009	0.68	0.038	0.006	0.04	0.004	< 0.004	0.006	0.039	0.003	0.005	0.015	0.011	0.0004

*Based on product analysis:
- Boron, lead and zirconium were below 0.005 wt% for the compositions measured.
- Tungstun was below 0.01 wt% for the composition measured.
- Cerium and antimony were below 0.002 wt% for the compositions measured.

M. RAMALINGAM and B. CHANDRAGUPTHAN,
Wood Plc., Chennai, India

Restaging/rerating of centrifugal compressors: Fundamentals, practices and challenges

The primary requirement for rerating or revamping an existing centrifugal compressor is to match the new operating requirements, such as increased or decreased flow, increased or decreased head, or a combination of both. Rerating or revamping is necessary where the existing compressor or compressor train is incapable of meeting the new operating requirement efficiently.

The rerating/restaging of operational existing compressors is an attractive cost-effective solution to address the latest development in process, changes in gas composition, debottlenecking of the existing plants and production maximization. Successful rerating/restaging plays a significant role in capital cost optimization processes.

Brief descriptions of fundamental concepts, practices, challenges and process checklists involved in the process of rerating/restaging of centrifugal compressors are discussed here.

Thermodynamic analysis. Centrifugal compressors are sensitive to operating conditions, molecular weight, gas properties, etc. However, the new operating environment may call for different operating scenarios, different molecular weights and different gas properties, as described in the subsequent paragraphs. During the restaging study, the adequacy of an existing compressor system will be analyzed and the requirements for modification or opportunities for improvement will be identified.

In centrifugal compressors, a decrease in inlet pressure will shift the operating envelope toward a lower flowrate, and the surge margin will decrease in proportion with the decrease in suction pressure. The compressibility factor (Z) also increases as the suction pressure/inlet pressure decreases, as the reduced pressure decreases while the reduced temperature remains constant. A decrease in inlet pressure decreases the gas density, which may result in higher power consumption.

Lower suction pressure results in a lower Reynolds number, influencing the boundary layer and friction loss. At a lower Reynolds number, friction loss will be higher, resulting in lower performance. As a result, a small fall in the inlet flowrate due to higher pressure at the inlet piping/nozzle often requires reduced rotational speed. On the other hand, higher suction pressure will result in higher discharge pressure at a given speed. As a result of a change in composition, the compressor operating envelope will change and consequently calls for revised operating procedures.

Temperature. An increase in the inlet/suction temperature will result in an increased discharge temperature; however, the influence of suction temperature is important when approaching the stonewall point (≥ mach flow). When the suction temperature is high at choke flow, the pressure ratio is reduced. The molar heat capacity has non-linear propositional relation with temperature, and an increase in temperature will result in a lower specific heat ratio. Additionally, higher inlet temperature will result in higher compressibility and lower gas density.

Lower suction pressure results in a lower Reynolds number because of lower density and influences on the induced boundary layer and frictional loss in the flowing path, leading to lower overall efficiency. When suction pressures increase, discharge pressure will increase and must ensure the sufficient flow/adjust speed to avoid surge. **TABLE 1** summarizes the impact of lower suction pressure and composition change.

The high specific heat ratio will result in higher discharge temperature and slightly lower discharge pressure at the same pressure ratio. On the other hand, lower specific ratio gases consume more specific power for a given pressure ratio.

Polytropic head will increase along with specific heat ratio. The head is increasing proportionally with the volume polytropic exponent, which in turn increases as the specific heat ratio goes up. However, the influence of the pressure ratio on the head value is less significant compared with volume polytropic exponent effect. The impact of gas heat ratio on the compressor head becomes more pronounced at high rotational speed. Operating range decreases as the specific heats ratio of the handled gas reduces.

Polytropic head is influenced by gas constant (R), which decreases as molecular weight increases. Compressor efficiency is also affected by gas constant. The high molecular weight value leads to a reduction in the gas constant, yielding a lower volume polytropic exponent, which is inversely related to the stage efficiency. The required polytropic head of low molecular weight tends to increase as the flowrate reduces. This indicates higher frictional losses associated with low gas density and viscosity.

The effect of gas molar mass on the compressor head causes the required number of mechanical stages to vary. The low molecular weight gas raises the required head to achieve the desired discharge pressure, leading to greater pressure coefficient on the impeller blades.

During rerating, the probability of formation of deposits/hydrates on the impeller and diffuser surface of the compressor

TABLE 1. Effects of composition/molecular weight changes

Causes	Primary impact	Effects on compressor
Change in composition	Higher average molecular weight	1. Polytropic head increases
		2. Pressure ratio increases
		3. Reduction in surge margin (stability region)
		4. Increased stage efficiency
	Lower average molecular weight	1. Pressure ratio decreases
		2. Lower efficiency
		3. Raises required head to meet the discharge pressure
Low suction pressure	1. Lower density	1. Lower discharge pressure
	2. Compressibility factor (Z) increases	2. Lower power requirement
	3. Lower N_{Re} and higher friction loss	3. Slightly higher polytropic head at same pressure ratio
		4. Lower rotational speed to avoid surge
		5. Lower overall efficiency
		6. Compression ratio through impeller is reduced

must be evaluated to find the suitable solvent injection requirements to avoid costly, time-consuming offline cleaning. Normally, the amount of solvent required should not be more than 3% of the total flowrate, and excessive flow can lead to serious erosion problems.

Settle-out pressure should be estimated for a rerated/restaged compressor system and the design adequacy of the existing system—including the knockout drum (KOD), inter-stage coolers, piping system, pressure relief valve, blowdown system and associated systems like the flare system—should be checked. Vibration analysis of the piping system is required to avoid acoustic-induced vibration/flow-induced vibration.

Requirements of alarm and trip schedule changes should be addressed based on the rerated or restaged compressor operating conditions and composition. The adequacy and requirements of the lube oil system, sealing system, bearing cooling water system, inter-stage cooler load and KOD must be checked. Brief adequacy check requirements are highlighted in TABLE 1.

While rerating with material of different gas composition, compatibility with respect to the new composition should be studied. As per API 617,[1] casing should be radially split when the partial pressure of hydrogen (H_2) at maximum allowable working pressure (MAWP) exceeds 200 psig. The presence of hydrogen sulfide (H_2S) in the gas composition should be considered to check the material compatibility, as per NACE MR 0103, NACE SP 0472 and NACE MR 0175. Gas service where the partial pressure of H_2 exceeds 100 psig or H_2 concentration exceeds 90 mol% at pressure should be considered as hydrogen service, and the compatibility should be checked during the rerating of compressors.

Compressor discharge temperature should be limited to 150°C (302°F) for natural gas services to avoid polymerization of hydrocarbons (fouling in the impeller), possible decomposition/cracking, auto-ignition hazards and seal/lube system limitations, even though the compressor components can withstand higher temperatures. Discharge temperature should be estimated based on the new composition and operating conditions.

The following rules of thumb have been deduced for ease of understanding and application:

- **Rule of thumb 1:** The head of a compressor varies as the square of the tip speed and flow handled by the compressor varies with tip speed and impeller diameter.
- **Rule of thumb 2:** A 1% increase in speed corresponds to a 3% increase in flowrate.
- **Rule of thumb 3:** A velocity of 38 m/sec–45 m/sec is generally considered as the upper limit for an inlet nozzle operating on air or gases with acoustic velocities like air.
- **Rule of thumb 4:** Higher molecular weight or lower temperature may reduce the allowable flow through the nozzle.
- **Rule of thumb 5:** Volumetric flow and molecular weight define the size of the compressor.
- **Rule of thumb 6:** In general, reduced gas molecular weight reduces pressure ratio surges at lower flowrates.
- **Rule of thumb 7:** Lower suction pressure affects the overall efficiency of the compressor.
- **Rule of thumb 8:** Excessive fluctuation in the molecular weight causes change in the incidence angle to the entry of the diffuser vane.

Compared to an isentropic process, the discharge temperature at the impeller exit is greater in the polytropic process. Therefore, the provided work by the impeller is higher in the case at constant discharge pressure. Even though the exit pressure of both polytropic and isentropic processes are equal, the discharge temperature and enthalpy differences are greater in the polytropic process. Discharge temperature in both isentropic and polytropic processes is a function of the pressure ratio, suction temperature and process exponent. The polytropic process is a function of inlet temperature, pressure ratio, compressibility factor and molecular weight.

Fouling/scaling. Fouling is normally accompanied by lower efficiency and decreased head due to changes in aerodynamic performance and flow restrictions. One of the early warning symptoms is a decrease in the amount of turndown to surge, i.e., an increase in the minimum flow. This is normally caused by deposits in the diffuser/guide vane, which offers flow restrictions that often result in surging. Online chemical wash-

TABLE 2. Dimensionless number analysis

Dimensional number	Significance	Normal range	Note
Heat coefficient or pressure coefficient	Relates head capabilities of a wheel with its peripheral velocity	0.48–0.54	It can be increased by increasing the number of blades in the impeller
Flow coefficient	Relates flow, tip speed and impeller diameter	0.01–0.1	Minimum discharge coefficient is 0.008–0.01 Peak efficiency occurs around mid-range 0.04–0.05
Mach number	Relates velocity of gas to velocity of sound at operating conditions	0.6–0.7 (at inlet)	Many compressors are operating above mach number, but the OEM shall be consulted. It should be limited to 0.9
Reynolds number	Relates inertial and viscous forces	Turbulent flow but less than mach velocity	Used to characterize the flow regime and is useful to find friction loss

ing/offline removal techniques improve the performance of the compressor. This requirement can be identified during the design stage and appropriate provisions can be provided. Water-based or petroleum-based solvents can be used to dissolve the contaminations.

- **Rule of thumb 9:** Generally, petroleum-based solvents are not useful to remove salty deposits.
- **Rule of thumb 10:** The amount of injected solvents should not be more than 3% of the total flowrate.

Capacity enhancement. Existing compressor system capacity can be enhanced by the following methods or a combination of the following methods:

- Utilization of design margin
- Addition of stages/impellers
- Optimizing impeller tip speeds
- Adding a parallel compressor train
- Optimizing the impeller design
- Suction boosters
- Eliminating the compressor losses.

DIMENSIONLESS PARAMETERS ANALYSIS AND FEASIBILITY ANALYSIS

The following dimensional number analysis (TABLE 2) will provide the scope for restaging/rewheeling of the compressor. A rationalized approach to describe the aerodynamic characteristics of compression machinery can be used for analysis.

Polytropic head per impeller. As per Simmon's method,[2] the maximum polytropic head can be approximately 30 kJ/kg (3,058 m) for an operating pressure < 100 bar, whereas the maximum head is limited to 20 kJ/kg (2,038 m) when the discharge pressure exceeds 100 bar (FIG. 1). In low-pressure services (> 100 bar), the maximum head values must be corrected based on molecular weight using the Brown method.

As per the Brown method, the value of 30 kJ/kg (3058 m) is to be used for molecular weight between 28 and 30. For molecular weight above this value, 0.3 kJ/kg (31 m) is to be subtracted from this head value for every unit increase in molecular weight, whereas 0.6 kJ/kg (61 m) head is to be added for every unit decrease in molecular weight. In general, a single-stage closed impeller compressor can raise the head up to 42 kJ/kg (4,281 m).

The change in molecular weight will have an impact on the number of stages (FIG. 2) of the compressor since a lower molecular weight calls for more required head to achieve the desired pressure, leading to greater pressure coefficient on the impeller.[3,4,5,6] It is always better to review the number of impellers/stages required with respect to all possible operating scenarios and molecular weight to avoid unnecessary cost and time delay at a project's later stages.

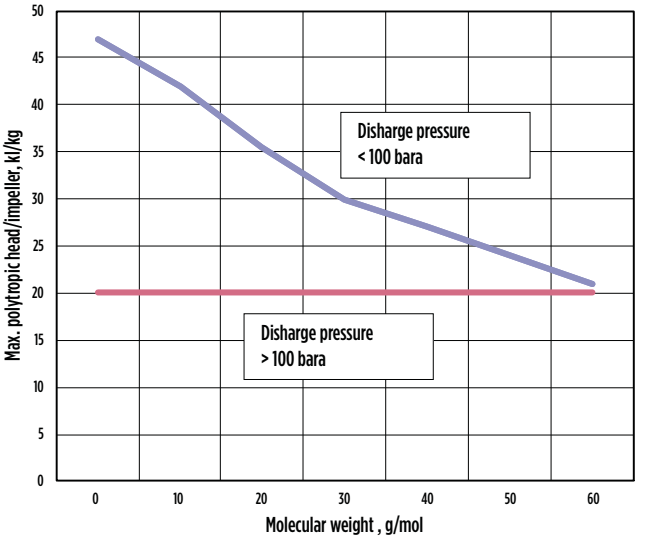

FIG. 1. The maximum polytropic head can be approximately 30 kJ/kg (3,058 m) for an operating pressure < 100 bar, whereas the maximum head is limited to 20 kJ/kg (2,038 m) when the discharge pressure exceeds 100 bar.

- **Rule of thumb 11:** Polytropic head per impeller and the number of stages of a compressor depend on the molecular weight of the gas being compressed.

Optimum impeller tip speed. Optimum tip speed depends mainly on the type of impeller, molecular weight, material strength and tip mach number. TABLE 3 can be used for preliminary design. However, for corrosive and low-temperature service [below –50°C (–58°F)], maximum tip speed is normally limited to 250 m/sec even though the molecular weight is < 35. Apart from these criteria, rotational stress, critical speed (mechanical resonances) and driver capabilities must be considered.[7,8,9]

During rerating, tip speed can reach up to 274 m/sec with careful engineering. Gas acoustic velocity is directly related to specific heat ratio and temperature and inversely proportional to molecular weight. Higher molecular weight gases are associated with lower acoustic velocities and lower allowable tip speed. It should be noted that the impeller material stress level is directly proportional to the square tip speed. Material strength often plays a critical role when low molecular weight gas is being handled with high head requirements. Cases exist

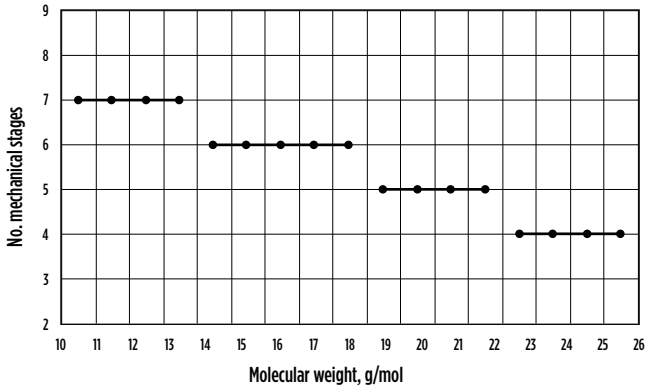

FIG. 2. The change in molecular weight will have an impact on the number of stages of the compressor since a lower molecular weight calls for more required head to achieve the desired pressure, leading to greater pressure coefficient on the impeller.

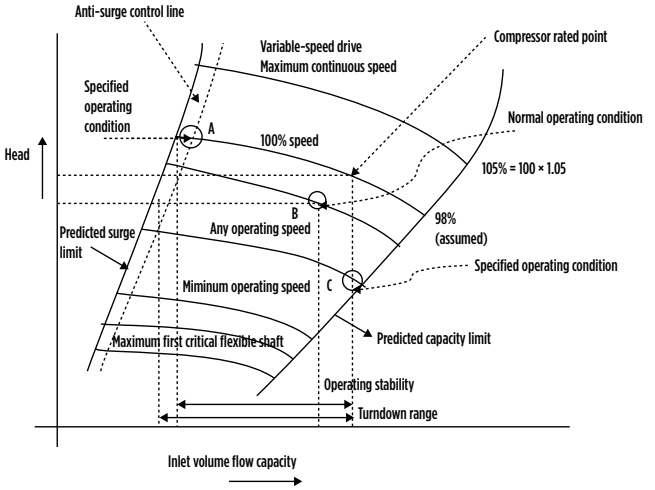

FIG. 3. The diagram presented in API 617 outlines the compressor stability requirements.

in which machines are operated at more than machine mach number without any issues—the important factor is the inlet relative mach number, which is proportional to the machine mach number and flow coefficient. Speed shall be optimized with respect to lower/upper critical speeds. The maximum speed is limited by aerodynamic and mechanical limitations.

- **Rule of thumb 12:** Impeller maximum speed is limited by mach number, material strength (yield stress at maximum continuous speed) and critical speed (resonance).
- **Rule of thumb 13:** Some original equipment manufacturers (OEMs) set the overload limit based on the relative Mach number of 0.96 or lower.

Utilization of design margin. Utilizing the existing overload limits is a common method of optimization. However, such limits are based on experience and function of machine mach number limitations, gas composition, number of stages, etc. It is well known that a compressor running at a high machine mach number or handling high molecular weight gases will have less overall flow range than a compressor that runs at a low machine mach number or handles low molecular weight gases. Therefore, the allowable overload margin may vary. For example, the high molecular weight compressor with an overload margin of 120% will have a 140% design margin when it handles low molecular weight.

TABLE 3. Tip speed limitation

Molecular weight	Average tip speed m/sec
< 35	310
< 45	250
< 65	200
< 120	150

Adding additional trains. The addition of parallel compressor trains is quite common in the oil and gas industry; however, deciding the parallel configuration option—a series-parallel (each casing will have independent driver) and tandem-parallel (single driver for multiple casings)—plays a key role in plant reliability, turnaround capabilities and efficiency.[10,11,12]

In general, a tandem-parallel arrangement requires more casing compared to a series-parallel arrangement for the given flowrate, resulting in higher increased fixed capital. More casing calls for more piping, sealing, lube system and accessories, which adds to the cost in a tandem-parallel arrangement. The loss of a compressor in a series-parallel arrangement is associated with variation in the inter-stage pressure, and the impact should be studied during the engineering stage. The loss of driver in the series-parallel will result in flow instabilities in the other stage. Loss of driver in the tandem-parallel will result in capacity reduction. The tandem-parallel represents a simple control system. Careful analysis of the configuration during the revamp/installation of additional trains should be exercised with respect to reliability, availability, safety, capital cost, space constraint and turndown flexibility.

Number of impellers. The number of impellers can be estimated by dividing the total polytropic head by the maximum head per impeller. The inlet flow coefficient can be improved by improving the eye diameter and impeller diameter ratio. Normally, it is preferred to have the same diameter for smooth flow. However, the maximum number of impellers in a single casing is normally limited to 10 (or 10 impeller stages) due to rotodynamic, aerodynamic, operational and design constraints.

Casing. Horizontally split casings are typically used for lower pressure applications (up to approximately 40 bar discharge pressure), while vertically split (barrel type) casings have successfully been used for discharge pressures up to 800 bar. During rerating/restaging, casing will not usually be modified.

Compressor stability. Both operational and aerodynamic stability should be considered during the rewheeling/rerating of compressors. **FIG. 3** presented in API 617 outlines compressor stability requirements.

Suction boosters. Gas density can be increased by many ways, including suction boosting and refrigeration. Simple suction boosting is considered as an additional stage.

TABLE 4. Process system

Process system	Minimum process adequacy/Limitations check requirements
KODs	• Separation adequacy, adequacy against revised design conditions/settle out conditions, revisit PRV systems, adequacy of inlet/outlet and orifice size of PSVs, revisit alarms and trip settings, revisit emergency depressurization system, re-run depressurization study (fire case and adiabatic case) and ensure the ESDV system is adequate and low temperature compatibility of the material, check MOC compatibility against new composition/condition
Nozzle	• Check nozzle pressure drop, velocity criteria, ρV^2 criteria, noise criteria
Piping system	• Pressure drop, velocity criteria, ρV^2 criteria, noise criteria, re-routed piping must be checked
	• Adequacy of existing drain header, vent header and other piping must be checked
Heat exchangers/coolers	• Check adequacy against revised duty
	• Check material compatibility
	• Check vibration/two-phase flow
	• Check design conditions for revised settle out/design conditions
	• Check adequacy of final protection elements
Alarms and trips	• Check requirement revising alarm settings
	• Check requirement revising trip settings
	• Margin between the operation, alarm and trip must revisit along with operation team to avoid frequent alarm, trip and maintain operator response time
Lube/seal systems	• Check compatibility against the new composition
	• Check against new operating and design conditions
	• Check the adequacy in terms of load, capacity, consumption, lube pump/driver capacity, relief system capacity
	• Check viability of other techno-economical viability available in the market
Material	• Compatibility with respect to new composition and operating and design condition must be checked
	• Hazardous area classification/temperature class of the equipment/electrical/instruments should be checked against new composition/operating and design condition
Driver capabilities	• Driver capabilities against required duty, speed
	• Changes in the utility/ambient conditions on turbine, motor to be reviewed
Operating envelope	• Check impact on the downstream equipment/piping/instrument for revised operating and design conditions
	• Check alarm, trip, PSV set pressures, ESDV set pressures against revamped conditions
	• Update the operating procedures
Utiilty system	• Check the additional utility required and availability
	• Perform adequacy check of existing utility lines/facilities
	• Perform adequacy check of vent/flare/relief headers
Other	• Space constraint for additional/rerouting of equipment/piping must be checked
	• Adequacy of DCS/ESD system for additional/modification of inputs/alarms/trips to be checked
	• Aging factor/structural strength of the supports must be considered for revamping the system
	• Existing piping/equipment adequacy for revamping condition shall be checked for adequacy with respect to available thickness (inspection report based)
	• Integrity assessment, design review and risk assessment to be carried out and recommendations of these reviews must be incorporated
	• Requirement of hot/cold anti-surge staged anti-surge/capacity control measures must be checked
	• Adequacy of existing anti-surge system must be checked

Process challenges and the ripple effect on a process system. KODs, piping/nozzles, relief systems, interstate/discharge coolers, drain and vent systems, emergency shutdown and depressurization systems, alarm and trips schedule, area classification and its impact, impact on material corrosion, lube and seal systems, utility requirements, rerouted piping system, operating envelop, driver capabilities, etc., should be revisited during the restaging/revamping of the compressor system, as tabulated in **TABLE 4.**

Impeller trimming. Impeller trimming is often used to improve energy efficiency to optimize the oversized compressor and alter the exit mach number of an impeller for different molecular weight.

In radial trimming, the outlet of the impeller will be trimmed in the radial direction by reducing the diameter. Normally, radial trimming is preferred where the reduction in pressure rise across the impeller is required. This is simple and does not require modification in shroud; however, it will change the fluid exit angle, which often calls for diffuser redesign. This option is not preferred for high-speed wheels since it will result in lower efficiency, whereas in low-specific speed wheels, it improves the specific speed value closer to optimum value, and radial trimming does not alter the flow coefficient at the inlet.

Axial trimming involves the reduction of impeller blade height at the outlet of the impeller without changes in the inducer. This is preferred for high-specific speed impellers. Reducing the outlet height will lower the specific speed of the impeller. Trimming to control the losses due to tip gap (clearance between impeller and shroud) should be checked and revisited. It should be noted that the tip gap for the given operating speed is generally based on material distortion, which is greatest at the outer diameter where centrifugal forces have the strongest effect. It is normally expected that axial trimming will result in an efficiency decrease and narrow choke margin but will have no major effect on the flow range of the compressor in the initial stages.

TABLE 5. Major factors considered during the decision-making process

Major process variables	Capital cost	Driver cost
		Equipment cost
		Installation cost
		Auxiliary equipment/piping/software cost
		Foundation cost
	Operating cost	Plant life
		Service cost
		Maintenance cost
		Utility/chemicals cost
		Efficiency
		Cost of spares
	Logistics	Suitability for future modification
		Field/location accessibility
		Operating experience
		Supply chain (single/multiple location)
		Installation equipment/utilities
		Temporary facility/resources
		Packing and delivery
	Economy and safety	Payback period
		Reliability, availability and maintainability (RAM)
		Shutdown requirements: production loss, impact on customers
		Opportunity cost
		Plant and personal safety
	Environmental	Noise
		Vibration
		Emissions, gas and vapor
		Liquid discharge
		Toxicity
		Hazardous waste management
		Drain and vent management
		Regulatory requirements
	Other	Reusability of existing spares/equipment
		Material compatibility
		Training requirement
		Operability
		Schedule

Control of losses. The following losses are normally encountered in the compressors, affecting performance. By controlling these losses, the compressor system can be optimized.

- Disk friction loss due to adhesive forces between rotating disk and fluid. The shear force acting between the impeller back face and the stationary surface is to be overcome by cost of power. Generally, it increases with rotational speed and impeller exit radius.
- Skin friction loss due to adhesive forces between the channel surfaces and the fluid. Channel surfaces includes the hub, blades and shroud.
- Incidence loss caused by the direction of the gas flow diffusing from blade angle. The deviation between the relative inlet angle of the gas and the actual blade angle causes the gas to change its direction, resulting in (energy loss) incidence loss. Incidence loss occurs when the relative fluid flow angle of fluid entering the impeller deviates from the actual blade inlet angle. This loss can be minimized by adjusting the blade angle closer to the relative flow angle, curving of the blade in the direction of the entering flow, and by improving the inducer (initial part of the impeller) design.
- Blade loading loss due to a pressure difference between blade to blade. Blade loading loss is due to the growth of the boundary layer in the impeller and is highly dependent on the diffusion of working fluid to the impeller. Blade loading loss is a function of the diffusion factor and the tangential impeller velocity. It can be optimized by increasing the rotational speed or by increasing the flowrate. Changing the relative flows (inlet and exit) and the tangential impeller exit speed will result in a change in blade loading loss.
- Recirculation loss caused by the back flow of fluid to the impeller, which requires additional power to overcome the backflow.
- Clearance loss due to significant flow leakage through the clearance between the impeller and casing due to pressure difference. This will form a small vortex on the suction side (low-pressure side) of the impeller vane outer tip. It affects both the suction side and discharge side.
- Leakage loss caused by the leakage of fluid through compressor seals. Seal loss decreases the energy available to convert into pressure head due to internal recirculation inside the compressor.
- Vaneless diffuser loss in the vaneless diffuser space as a result of friction and the absolute flow angle. Whether the compressor has a diffuser or not, a vaneless space is always directly flowing through the impeller where the

flow is diffused. In this space, primary and secondary flows mix, which results in friction loss and other losses referred to as vaneless diffuser loss.
- Vaned diffuser loss depends on diffuser shape, blade loading factors, incidence angle and surface friction of the vane.
- Mixing loss is also defined as slip of the flow field against the direction of rotation from pressure to suction side. After the flow has left the impeller, the primary and secondary flows mix. This is not ideal and energy loss and more recirculation will take place.
- Wake mixing loss due to mixing with jet flow right after impeller exit.
- Super critical mach number loss due to shock wave loss.
- Chocking loss due to the relative mach number at the throat.
- Incidence loss due to the difference between the inlet blade angle and flow angle.
- Entrance diffusion loss due to the diffusion inlet to throat.
- Mechanical losses include power dissipated through bearings, seals, shaft-driven lube pumps and gear boxes.

The role of OEMs. OEMs play a critical role in the restaging/rewheeling of compressors. Normally, all mechanical, rotary modifications, rewheeling, internals modification and restaging are carried out by OEMs due to their expertise, experience, facilities and tools. OEMs will conduct the thermodynamic, mechanical, rotary, aerodynamic and vibration studies, and will establish the safe operating envelop and provide performance guarantees. An engineering contractor or in-house engineering team can study equipment and processes upstream and downstream of the compressor unit.

Performance test. A centrifugal compressor's performance estimation can be done by three methods: the adiabatic method, N-method and Mollier method. In the adiabatic method, the compression process is completely reversible (isentropic), meaning that the input power is completely converted into pressure energy, which is not the practical case. The N-method is named based on a polytropic exponent (n) that is used to estimate discharge conditions and is independent of the state of compressed gas, and the polytropic head is the sum of each stage head, which are not true in adiabatic processes. Mollier diagrams are generally preferred for pure gases.

A performance test run of the rerated/restaged compressor can be carried out as prescribed in ASME PTC 10 and API 617. However, an agreement with the client and the OEM on PTC 10 test class and methodology is precedent. A complete unit test—including casing, gear, driver and auxiliary units—for evaluating performance is always recommended. Shop performance test limitations must be considered.

Decision-making process. A payback period of up to 5 yr can be considered as a potential opportunity for improvement. If the payback period is less than 2 yr, it requires urgent rerating/restaging. However, **TABLE 5** details some of the major factors considered during the decision-making process.

Takeaway. Gas molecular weight, gas property, suction operating conditions, upstream and downstream equipment limitations, and existing compressor data are playing a vital role in the analysis of rerating/restaging. Deep analysis on compressor stability is often required during the rerating study. However, rerating/restaging is an attractive and cost-effective solution to maximize the utilization of available resources (optimization) and address the changes in process and plant requirements. Rerating is often used to reduce the capital cost and improve the viability of a project.

Rerating or restaging often calls for multi-disciplinary input and knowledge and should, in general, be carried out in consultation with the OEM. The ripple effect on upstream and downstream equipment and units should be a part of any study. The outlined guidelines and limitations will help designers to carry out a feasibility study of rerating/restaging. HP

LITERATURE CITED

[1] API Standard 617, "Axial and centrifugal compressors and expander-compressors," 8th Ed., September 2014.
[2] Simmons, P., B. Nesbitt and D. Searle, *Guide to European compressors and their applications: The complete practical reference guide to compressors design, operation and applications,* Vol. 2, Professional Engineering Publishing, London, U.K., 2003.
[3] Khan, M. O., "Basic practices in compressors selection," International Compressor Engineering Conference, Purdue University, West Lafayette, Indiana, 1984.
[4] Ludtke, K., "Rerate of centrifugal process compressors—Wider impellers or higher speed or suction side boosting?" 26th Turbomachinery Symposium, College Station, Texas, 1997.
[5] Blahovec, J. F., *et al.,* "Guidelines for specifying and evaluating new and rerated multistage centrifugal compressors," 27th Turbomachinery Symposium, College Station, Texas, 1998.
[6] Ludtke, K., "Twenty years of experience with a modular design system for centrifugal process compressors," 21st Turbomachinery Symposium, College Station, Texas, 1992.
[7] Sorokes, J. M., E. A. Memmott and S. T. Kaulius, "Revamp/rerate design considerations," 42nd Turbomachinery & 29th Pump Symposium, Houston, Texas, 2013.
[8] Garcia, D., *et al.,* "Restage of centrifugal gas compressors for changing pipeline landscapes," IAGT 2015 Symposium, Banff, Alberta, Canada, 2015.
[9] Gutierrez Velasquez, E. I., "Determination of a suitable set of loss models for centrifugal compressor performance prediction," *Chinese Journal of Aeronautics,* October 2017.
[10] Li, P.-Y, C-W Gu and S. Yin, "A new optimization method for centrifugal compressors based on 1D calculations and analyses," *Energies,* Department of Thermal Engineering, Tsinghua University, Beijing, China, 2015.
[11] Albusaidi, W. and P. Pilidis, "An iterative method to drive the equivalent centrifugal compressor performance at various operating conditions: Part II Modelling of gas properties impact," *Energies,* School of Aerospace, Transport and Manufacturing, Cranfield University, Bedfordshire, U.K., 2015.
[12] Botha, B. W. and A. Moolman, "Determining the impact of the different losses on centrifugal compressor design," *R & D Journal,* 2005.

MURALITHARAN RAMALINGAM works as Group Manager, Process Engineering, at Wood Plc. India (previously Amec Foster Wheeler India Private Ltd.) and leads a team of more than 100 process engineers. He has more than 30 yr of post-graduate experience in oil and gas, FPSO, upstream and downstream projects execution, plant operation and commissioning. He has successfully handled numerous projects ranging from conceptual studies to commissioning, feasibility studies, optimization, troubleshooting and revamp/retrofitting engineering over the past two decades. He holds BS and MS degrees in chemical engineering from Anna University, India, has mentored numerous junior engineers and trainees, and has presented numerous design concepts and studies in in-house training. Mr. Ramalingam is an Associate of Chemical Engineers Association, India. He can be contacted at m.ramalingam@woodplc.com.

CHANDRAGUPTHAN BAHUBALI works as a Senior Principal Process Engineer at Wood Plc. India (previously Amec Foster Wheeler India Private Ltd.). He has more than 15 yr of post-graduate experience in oil and gas projects. He holds an MS degree in refining and petrochemical engineering from the University of Petroleum & Energy Studies and a BS degree in chemical engineering from Madras University, India. Mr. Bahubali has successfully completed many AIChE certificate courses in process safety as well as many international certification courses. He has also authored numerous papers on flow assurance, gas hydrates, fixed-bed reactors and economics. He can be contacted at c.bahubali@woodplc.com or b.chandragupthan@gmail.com.

M. CALVERT, Servomex, Crowborough, UK

How maintenance and reliability in gas analysis supports hydrocarbon processing installations

Industrial plants depend on accurate, reliable gas analysis for process control, efficiency, safety and emissions monitoring. When analytical systems perform poorly, it can increase costs and affect the quality of the final product. If the system fails, it can lead to very expensive downtime.

The COVID-19 pandemic has brought the need for preparation into sharp focus for industrial plants. Maintaining equipment reliability and minimizing downtime have taken on new levels of importance, and it has become essential to ensure the right spare parts, consumables and other equipment are available when needed.

Even the most reliable analyzers benefit from regular, planned maintenance. Getting the necessary level of service support can be the difference that keeps a plant operating reliably and profitably, even during pandemic restrictions.

Industrial plants that have addressed this by being in a service agreement will be far better prepared to cope with the stress of unplanned downtime, as well as an emergency response when a crisis (e.g., COVID-19) makes rapid reaction much more challenging. It also ensures they have better access to tailored support, including staff training and critical spares packs, giving them full peace of mind that they are prepared for any eventuality.

The benefits of good maintenance. The most basic level of maintenance is to wait until something goes wrong and then fix it. What this means for industrial plants is potentially lengthy downtime while an engineer identifies the problem, obtains the necessary part(s) and rectifies the issue.

Often, the expense involved—primarily from lost production—far exceeds the cost of even the most comprehensive service support packages. Regular inspection is a far more proactive approach to maintenance that significantly reduces the risk of unplanned downtime. It helps to identify any developing problems or unexpected damage and allows for the planned replacement of consumable parts.

For example, if a process must be stopped temporarily to replace an aging sensor cell, properly planned maintenance means this scheduled window can be used to address any other problems that may have been identified. Otherwise, left unattended, these issues could lead to an unexpected breakdown or affect the accuracy of the gas measurements.

The other side of this process is that regular maintenance means plant operators have to make 'just in case' replacements—inspections will reveal if a product is working as intended and does not need servicing.

Many modern plants operate with minimal staff, with some functions carried out entirely remotely. Quite commonly, the time and expertise to carry out even minor maintenance is not available. In the past, plant personnel have built up a good knowledge of the gas analyzers they use over time and learned to spot any problems. Changing work practices and the movement of experienced staff out of the industry means that much of this onsite expertise has been lost.

Forging an ongoing partnership with a service network ensures that processing plants have access to trained, expert engineers who have a deep understanding of the gas analysis systems and how they work within an application. It means that busy personnel do not have to be switched from other tasks to carry out inspections—the maintenance becomes part of an organized schedule that supports the continuous operation of the plant.

In the author's experience, visiting engineers are often seen as a key part of the plant's team and build a strong relationship with the customer. Operating out of regional service centers, the author's company's personnel have an excellent knowledge of the technologies involved, as well as the process and application, which helps them achieve better results. By attending the site regularly, they increase their understanding of each plant's individual needs, ensuring a tailored service beyond simple analyzer inspection and looking at entire process requirements.

How service supports industry. Reliability is achieved through good maintenance. However, this can mean different things to different operators, as plant requirements can vary greatly according to such factors as the applications involved and the gas analysis technology being used.

For this reason, the best approach is to offer a flexible, customized service that can adapt to meet the individual needs of each customer. This may range from the standard support and protection provided alongside every analyzer purchase, to a full partnership across the lifecycle of the gas analysis equipment.

Service support typically embraces several different products that can be combined into a custom plan to ensure the necessary assistance each plant requires. For example, regional service centers provide customers with rapid access to expertise, analyzer repairs, preventative maintenance and upgrades. They can also serve as hubs for locally based teams offering the onsite service support needs of industrial plants, ranging from emergency assistance to routine maintenance. This may also involve equipment health checks—where ex-

pert personnel attend to assess analyzer performance and detect anomalies before they develop into costly problems—and commissioning. Commissioning is the inspection of an installation—including the set-up and configuration of gas analyzers—by highly trained engineers to ensure peak system performance from the outset.

Even the most reliable analyzers benefit from regular, planned maintenance. Getting the necessary level of service support can be the difference that keeps a plant operating reliably and profitably, even during pandemic restrictions.

Service departments can get involved even before the commissioning stage by providing a factory acceptance test (FAT). This test is conducted in partnership between the customer and supplier to ensure the gas analysis system meets specifications prior to dispatch.

Service centers may also offer plant owners rapid access to high-quality spare parts and consumables for their gas analysis equipment. This service often extends to providing complete gas analyzers for hire, providing a temporary replacement that can be delivered quickly and with confidence that it will operate correctly.

Finally, many service networks are responsible for offering training to plant staff. This may be delivered onsite or at a training center and helps ensure that staff get the best performance from their gas analyzers.

Getting started with service support. The best way to begin a service partnership is to organize a health check for your gas analysis products. This validates the product performance and checks the state of the instrument. When engineers carry out these checks, they provide a written report on the work required, if any. Plant operators often want to go straight into a service contract. Even in these cases, a health check should be conducted to establish what sort of support is necessary. Once the health check has been completed, the level of support needed can be determined.

Commonly, plant operators are protective of their analyzers and dislike any interference with the product that might compromise the measurement. By partnering with the service division of an expert gas analysis supplier, they get total peace of mind that the engineer understands the product and knows how to get the best performance from it. Typically, onsite visits to inspect, service and maintain gas analysis equipment are scheduled for every 6 mos. The same regionally-based engineers are likely to attend each time, so trust is quickly established between them and the plant operator.

If it has been installed and configured correctly, a gas analysis system operates very reliably for many years, so this long-term relationship becomes very important. Additionally, the support required depends very much on the gas analysis equipment used. The key, of course, lies not merely in obtaining the diagnostic data from the analyzers, but also understanding it, which is where a partnership with an expert service network comes in. By monitoring the diagnostics, such as detector signals over the course of many years, any decline in performance can be identified early, allowing scheduled maintenance or replacement with minimal disruption to the process and no loss of measurement accuracy. In this way, the plant operator can be confident that the measurement they receive from their gas analysis system remains accurate, even late into the lifecycle of the analyzer.

The impact of COVID-19 on maintenance. The restrictions and safety concerns accompanying the global COVID-19 pandemic have had a significant impact on how service is carried out for industrial plants in all regions. Having an established service network that operates globally but at a local level, works very effectively. It means engineers are familiar with local restrictions and international travel is minimized.

Having built a good relationship with the plant personnel, engineers are able to more quickly adapt to any new procedures adopted to prevent the spread of the virus. They are also able to put their existing familiarity with the plant and its processes to good use through remote support.

Many gas analyzers have advanced digital communications options, which can be used to send diagnostic data to the engineer without them needing to attend the site. They also have auto-calibration and auto-validation capabilities that support ongoing reliability and make remote monitoring easier. Additionally, an existing service partnership can provide more secure spares support. The engineer can advise what spares need to be kept onsite and has rapid access to global stockpiles of these parts, along with an existing distribution network. Therefore, if disruption occurs as an essential part is needed, the problem is mitigated by the service arrangement.

While the pandemic is, hopefully, becoming less of an issue, it is comforting for plant operators to know that the procedures and technologies already in place will help service networks to provide continuous maintenance coverage even when the unexpected happens.

Takeaway. Ultimately, the goal of service is to support the customer throughout the entire lifecycle of the gas analysis product. It ensures that the plant starts up correctly, on time and on budget, and looks after the equipment until the time comes when it eventually needs replacing.

Good maintenance ensures maximum uptime and the best return on investment. It goes together with analyzer performance, delivering the measurements that plant operators need, whenever they need them. HP

MARK CALVERT is the Global Head of Service for Servomex. He is responsible for the coordination of Servomex's global service teams, ensuring that customer support and service delivery are provided quickly and effectively, while promoting best practices and maintaining the same high standards of service globally.

E. PARVIN and A. ROBINSON,
Parv Process Consulting and Engineering, Denver, Colorado

Isentropic effects: Application and simulation

A process safety risk in industry is having unknown problems that are not accounted for. Although the cause of many issues can be determined, others cannot be quantified without awareness. This article reviews an issue with high-velocity gases in piping systems, otherwise known as isentropic or kinetic effects. This issue can be difficult to detect and is often missed in most process engineering evaluations. It can result in temperature variances that metals, soft goods or internals in a system are not designed to tolerate. Most process simulations are not suited for identifying isentropic effects or require the implementation of a non-default setting. To avoid "traps" from simulations and an increased risk of damage to a system, identifying the characteristics of isentropic effects and how to physically address them is vital. The following are several case studies to demonstrate this effect.

Case study 1: Discovery. Hydrogen experiences a flat or reverse adiabatic effect with pressure drop. During a site visit, a 99.9% hydrogen stream was venting to flare. The temperature on the pipe indicated the occurrence of the reverse-adiabatic effect. Upon further examination, cooler than expected temperatures were detected at the valve outlet. A forward-looking infrared (FLIR) camera was utilized to measure the temperatures at and around the hydrogen valve. The images collected by the FLIR camera are shown in FIG. 1.

The FLIR images show that while the inlet and outlet temperatures from the hydrogen valve are relatively equal as expected, the temperature at the 1-in. valve connection was approximately 16°F lower. Since the fluid is hydrogen, the adiabatic or Joule-Thompson (JT) effect can be neglected. This temperature variance was not immediately explained by common knowledge or past simulation results.

It should also be noted that the temperature reversed over 3–5 pipe diameters out of the expander as the velocity decreased (FIG. 2). By investigating the principles that govern the kinetic effects, the cause of the velocity impacts on the temperature of the fluid can be determined. Simply put, when gas is flowing at a high velocity, it robs the temperature of the fluid to achieve that velocity. Through energy balances, the relationships between temperature, velocity and other variables demonstrate how isentropic effects impact a system.

Isentropic effect fluid correlations. During this evaluation, an isentropic model is assumed. No heat is added to the system; therefore, being adiabatic, and reversibility is achieved since viscosity effects, thermal conductivity and mass diffusion are absent. Application of the second law of thermodynamics captures any potential irreversibility in the process and accounts for the grade of conversion between work, heat and system energy change. Combining the second law and the first law of thermodynamics (Eq. 1) with no reactions while ignoring intermolecular forces, results in a thermally perfect gas.

$$S_2 - S_1 \square c_p \times \ln\left(\frac{T_2}{T_1}\right) - \frac{R}{MW} \times \ln\left(\frac{P_2}{P_1}\right) \quad (1)$$

where:

S_1 and S_2 = the initial and final entropy; [Btu/(lb × R)] (J / kg × K)

c_p = heat capacity; [Btu/(lb × R)] (J/(kg × K))

T_1 and T_2 = the initial and final temperatures; °R (K)

R = the universal gas constant; 1.985 (Btu/mol × R) [8.314 (J/(mol × K)]

P_1 and P_2 = the initial and final pressure; psia (Pa)

MW = molecular weight; lb/lbmol (kg/kmol)

To isolate and explain the temperature variance, a steady-state energy balance is created from inlet and outlet conditions to derive Eq. 2 for the isentropic assumptions (left hand side of Eq. 1 is set to zero) by algebraic rearrangement and with the utilization of the Mach number expression in Eq. 3. Via Eq. 4, the speed of sound for a given fluid can be calculated with the fluid properties.

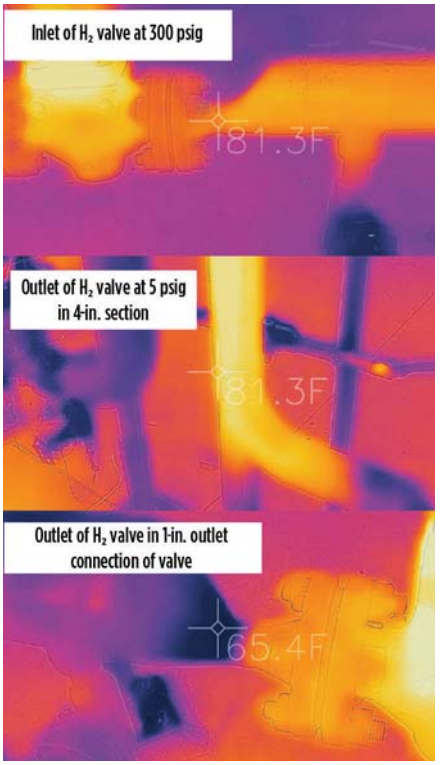

FIG. 1. FLIR camera imaging of inlet temperature, outlet temperature, and 1-in. valve connection temperature for pure hydrogen.

$$T = \frac{T_S}{\frac{k-1}{2} \times M^2 + 1} \quad (2)$$

$$M = V / c \quad (3)$$

$$c = \sqrt{\frac{kRT_S}{MW}} \quad (4)$$

where:

T_s and T = the stagnation temperature and the high-velocity temperature; °R (K)

V = velocity of the fluid; ft/sec (m/sec)

c = speed of sound of the fluid; ft/sec (m/sec)

M = Mach velocity of the fluid

k = ratio of specific heats (C_p/C_v at the T_s location)

R = the universal gas constant; 10.73 (ft³ × psia)/(lbmol × R) [8.314 (m³ × Pa)/(mol × K)]

By applying the proper unit conversion necessary for U.S. customary units, Eq. 4 can be simplified to Eq. 5.

$$c = \sqrt{\frac{kT_S R'}{MW}} \quad (5)$$

where:

R' = converted universal gas constant; 49,713 ft²/sec²

Since the Mach number is influenced by a direct relationship with the velocity of the fluid, an increase in velocity will result in a lower fluid temperature, which was observed through FLIR imaging of the hydrogen valve. Once the velocity of the fluid slows, the system's energy is maintained and is returned to the fluid temperature.

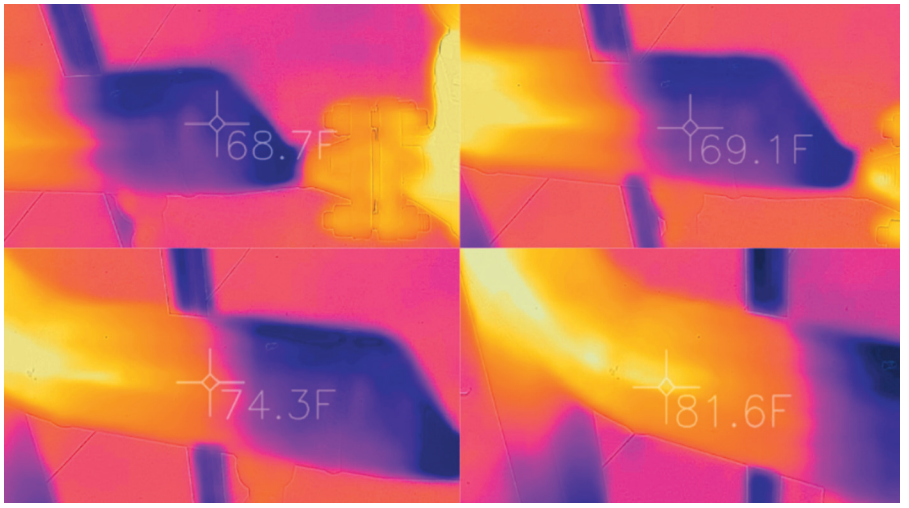

FIG. 2. Temperature increases approximately 3–5 pipe diameters from the reducer, as the velocity of the fluid decreases from top left to the bottom right.

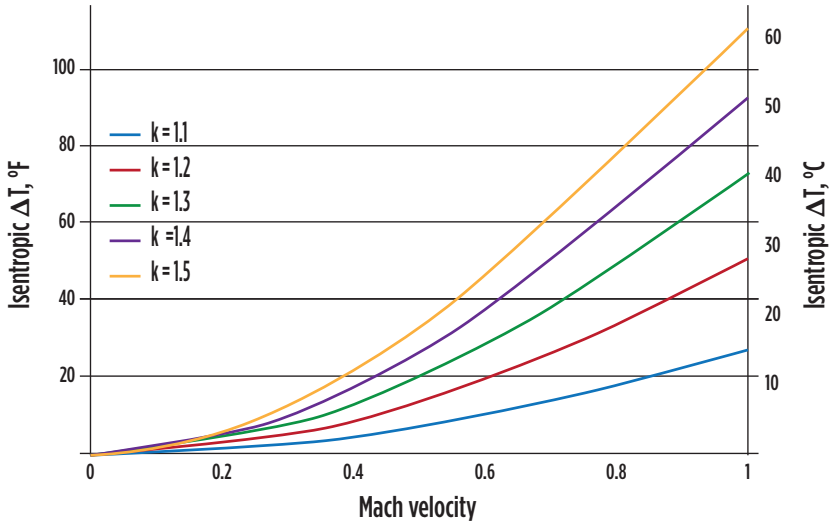

FIG. 3. Isentropic ΔT (°F or °C) vs. Mach velocity for k-values ranging from 1.1–1.5.

Similar equations (Eqs. 6 and 7) can be derived that pertain to the fluid's pressure and density within the system to account for all other variations from isentropic effects:

$$\frac{P_S}{P} = \left(\frac{T_S}{T}\right)^{\frac{k}{k-1}} = \left(\frac{k-1}{2} \times M^2 + 1\right)^{\frac{k}{k-1}} \quad (6)$$

$$\frac{\rho_S}{\rho} = \left(\frac{T_S}{T}\right)^{\frac{1}{k-1}} = \left(\frac{k-1}{2} \times M^2 + 1\right)^{\frac{1}{k-1}} \quad (7)$$

where:

P_s and P = the stagnation pressure and the current pressure; psia (Pa)

ρ_s and ρ = the stagnation fluid density and the current fluid density; lb/ft³ (kg/m³)

Hydraulic modeling can be used to determine the Mach number for the flow reading in addition to the relevant k values to find the pressures, densities and temperatures for a fluid.

Calculation vs. FLIR imaging. For the hydrogen valve, the FLIR camera recorded a temperature of 65.4°F. By using hydraulic modeling for the flow reading, the Mach number was found to be approximately 0.4, with a k-value of about 1.42. Eq. 2 is used with a stagnation temperature of 81.3°F to yield the following results:

$$T = \frac{81.3 + 458.67}{\frac{1.419 - 1}{2} \times 0.4^2 + 1} - 458.67$$

TABLE 1. K-values for fluids at 14.7 psia and 100°F or at fluid's dew point if above 100°F

Fluid	C_p/C_v
Hydrogen	1.413
Helium	1.666
Nitrogen	1.4
Carbon dioxide	1.279
Hydrogen sulfide	1.326
Methane	1.298
Ethane	1.186
Propane	1.127
i-Butane	1.097
n-Butane	1.097
i-Pentane	1.081
n-Pentane	1.081
Water	1.331
Air	1.409

Source: Proprietary software[a] simulation using Peng-Robinson equation of state.

$T \approx 63.8°F$.

The calculated temperature through Eq. 2 is slightly lower than the value found by the FLIR camera but is within reason due to uncertainties in the flow measured (orifice meter with known drift) and heat transfer through the wall of the pipe. The principles applicable to Eq. 2 accurately represent the steady-state system of interest.

When to consider isentropic effects? Isentropic effects are relevant for numerous systems in industry, including control valves, pressure safety valves (PSVs), flare headers, compressor station designs and others. It can also potentially explain failures in a system due to exceeding the minimal design metal temperature (MDMT) when conventional modeling does not predict colder conditions. On a practical level, it can also explain icing on the outside of piping when modeling predicts higher than freezing temperatures. The relationship of isentropic change in temperature with increased Mach velocity for different *k*-values can be found in **FIG. 3.**

The *k* or C_p/C_v values for a list of fluids can be found in **TABLE 1.** When a fluid is examined with various starting or stagnation temperatures, the resulting isentropic change in temperature varies. In **FIG. 4,** a fluid with a *k*-value of 1.3 is examined over a range of starting temperatures.

Why consider isentropic effects? Consideration of the design of valves (both the metal body and the internal soft goods), thermowells and pipe wall material are important considerations in industry. For example, soft goods within valves (e.g., PSVs and manual block valves downstream) may not be able to endure the low temperatures that occur from isentropic effects, as demonstrated in the next two cases.

Case 2: Retail city gas to flare. For one client, retail city gas is injected at 440 psig into a flare at below 5 psig to meet new regulatory Flare RSR (40CFR63.670) requirements. The gas can reach 20°F at 440 psig in the winter, and the valve adiabatic temperature loss is approximately 40°F. The outlet velocity can reach about 0.9 Mach. The system utilizes normal carbon steel piping and the outlet temperature is roughly –20°F by accounting for the JT effect and as per simulation results. At a velocity of 0.9 Mach, the isentropic change in temperature was found to be 50°F, resulting in a 90°F temperature drop from the starting temperature of 20°F for a minimum outlet temperature of –70°F at the high-velocity point. This requires ANSI B31.3 pipe stress test analysis for typical carbon steel (e.g., A106) or a different metallurgy selection (e.g., stainless steel). It was found that the A106 piping at this system's pressure was adequate, but the manual block valves' internal soft goods were only adequate for –50°F. A change in design was required for this system's valves. In addition, thermal shock for the sudden change in temperature was evaluated and found not to be an issue but should also be considered in designs.

Case 3: Operating valve. A different city gas supply was utilized at 450 psig at inlet temperatures of 20°F–40°F in the winter and 100°F in the summer. The system regulates pressure 40 psig–60 psig downstream through a 1-in. regulator. Operations measured 1 MMsft³d gas flow. Ice forms on the system's 1-in. outlet connection almost year-round, baffling operations and engineers at the site in the summertime where the simulation showed that the valve outlet temperature should be typically 40°F or higher. Isentropic effects and comparisons to simulation data are presented in **TABLE 2** at the valve outlet connection.

Due to low-temperature results with lower pressure or lower inlet valve temperature, a mechanical stress test study was required. The existing piping system downstream of the regulator was not designed for these conditions and the system was routinely below the MDMT of the metal, posing a risk to failure long-term. The regulator size was increased to 2-in. to eliminate any 1-in. section of piping and decrease the velocity, thereby increasing valve outlet temperature. The resulting operation showed no more icing in the summer and operating temperatures above the MDMT in the winter.

Case 4: PSVs/flare headers. Most PSVs generally have a Mach velocity across the throat of the PSV, and Mach velocity is common in tailpipes. Some engineers avoid Mach on headers for acoustic vibration reasons. Others try to avoid Mach by wrongly assuming it is a design or code compliance constraint. In addition, the temperature at the tees is seldom examined. In multiple cases, it

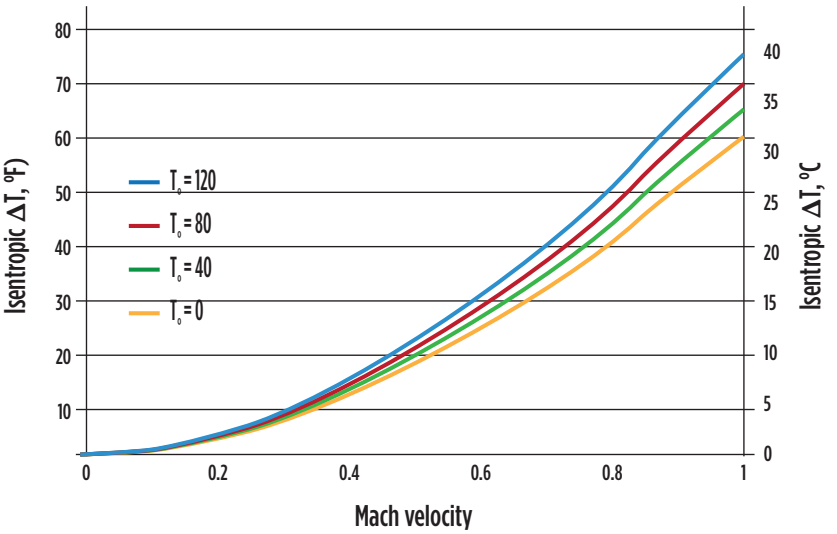

FIG. 4. Isentropic ΔT (°F or °C) vs. Mach velocity at *k*-value of 1.3 for various starting temperatures.

TABLE 2. Outlet temperature vs. isentropic effect temperature of the system with different operating pressures and starting temperatures

	Inlet temperature, °F	Simulation predicted outlet adiabatic temperature, °F	Pressure, psig	Mach velocity	Isentropic, ΔT, °F	Actual valve temperature, °F
Case 1	80	35	60	0.338	9	26
Case 2	20	–22	60	0.388	9	–31
Case 3	20	–25	40	0.44	14	–39

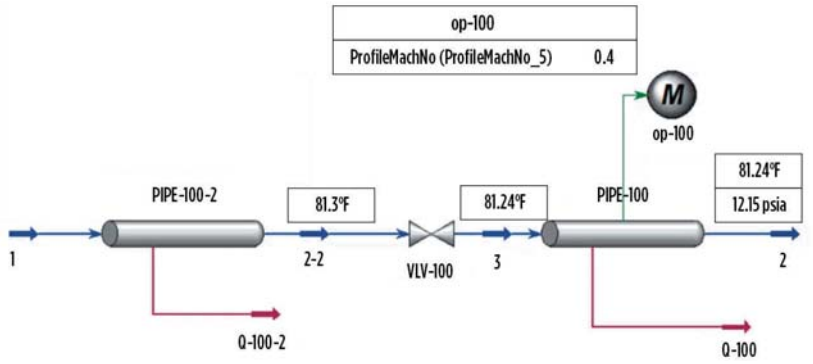

FIG. 5. Simulation—using proprietary software[a]—of the hydrogen valve example from FLIR camera imaging.

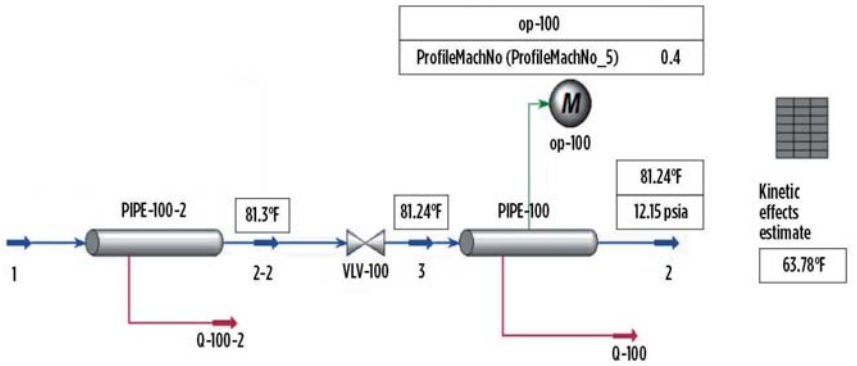

FIG. 6. Adjusted simulation—using proprietary software[a]—to account for isentropic effects for hydrogen valve.

has been identified that the tee at Mach velocity to a flare header can experience temperatures below the MDMT. At this point, a mechanical stress analysis should be performed to determine the risk. In most cases, the mechanical stress analysis passes. In some cases, it identifies the need to consider the risk of exceeding the stress analysis for a limited amount of time while the PSV is opened, requiring determination of whether the entire pipe metal wall can sustain these temperatures below MDMT. If the risk is high enough, then a change in flare header design is merited.

Modeling of isentropic effects. It is commonly assumed that process simulators are an accurate method of indicating the temperatures and behaviors of a system. However, steady-state simulators do not predict isentropic behavior. Proprietary software[b] can predict this behavior but only in Dynamics mode and requires user knowledge to implement the setting to report it. Any user can build it out themselves. For example, the results of a default simulation for the 99.9% hydrogen valve example is shown in FIG. 5.

The isentropic temperature for the hydrogen valve example should be approximately 65°F, unlike the simulation calculated value of 81°F. To measure the temperature accurately by using steady-state simulation, a spreadsheet or other embedded calculation should be created to report the change in temperature via the isentropic effect, along with the final temperature. An example of what this looks like for the hydrogen valve is displayed in FIG. 6, showing the 65°F, which aligns closely with the FLIR camera imaging.

Proprietary flare modeling software[c] can be used. However, the default settings do not predict the behavior of isentropic effects. The user must change the settings to "include kinetic effects." Other simulators have not been explored in detail.

Where to consider isentropic effects? Isentropic effects can create issues with many elements of a system, including areas that have not yet been studied. These include but are not limited to:

- Icing effect on the integrity of metal and soft goods in PSVs, flare headers and other constituents
- PSV tailpipe and flare header evaluations/metallurgy
- Pressure drop calculations that can be marginally impacted
- Blowdown valves (potential pipe embrittlement)
- Ejectors on top of vacuum towers or systems
- Potentially on heat exchanger performance impacting the heat release curves (though very rare due to velocities < 0.3 Mach for standard exchanger designs).

There is also an ongoing study regarding how hydrate formation may be impacted at higher velocities.

Takeaway. To ensure systems are running safely, isentropic effects must be considered where high-velocity gases occur or where lower than expected temperatures may impact design or operation. While steady-state process simulators do not easily simulate isentropic behavior, the implementation of spreadsheets or additional settings can aid in improved predictions. By being able to determine when and where isentropic effects are relevant and how to address them, any risk to a system's integrity, safety and longevity can be reduced. HP

ACKNOWLEDGEMENTS

The authors would like to send special thanks to Bart Carpenter, Parv Consulting, and Ben Day, Tailwater Technical.

NOTES

[a] Aspen HYSYS
[b] VMG Symmetry by Schlumberger
[c] Aspen Flare System Analyzer

ERIC PARVIN is the Founder and Principal Consultant of Parv Consulting in Denver, Colorado. He has extensive experience in upstream, midstream, refineries, rail car facilities and petrochemicals, with expertise in simulations, towers/trays, flares, debottleneckiing and PSM/PSV evaluations. With more than 24 yr experience, he also serves as adjunct professor at the Colorado School of Mines, is an editorial contributor of the "GPSA Engineering Data Book" and member of API 520 and 521. Mr. Parvin earned a BS degree in chemical engineering from Louisiana State University and is licensed in multiple states and Alberta, Canada.

ADRIANA ROBINSON is a Process Engineer at Parv Consulting. She has recently completed her BS degree in chemical engineering from the University of Colorado Boulder, with a minor in space and an emphasis in energy process engineering.

S. CHIDAMBARAM, Central Mechanical Research Institute, Durgapur, Indi

Thick-wall reactor shell repair procedure after damage detection at an interface in a hydrocracking unit

The vessel and reactor operating in a refinery may undergo various deteriorations due to their operating conditions.[1] Therefore, to protect the vessel and reactor from such deteriorations, the inner surface of the wall should be cladded by stabilized austenitic stainless-steel grades like SS321 and SS347. However, reactors and/or vessels are often composed of mostly chromium molybdenum (Cr-Mo) alloy steel grades, which is enough to maintain structural stability during operations at full capacity load. The combination of low-alloy steel with stabilized austenitic steel grades was obtained by dissimilar welding processes between clad plates or by a weld overlay.[2]

One such similar combination (i.e., a vessel or reactor wall made up of dissimilar welding) was affected by lamination defects after a few years of operation. The lamination-like defects were observed on a weld overlay of the vessel shell during non-destructive testing (NDT). The cause of this defect was identified as disbonding, which is defined as the failure of a coating to adhere to the substrate to which it was applied.[3] These disbonding defects were observed between stainless-steel (SS309) layers—i.e., the first layer of the weld overlay and the parent shell wall of the reactor vessel. It was found that, during initial fabrication, there were no defects observed at these interface junctions, and these defects were initiated during long-term exposure of service.

A schematic representation of the reactor shell configuration, heavy-wall thick alloy steel (parent metal) and weld overlay within a reactor shell in transverse direction is shown in FIG. 1. An arbitrary disbonding defect parallel to the inner wall surface is shown in FIG. 2. The flaw is represented in a general manner in the current study, but actual flaw dimensions (e.g., flaw shape, size and orientation) are dependent on many factors, such as microstructures at interfaces, fracture toughness at interfaces and material properties. These all play a vital role in structural integrity. A schematic of the vessel shell adjacent to the internal load bearing is shown in FIG. 3.

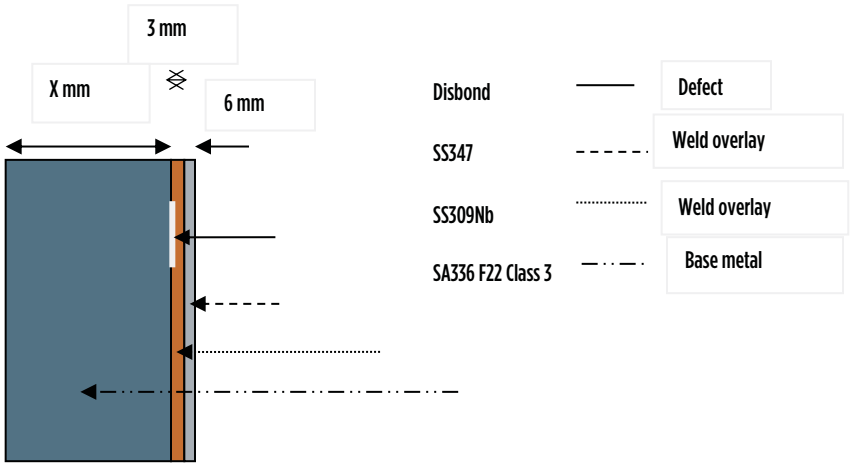

FIG. 1. Schematic of the reactor wall in transverse direction and corresponding material of construction.

Repair procedure. There are two scenarios to consider for repair procedures, and these are 1) if the defect has not damaged or affected the parent base metal shell,[4] or 2) if the defect has damaged the parent base metal (and if the defect damaging the vessel shell is assumed to be affected by hydrogen damage).[4]

Repair that has not affected the parent base metal. If the defect has not affected the parent base metal, then the following repair steps should be implemented:

- **In-situ metallography:** Prior to the repair process, an in-situ metallographic study is recommended on the weld overlay region to access the nature and type of material behavior induced in the material during long-term exposure of service. If any crack is discovered in the grinding process during

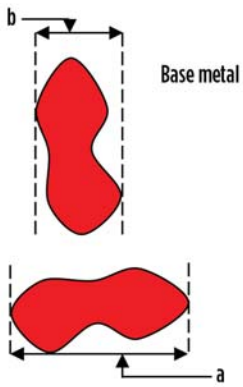

FIG. 2. Schematic view of the arbitrary disbonding defect in parallel to the base metal at the vessel's wall surface, with (a) and (b) representing arbitrary defect sizes.

repair activity, then that cracked portion and nearby area should be subjected to additional in-situ metallography studies for further assessment.

- **Prior cleaning:** Before starting the grinding process, the surface of the weld overlay metal should be cleaned thoroughly to remove scales, rust, carbon or any hydrocarbon deposits. After removing 3 mm from the weld overlay portion, the fresh surface should be cleaned thoroughly to remove any oxide scales. If any cracks are discovered, they should be verified by visual examination and dye penetrant testing.
- **Grinding:** The disbonding at an interface should be repaired as per the applicable construction code. Depending on the type of flaw and locations, as well as the type of weld overlay material and base metal, the flaw should be ground out. It is recommended not to use thermal gouging during the flaw removal process. The grinding should be initially at the weld overlay portion, and grinding wheels should be used as with the same stainless-steel grades of the weld overlay. Grinding should be optimized by controlling the speed of the grinding wheel to remove the weld overlay portion, and enough care should be taken to not overload the speed of the grinding wheel or the metal removal rate. The removal of metal in the weld overlay region should produce an even surface finish throughout the repair process, and the grinding load should be light enough to avoid any unwanted defects. Preheating before grinding is recommended to produce smooth surfaces and to promote easy removal of the weld overlay metal until the wheel reaches the base metal. However, the parent metal should not be ground out unless other directions were provided to do so after obtaining all assessment reports from metallurgical and NDTs.
- **Hydrogen bake-out:** After removing the weld overlay, a spot dehydrogenation heat treatment is recommended on the parent metal for at least 1 hr. The heating rate is 100°C/hr/in. and the soaking temperature should be 300°C/hr/in., followed by air cooling at 100°C/hr/in. If any diffusible hydrogen content on the parent metal is found, it should be removed prior to starting any welding process.
- **Design to meet ASME standards:** After removing the weld overlay portion inside the reactor, the repair should be carried out to rebuild the wall thickness as per the original specified drawings. The flawed portion removed from the weld overlay should be prepared for welding, and adequate access should be provided for the welding operation to avoid lack of penetration, slag entrapment and improper fusion. Prior to welding loosening or the detaching of stiffener rings, the installation of insulation support rings and a reinforcing saddle should be carried out.
- **Welding:** The welding should be produced via applicable construction codes as per welding procedure specifications. If any defects need to be removed on the parent metal, then the parent metal should be preheated to 315°C/hr/in. and, subsequently, the weld should be built up by E8018 B3L or E-80S B3L electrode or filler wire, depending on the type of welding process.
- **Heat treatment:** The parent base metal should be spot-heat treated, and the heat treatment should be completed on the base metal prior to starting the weld overlay. Based on various metallography and other test results, the spot-heat treatment should be recommended on the intended repair area. The heat treatment procedure is shown in TABLE 1.
- **Weld overlay restoration:** After completing the heat treatment on the parent metal, the weld should be overlaid on top of the parent metal as per the welding procedure specification.[1,2]

Repair that has affected the parent base metal. If the defect has affected the

The vessel and reactor operating in a refinery may undergo various deteriorations due to their operating conditions. Therefore, to protect the vessel and reactor from such deteriorations, the inner surface of the wall should be cladded by stabilized austenitic stainless-steel grades.

TABLE 1. Heat treatment procedure in repair work[5]

Parameters	Minimum criteria per ASME code
Heating rate	100°C/hr/in. thickness
Soaking time	1 hr/in. thickness
Soaking temperature	675°C (min.)–730°C (max.)
Cooling rate	100°C/hr/in. thickness
Heating methods	Electric resistance/ induction heating
Cooling methods	Air cooling

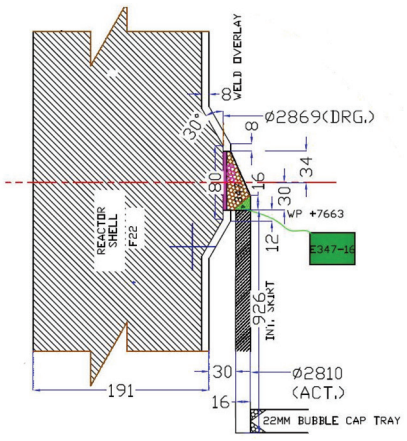

FIG. 3. Schematic of the vessel wall adjacent to the internal load-bearing section.

TABLE 2. Welding procedure specifications for the SMAW process

Welding procedure specification no.			
Welding process		SMAW	
Joint (QW-402)			
Joint design		Corrosion-resistant weld overlay	
Root spacing		Not applicable	
Backing		Yes	
Backing material		Base metal and weld metal	
Base metal (QW-403)			
P. no.	P5A	P. no.	–
Group no.	1	Group no.	–
Thickness range	8 mm	Thickness range	–
Base metal groove	Not applicable	Base metal groove	Not applicable
Filler metal (QW-404)			
Specification no. (SFA)		Barrier layer	Subsequent layer
AWS no. (class)		E-309 Nb	E-347
F-No.		5	5
A-No.		8	8
Size of filler metals		3.15, 4φ	3.15, 4φ
Fillet		Not applicable	Not applicable
Electrode flux (class)		Not applicable	Not applicable
Flux type		Not applicable	Not applicable
Flux trade name		Not applicable	Not applicable
Consumable insert		Not applicable	Not applicable
Other		Chemical composition should be specified	Chemical composition should be specified
Backing: Yes/No		Yes	Yes
Backing material (type)		Parent metal	Weld metal
Root spacing		Not applicable	Not applicable
Maximum pass thickness: 0.5 in. (13 mm) (Yes) (No)		No	No
Filler metal product form		Not applicable	Not applicable
Supplemental filler metal		Not applicable	Not applicable
Positions (QW-405)			
Position of groove		All	
Welding progression		Uphill	
Preheat (QW-406)			
		Barrier overlay	Weld overlay
Preheat temperature: Minimum		125°C	25°C
Interpass temperature: Maximum		175°C	175°C
Preheat maintenance		250°C	Not applicable
Other: Continuous or special heating, where applicable, should be recorded		Method of applying heat for preheat and interpass temperature: Electric coil heating, which should be checked by a Thermapen	
PWHT (QW-407)			
		Barrier overlay	Weld overlay
Temperature range		Not applicable	Not applicable
Time range		Not applicable	Not applicable
Soaking temperature		Not required	Not required
Heating rate		Not required	Not required
Cooling rate		Not required	Not required
Method of heating		Not required	Not required
Method of cooling		Not required	Not required

TABLE 2. Welding procedure specifications for the SMAW process (CONT.)

Gas (QW-408)			
	Gas	% composition (mixture)	Flowrate
Shielding	Not applicable	Not applicable	Not applicable
Trailing	Not applicable	Not applicable	Not applicable
Backing	Not applicable	Not applicable	Not applicable

Electrical characteristics (QW-409)								
		Filler metal		Current type	Ampere	Travel speed in	Volts in	
Weld passes	Process	Classification	Diameter, mm	and polarity	in range	range, mm/min	range, v	Energy input
Barrier overlay	SMAW	E-309 Nb	3.15	DCEP	80–100	107–140	22–26	1.6
Barrier overlay	SMAW	E-309 Nb	4	DCEP	100–130	127–165	22–26	1.6
Weld overlay	SMAW	E-347	3.15	DCEP	80–100	Not available	22–26	Not applicable
Weld overlay	SMAW	E-347	4	DCEP	100–130	Not available	22–26	Not applicable
Tungsten electrode size and type				Not applicable				

Welding technique (QW-410)	
String or weave bead	String or weave bead
Orifice, nozzle or gas cup size	Not applicable
Initial and interpass cleaning (brushing, grinding, etc.)	Stainless-steel wire brush or stainless-steel wheel grinding
Method of back-gouging	Not applicable
Oscillation	Not applicable
Contact tube to work distance	Not applicable
Multiple passes or single pass (per side)	Multiple passes per side
Multiple or single electrodes	E-309 Nb followed by E-347
Electrode spacing	Not applicable
Peening	No peening

parent base metal, then the following repair steps should be implemented:

- **Evaluating severity:** The weld overlay material from the inner diameter of the reactor within the disbonded region—comprising an SS347 corrosion-resistant layer and an SS309 barrier layer for the load-bearing section—should be chipped off. Both samples should be evaluated by digestion techniques to measure dissolved hydrogen. If hydrogen content is zero, then it is assumed that no hydrogen has diffused within the Cr-Mo steel parent metal. However, if enough hydrogen is observed, then the procedure detailed below should be used. If hydrogen attack is detected in the barrier layer and the corrosion-resistant layer, then the parent metal should also be subjected to hydrogen measurement techniques.

  Radially, the same area of the parent material should be evaluated. In addition to in-situ metallography on the parent metal, the digestion techniques should be engaged to measure the dissolved hydrogen content. If the dissolved hydrogen content is above the specified value (4 mL/100 g), then hydrogen bake-out should be carried out on the parent metal.[6] The dissolved hydrogen in the base metal should be removed completely as per design codes and conditions. In addition, before starting the repair process, the reactor shell should be evaluated for internal bulging on both the internal diameter and the external diameter.[7]
- **Prior preparation before shell replacement:** After excavating the damaged material, a new plate should be used to replace the damaged portion of the parent base metal. Parent metal replacement in pressure-retained areas is required for areas with hydrogen embrittlement cracking or any hydrogen damages (e.g., blisters). Before replacing the shell wall, it should be evaluated for distortion. The curvature of the shell wall should also be evaluated to match with an existing shell curvature. The defect section on the shell should be ground out by thermal gouging or grinding methods. The edges of the ground portion should be smooth, and all sharp edges and corners should also be ground out to produce a uniform surface finish. The same material of removed thickness and removed dimensions should be purchased and prepared. The construction material should be of the existing parent metal (SA336 F22CL3), and dimensions should be equal. The new plate thickness should be equal to the nominal thickness of the parent material.
- **Replacement of the shell's material.** The rectangular and square plates should be used, with their corners rounded to a radius of at least 150 mm. The new plate material should be manufactured and supplied in the conditions as the existing shell (i.e., a quenched

TABLE 3. Welding procedure specifications for the GTAW process

Welding procedure specification no.			
Welding process		GTAW	
Joint (QW-402)			
Joint design		Corrosion-resistant weld overlay	
Root spacing		Not applicable	
Backing		Yes	
Backing material		Base metal and weld metal	
Base metal (QW-403)			
P. no.	P5A	P. no.	–
Group no.	1	Group no.	–
Thickness range	8 mm	Thickness range	–
Base metal groove	Not applicable	Base metal groove	Not applicable
Filler metal (QW-404)			
Specification no. (SFA)		Barrier layer	Subsequent layer
AWS no. (Class)		E-309 Nb	E-347
F-no.		5	5
A-no.		8	8
Size of filler metals		3.15, 4φ	3.15, 4φ
Fillet		Not applicable	Not applicable
Electrode flux (class)		Not applicable	Not applicable
Flux type		Not applicable	Not applicable
Flux trade name		Not applicable	Not applicable
Consumable insert		Not applicable	Not applicable
Other		Chemical composition	Chemical composition
Backing: Yes/No		Yes	Yes
Backing material (type)		Parent metal	Weld metal
Root spacing		Not applicable	Not applicable
Maximum pass thickness: 0.5 in. (13 mm) (Yes) (No)		No	No
Filler metal product form		Not applicable	Not applicable
Supplemental filler metal		Not applicable	Not applicable
Positions (QW-405)			
Position of groove		All	
Welding progression		Uphill	
Preheat (QW-406)			
		Barrier overlay	Weld overlay
Preheat temperature: Minimum		125°C	25°C
Interpass temperature: Maximum		175°C	175°C
Preheat maintenance		250°C	Not applicable
Other: Continuous or special heating, where applicable, should be recorded		Method of applying heat for preheat and interpass temperature: Electric coil heating, which should be checked by a Thermapen	
PWHT (QW-407)			
		Barrier overlay	Weld overlay
Temperature range		Not required	Not required
Time range		Not required	Not required
Soaking temperature		Not required	Not required
Heating rate		Not required	Not required
Cooling rate		Not required	Not required
Method of heating		Not required	Not required
Method of cooling		Not required	Not required

TABLE 3. Welding procedure specifications for the GTAW process (CONT.)

Gas (QW-408)								
	Gas			% composition (mixture)		Flowrate		
Shielding	Not applicable			Not applicable		Not applicable		
Trailing	Not applicable			Not applicable		Not applicable		
Backing	Not applicable			Not applicable		Not applicable		
Electrical characteristics (QW-409)								
		Filler metal		Current type	Ampere	Travel speed in	Volts in	
Weld passes	Process	Classification	Diameter, mm	and polarity	in range	range, mm/min	range, v	Energy input
Barrier overlay	SMAW	E-309 Nb	3.15	DCEP	80–100	107–140	22–26	1.6
Barrier overlay	SMAW	E-309 Nb	4	DCEP	100–130	127–165	22–26	1.6
Weld overlay	SMAW	E-347	3.15	DCEP	80–100	Not available	22–26	Not applicable
Weld overlay	SMAW	E-347	4	DCEP	100–130	Not available	22–26	Not applicable
Tungsten electrode size and type				Not applicable				
Welding technique (QW-410)								
String or weave bead				String or weave bead				
Orifice, nozzle or gas cup size				Not applicable				
Initial and interpass cleaning (brushing, grinding, etc.)				Stainless-steel wire brush or stainless-steel wheel grinding				
Method of back-gouging				Not applicable				
Oscillation				Not applicable				
Contact tube to work distance				Not applicable				
Multiple passes or single pass (per side)				Multiple passes per side				
Multiple or single electrodes				E-309 Nb followed by E-347				
Electrode spacing				Not applicable				
Peening				No peening				

and tempered condition). No defect should be present on the new parent plate metal. The minimum diameter of the new plate should be at least 380 mm, with a maximum of 2,184 mm, depending on the location of the replacement and considering cutouts for attached piping or any other system (e.g., nozzles). This cutout in the reactor wall should be assessed and prepared as per original drawings. The edges of the new plate should be prepared by machining or grinding. The edges should be subjected to NDT, and all defects must be removed and repaired. Additionally, the edge alignment of the new plate should be within the applicable design code.

- **Welding:** The welding should be a full-penetration butt weld of the double-v groove joints. The filler metal and electrode chosen should be based on the type of welding process. Before the joint is welded, it should be preheated to a maximum of 315°C/hr/in. thickness. The weld joint should use an E8018 B3L electrode or E-80S B3L filler wire for single-metal arc welding (SMAW) or gas-tungsten arc welding (GTAW), respectively. Prior to welding, any grease, oil and/or scales must be cleaned off to avoid weld contamination. Welding procedure specifications for SMAW and GTAW are detailed in TABLE 2 and TABLE 3, respectively.
- **Quality before post-weld heat treatment (PWHT):** The final weld joint should be produced with minimum distortion, as well, to avoid a lack of fusion and penetration or any other defects. The final weld should have a smooth surface finish. The welding procedure qualification (WPQ) of the parent metal welding should be subjected to impact tests. An impact test is mandatory for WPQ to produce reliable weld metal. The new plate should be 100% radiographed. After completing the weld, the full penetration joint should be 100% radiographed to ensure sound weld quality.
- **PWHT of the replaced plate:** After ensuring quality, the thick-welded joint should undergo PWHT, which should be carried out only in weld joints. The PWHT chart should be equivalent to TABLE 1.[5]
- **Non-destructive evaluation after PWHT:** After completing the PWHT, the weld joints should be subjected to 100% radiography. This will ensure that no new defects were generated after the PWHT process. Before resuming its service, the entire reactor, or at least the repaired portion of the reactor, should be subjected to a leak test or hydrotest to confirm the quality of the repair. HP

REFERENCES

[1] ASME BPV Code Sec 9
[2] ASME BPV Code Sec 8
[3] ASME BPV Code Sec 5
[4] ASME PCC-2
[5] ASME BPV Code Sec 2 A
[6] ASME BPV Code Sec 2 C
[7] API RP 579, Fitness for Service

K. BRASHLER and **Y. ALSHAHRANI,**
Saudi Aramco, Dhahran, Saudi Arabia

Use infrared thermal imaging for pump system condition monitoring and early failure detection

Thermal imaging technology has evolved over the years, and investment costs have decreased significantly. Early deployment of thermal imaging technology in industrial applications was primarily geared towards electrical inspections. In recent years, these thermal imaging cameras have been successfully implemented for mechanical inspections, including rotating equipment. Typical applications for thermal imaging fall under three main categories outlined here:

- Electrical
- Process/mechanical equipment
- Building inspections.

Mechanical equipment inspections, specifically for centrifugal pumps, will be the main focus of this article. Typical thermal imaging applications for pumps will be presented, including a specific case example showing an interesting case study that resulted in the identification of severe throttling/leakage across a multistage pump center-stage bushing.

TYPICAL INSPECTION METHODOLOGIES

Three main methodologies should be considered when implementing thermal imaging inspections as outlined here. The method applied depends on the equipment being inspected and the type of data required:

- Baseline
- Comparative
- Thermal trending.

Baseline method. Baseline inspection establishes a reference point of equipment operating under normal conditions and in good working order. The field of view (FOV) of the thermal camera may dictate taking several images to capture all components. For pump applications, it is advisable to take an image of the entire pump, including the entire casing, bearing housing(s) and mechanical seal support systems, including flush lines, heat exchangers, cyclone separators, etc.

Comparative method. Comparative inspection compares similar components operating under similar conditions to analyze the condition of the equipment being tested. When this method is applied correctly, the comparative difference will be indicative of the condition. For pump applications, an example could be several pumps operating in parallel with individual minimum flow recycle valves. A comparative analysis of all recycle valves can identify a possible passing condition of one or more of the recycle valves.

Thermal trending method. This method is used to compare temperature distributions of the same compo-

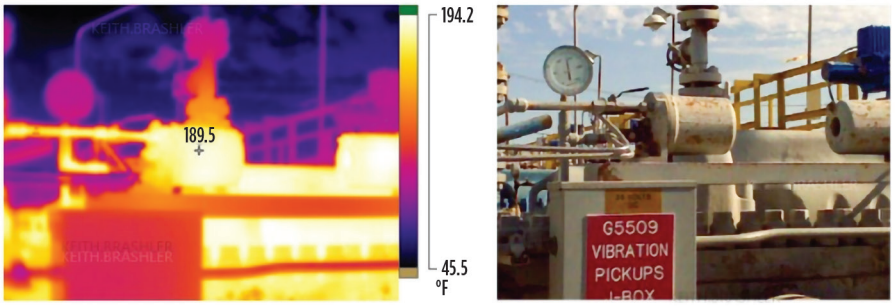

FIG. 1. An API Plan 21 seal support system with fouled exchanger.

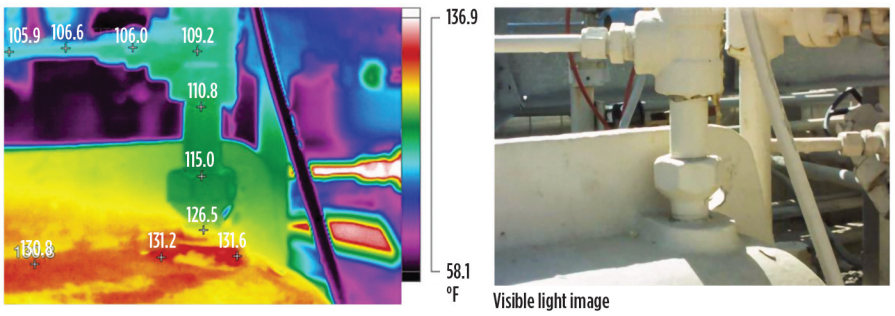

FIG. 2. A plugged API Plan 11 flush connection.

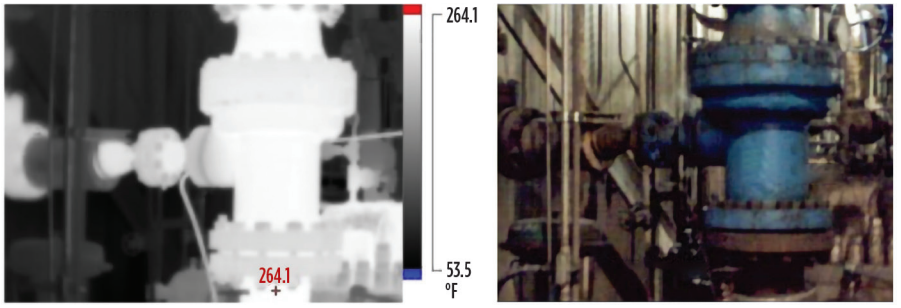

FIG. 3. Thermal signature of recycle valve passing condition.

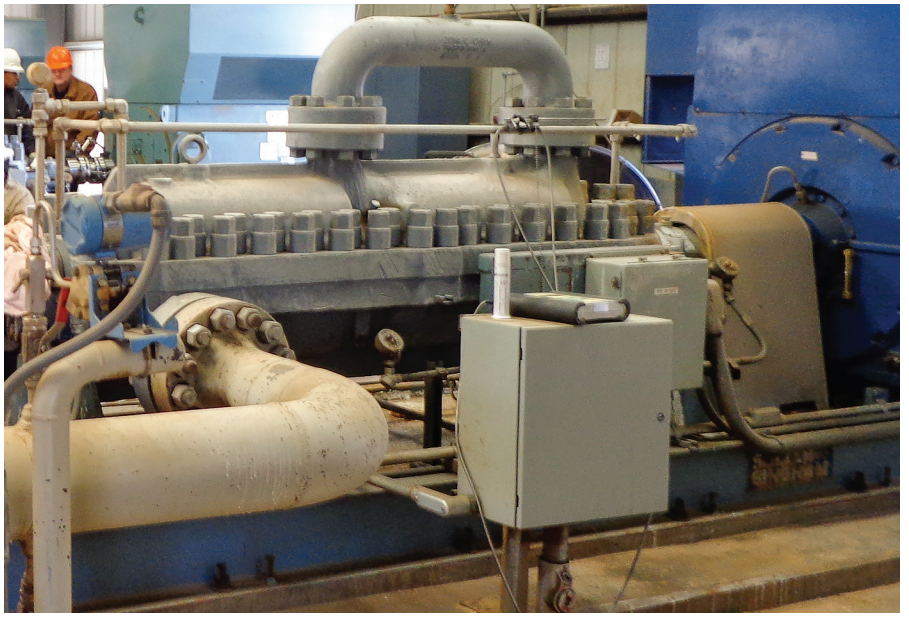

FIG. 4. Multi-stage, axially-split, opposed impeller pump.

nent over a period of time. This method works well for inspecting mechanical equipment when normal thermal signatures are complex. In these cases, thermal signatures indicate failure slowly, such as electrical components, valve leakage, seal flush line blockage or fouling, etc.

PUMPING SYSTEM PRACTICAL APPLICATIONS

The following outlines typical thermal imaging applications related to pumping systems:

- Pump and driver bearing housings to baseline, and detecting early bearing failure or oil and cooling system inadequacies
- Pump recycle and discharge check valve passing conditions
- Mechanical seal support systems, including flush lines, heat exchangers, cyclone separators and seal glands
- Pump casings to detect center-stage throttle bushing distress.

Mechanical seal support system. A thermal signature of a mechanical seal API Plan 21 seal flush system, including the heat exchangers, is shown in FIG. 1. Thermal imaging identified high skin temperatures on the heat exchanger shells resulting from fouling of the water side of the cooler.

FIG. 2 shows a thermal signature of an API Plan 11 seal flush line, which showed significant temperature difference (~26°F) between the take-off point and the downstream seal flush line. Periodic thermal scanning can quickly identify plugged seal flush lines, which can result in early mechanical seal failure.

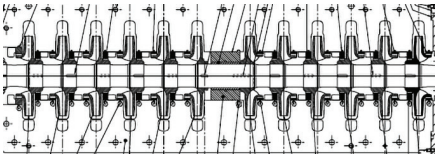

FIG. 5. A 12-stage, opposed impeller with center-stage bushing.

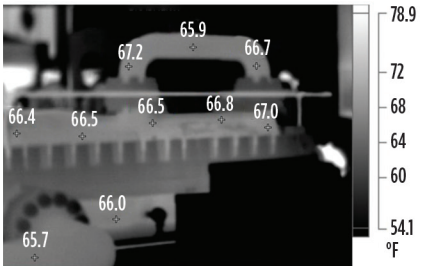

FIG. 6. Baseline signature with uniform casing temperature.

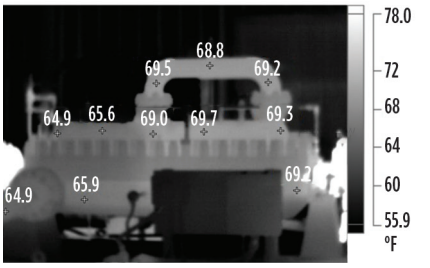

FIG. 7. Thermal signature with casing temperature anomaly.

Pump recycle valve passing condition. FIG. 3 shows a thermal signature of a boiler feedwater pump recycle valve, where the temperature profile across the valve clearly indicates a passing condition. As shown, the recycle line downstream of the recycle valve is similar to the process fluid temperature.

Multi-stage pump center-stage bushing failure. A typical axially split, multi-stage, opposed impeller design pump is shown in FIG. 4. The opposed impeller design is used by pump designers to balance axial thrust forces, and requires a center-stage bushing to isolate the higher pressure from the crossover stages.

FIG. 5 shows a 12th-stage, opposed impeller design with the center-stage bushing to isolate the 12th stage from the 6th stage. This center-stage bushing arrangement is designed for controlled throttling of this high differential pressure across the bushing, as well as for hydrodynamic support of the rotor.

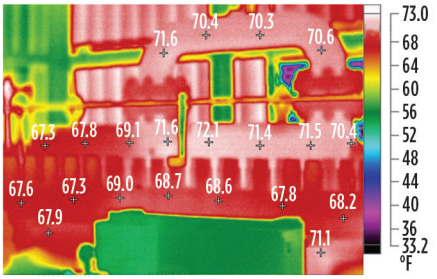

FIG. 8. Casing anomaly with high-resolution palette.

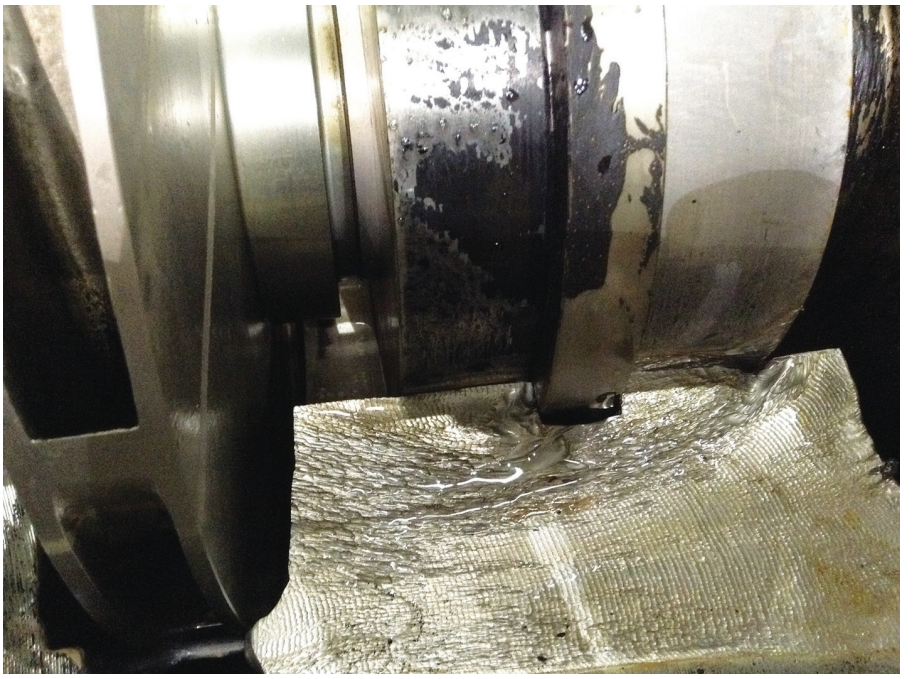

FIG. 9. Center-stage bushing and case split-line damage.

The subject-produced water injection pumps were critical to plant operations and, therefore, were tested annually to monitor and trend performance. Part of this testing included thermal imaging checks compared to baseline thermal signatures to identify any anomalies for early detection of failures.

A baseline thermal signature under normal conditions (**FIG. 6**) shows a uniform casing temperature across the pump with no more than 1°F (0.8°F) difference.

During subsequent tests, operations began to complain about a decrease in injection flowrate for this particular pump. This was confirmed during the performance testing, which indicated a significant amount of total dynamic head (TDH) deterioration (~6%). When the thermal imaging was conducted on the pump casing and compared to the baseline image, a significant temperature gradient was noticed across the center-stage bushing. The pump casing was now showing a temperature difference of ~4°F across the center-stage bushing (**FIG. 7**).

FIG. 8 shows the same casing thermal image with a high-resolution temperature palette applied, which clearly shows the temperature difference on both sides of the center-stage bushing.

FIG. 9 shows the results of the inspection of center-stage bushing, showing the significant erosion damage. This was confirmation of the identified anomaly detected with the thermal imaging.

Takeaway. Based on the casing thermal signature anomaly and the measured head deterioration, it was suspected that the center-stage bushing running clearance may have increased, resulting in excessive leakage across the bushing. With this condition, a temperature rise will occur due to the Joule-Thomson Effect. The temperature increase of the fluid leaking from 12th-stage discharge back to 6th-stage crossover resulted in the observed casing temperature profile. Based on these findings, it was recommended to inspect and overhaul this pump at the next opportunity.

Upon internal inspection, the center-stage distress was confirmed. The loss of center-stage bushing clearance, and subsequent excessive leakage rate, resulted in significant casing split-line damage from high-velocity cutting. Internal inspection also confirmed the presence of an abnormal amount of abrasive material, which was determined to be the root cause of the loss of running clearances.

The cost of thermal imaging equipment has become more economically attractive for maintenance and reliability professionals. Using thermal imaging for condition monitoring of pumps and other rotating equipment can identify thermal anomalies and provide early detection of pending failures.

The aforementioned case studies are good examples of how these techniques can be applied to pump condition monitoring. The case studies resulted in not only early detection of failures, but also can be used to identify energy savings potential, as with the case of passing pump recycle valves.

Many of the common pitfalls of using infrared devices, such as emissivity and other issues, were not addressed here. A slight learning curve exists for effective measurement and analysis.

Training and certification courses are readily available to maximize any return on investment of this technology. As with all field related activities, safety should come first. Thermal imaging in the field can inhibit the ability to keep "eyes on path," which can result in potential slips, trips and falls. HP

KEITH BRASHLER is a Pump Specialist with Saudi Aramco and has 31 yr of rotating equipment experience in refining, pipeline, power generation, pulp and paper, and nuclear facilities with emphasis on pump and system troubleshooting. He earned a BS degree in mechanical engineering from Washington State University, and is a Certified Vibration Analyst: ISO Category IV, and a Certified Maintenance and Reliability Professional (CMRP).

YASSER ALSHAHRANI is a Pump Engineer at Saudi Aramco. He has 6 yr of rotating equipment experience and is a Certified Vibration Analyst: ISO Category II. Mr. Alshahrani earned a BS degree in mechanical engineering and an MS degree in engineering management from King Fahad University of Petroleum and Minerals.

S. KNECHT, ITT Goulds Pumps,
Seneca Falls, New York

Ensuring safety in dynamic chemical manufacturing environments

As with all industries, chemical manufacturing is evolving in response to technical innovations, new customer requirements and increased global competition. As a result, batch production is becoming more common and specialty chemicals represent a greater percentage of orders.

For many manufacturers, greater product diversification and fluctuating demand translates into increased operational complexity, which can have a significant impact on workplace safety. That is because continual shifts in production can put considerable stress on pumping systems that are the heart of every production facility (**FIG. 1**).

In the interest of safety and flexibility, there is a trend among manufacturers to install heavy-duty API pumps, which are more robust and durable. Over the past decade, there has also been an uptick in the use of sealless pumps. These devices eliminate the need for mechanical seals that were necessary to reduce leakage and capture fugitive emissions.

These components have strong selling points; however, there are trade-offs. API pumps are more expensive and might not always be available in the required metallurgy. Sealless pumps can be more sensitive to less than ideal operating conditions and process upsets, which can result in increased maintenance.

Design considerations to ensure safe chemical pumping. To ensure safe chemical pumping, the best approach is the most obvious: install the right configurations for specific production needs. However, that is sometimes easier said than done. Operators with special chemical formulations may not have a reference list of chemical elements and specifications for safe pump configuration, which is an important first step in selecting the best pumping solution and pump material for construction.

In instances like that, which are becoming more familiar, the best option is to collaborate with experts to assemble a design solution. Original equipment manufacturers (OEMs) and suppliers have the experience, expertise and tools to assess risk factors and determine the best components to use.

Corrosion is the biggest concern because of the harm it can do to a pump and the increased possibility of leaks that result (not to mention the higher replacement rate and operating costs). Oftentimes, there is a bit of give-and-take between metallurgies when settling on the right material for combating corrosion. Engineers rely on charts that show the rate of corrosion to determine how long a pump will last when pumping various types of chemicals. Knowledge of the liquid properties relative to temperature and chemical concentration are significant factors in their calculations. Pumping 5% of chemical "X" can be vastly different than pumping 35% of the same chemical because, at higher concentrations, it may have much higher corrosive characteristics. A similar impact can be created if the temperature of a given liquid were to elevate due to a process upset condition. That could encourage a similar level of corrosive attack, even if the chemical concentrations remain the same.

Temperature and vibration are other important variables that can affect safe pumping operations. Too much of either can cause excessive wear and decrease pump life and performance. Plastic and metal have different tolerances; therefore, it is vital to match the right material with every application. When working with certain chemicals, plastic can be more forgiving than metals, which is why engineers will design pumps with plastic parts for optimal performance and safety.

Monitoring and maintenance. Designing for safety is one thing; consistently achieving that goal is another. However, like the design process, there is more than one way to get it right.

In most production facilities, engineers perform regular walkaround inspections to monitor equipment. For pumps that run continuously, these examinations might be part of a daily routine. For other pumps that run intermittently, a weekly or monthly check may suffice. Regardless of schedule, the key outputs typically monitored to assess pump performance and safety are temperature, vibration, pressure, power and flow.

During these inspections, the visual presence of leakage is a dead giveaway that something is not right. Failure of the shaft sealing systems are typically where pumps in chemical applications break down, and

FIG. 1. ANSI pumps running in a parallel system.

leakage is the visual tell of this wear. Depending on the chemical being pumped, the makeup could be very dangerous if leakage occurs. Plant personnel should set maintenance schedules based on applications, with more frequent monitoring for mission-critical processes.

The bigger the facility, the more potential trouble spots there are to inspect. Fortunately, plant operators have a powerful new ally in the form of remote monitoring technologies. These devices can easily integrate into existing systems and collect data around the clock. The information is relayed via Bluetooth or internet connection to a condition monitoring control center where operators can track daily and long-term performance.

Ongoing digital monitoring of equipment provides greater visibility into floor operations and enables swift and accurate decision making that can improve safety. For example, plant operators can track equipment breakdowns and ongoing maintenance costs. Armed with this information, they have a much better understanding of when it is time to replace components, thereby preventing a system failure that could potentially cause harm to workers and the environment.

In general, only around 20% of chemical manufacturing processes are equipped with monitoring devices. However, for mission-critical applications, the adoption rate increases to approximately 60%–70%. Given the costs associated with unplanned downtime, this is a reasonable approach. The average length of downtime is 4 hr and can result in $1 MM in lost revenue.[1]

However, it is also important to note that 70% of unplanned downtime events occur on second or third shifts, which are typically staffed with fewer workers. With digital monitoring, industrial operators have a 35% better chance of preventing unplanned downtime and the associated safety risks from equipment malfunction.[1]

Begin with the end in mind. When new chemical compounds are created, it is common to assign a pilot plant to develop the manufacturing process and document the ideal methods and materials for a pumping system. Typically, it is a trial-and-error process. The end result is a most effective technology, which can be shared, as appropriate, with manufacturing partners.

That same method can be applied to daily operations, especially as special orders and batch production become more common. Chemical manufacturing is a test-and-learn proposition. We always face new challenges, which is why our best practice must keep getting better. The more we can anticipate which production elements could be improved in the name of safety, more problems can be prevented. HP

LITERATURE CITED

[1] George, N., "i-ALERT: Learn how to get automated machine health diagnostics on your rotating equipment," ITT webinar, online: https://www.i-alert.com/videos/

STAN KNECHT is Vice President, Global Engineering for ITT Goulds Pumps. He has worked for the organization since 1987 in various leadership roles in product management, operations and product development. He is also a member of the Hydraulic Institute Board of Directors. Mr. Knecht earned a Bch degree in mechanical engineering from Rochester Institute of Technology.

P. M. MISAL, Fluor, New Delhi, India

Double-tubesheet heat exchangers: Necessities and challenges

Among all types of heat exchangers, shell-and-tube heat exchangers are in huge demand for industrial applications. They are suitable for highly corrosive operating fluids and are appropriate for a broad range of pressure and temperature conditions. These heat exchangers are equipped with a single partition between the shell-side and the tube-side fluid that is popularly known as a tubesheet.

Leakage can typically occur through the tube-to-tubesheet joint, which is generally the weakest point in heat exchangers. This leakage can contaminate the other side with lower operating pressure, adversely affecting process parameters. These leakages cannot be avoided even after properly designing the tube-to-tubesheet joint by using a strength-welded and light-expanded joint with an appropriate mockup in the fabrication stage.

This article discusses double-tubesheet exchangers with a covered connected-shroud shell arrangement and presents special precautions and guidelines for manufacturers during fabrication, testing and assembly of double-tubesheet heat exchangers. It also presents two different assembly sequences that, if implemented by manufacturers, can provide a quality product.

Double-tubesheet heat exchangers are used for applications where the mixing of tube-side and shell-side fluid must be avoided. For example, chlorosilanes—either on the shell or tube side—leak through the tube-to-tubesheet joint and mix with water. They readily react with water to form corrosive hydrogen chloride (HCI) gas and hydrochloric acid, along with heat. Many chlorosilanes evolve into flammable gaseous hydrogen gas during exposure to water. Such a scenario obviously prohibits the mixing of shell-side and tube-side fluids. A comparison between a typical shell-and-tube heat exchanger and a double-tubesheet heat exchanger is presented in FIG. 1.

Another example of leakage is condensers in power plants. In condenser applications, water is used as a cooling medium—the cooling water (raw water) can be sea water, river water, tank or pond water. Cooling water can be brackish and full of contaminants; since the steam side is under vacuum, this water can find a way into the steam-condensed water through a tube-to-tubesheet joint. The potential for leakage of cooling water arises from tube failures, which are caused by a variety of factors. Mixing of cooling water contaminates the feed water, leading to its unacceptable chemistry.

This condensate goes to the hot well and is then pumped to the boiler with the help of a boiler feed pump. The cooling water mixing with condenser water leads to many problems on the boiler side. The affected conductivity and pH level of the boiler water can disturb boiler performance.

The primary concern is preventing contamination of treated and demineralized water due to the leakage of circulating cooling water into the condenser steam space. To overcome this possibility, the provision of double-tubesheet construction for power station condensers is mandatory in some countries.

To date, no method of joining tube-to-tubesheet exists that completely eliminates the possibility of leakage. With double-tubesheet type construction, any leaks through a tube-to-tubesheet joint will accumulate in the space between two tubesheets rather than leaking and contaminating the fluid on the other side. Therefore, while double tubesheets will not negate leakage, they will eliminate the mixing of shell-side fluid with tube-side fluid.

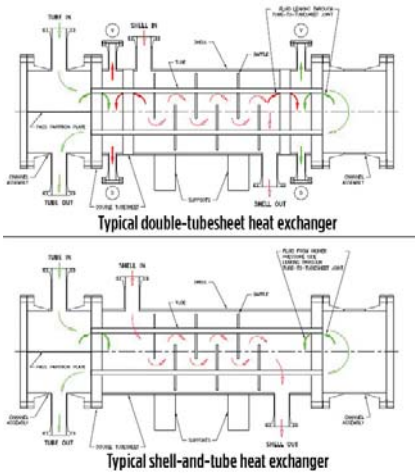

FIG. 1. A typical shell-and-tube heat exchanger vs. a typical double-tubesheet heat exchanger.

Construction. The conventional double-tubesheet exchanger has two tubesheets at both ends of the tubes. Generally, adjacent tubesheets are connected with each other by tubes. Alternatively, shroud shells can be used to cover the gap between two tubesheets. In this case, leaked fluid from either side is collected in a shroud shell.

The shell-side tubesheet of a double-tubesheet U-tube unit can be constructed with any attachment method suitable for removable bundle construction. In the case of a fixed-tubesheet arrangement, the shell-side tubesheet is welded with a shell, whereas the tube-side tubesheet may be bolted or welded with a channel. In the case of a drastic difference in mean metal temperature of the shell side and tube side and different metallurgy used for the shell-side and tube-side tubesheet, a shroud may be provided with an expansion bellow, as shown in FIG. 2.

Typically, the Tubular Exchangers Manufacturers Association (TEMA) covers three types of double-tubesheet

construction, shown in FIG. 3. In all three types of constructions, care should be taken while designing the tube-to-tubesheet joint. Primarily, the tube-to-tubesheet joint on the tube side must be strength-welded with light expansion (FIG. 4) to eliminate the possibility of a leakage of the tube-side fluid through the tube-to-tubesheet joint. On the other side, the tube-to-tubesheet joint on the shell side must be grooved with a minimum of two grooves and expanded to the full length, as shown in FIG 5. This grooved expansion joint must be selected considering the fact that on the tube-to-tubesheet joint of the shell side, welding is practically impossible.

Leakage can typically occur through the tube-to-tubesheet joint. Careful selection of the type of tube-to-tubesheet joint and the sequence of welding and expansion within the tubesheet are vital.

Design. In connected (FIG. 3B) and integral (FIG. 3A) double-tubesheets, axial load distribution is accomplished by an interconnecting element/shroud shell (in the case of a connected double-tubesheet) or an integral portion of the tubesheet (in the case of integral double-tubesheet). In the integral double-tubesheet construction, an interconnecting element is so rigid that it distributes thermal and mechanical radial loads between the tubesheets and prevents the individual radial growth of tubesheets. For both constructions, tubes can mutually transfer all mechanical and thermal axial loads between the tubesheets.

In general, various types of stresses originated in the construction include:

- Differential pressure stresses due to a difference in operating pressures between tube-side fluids and shell-side fluids
- Axial stresses due to tension or compression of the tubes; differential thermal expansion between shell and tubes is another parameter that induces axial stresses
- Shear stresses induced due to differential thermal expansion between the tubes and tubesheet in radial direction
- Thermal and pressure stresses induced due to upset conditions.

Interconnecting elements and tubes between tubesheets of the connected double-tubesheet must be designed according to these parameters:

- Interconnecting element—Radial shear stress at the junctions due to differential thermal expansion of the tubesheets
- Interconnecting element—The combined stresses due to bending and axial tension induced due to differential thermal expansion of tubesheets and thermal expansion of tubes, respectively
- Tubes—Axial tensile or compressive/buckling stresses acting due to operating pressure and thermal expansion.

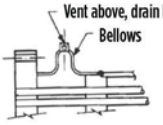

FIG. 2. With a drastic difference in mean metal temperature of the shell side and tube side and different metallurgy used for a shell-side and tube-side tubesheet, a shroud may be provided with an expansion bellow.

Fabrication and testing. Tube-to-tubesheet leak tightness is directly affected by how the double-tubesheet exchangers are manufactured. High-quality tubesheets, baffles and tube supports are produced by drilling holes—either individually or in a stack—with the help of computerized numerically controlled (CNC) machines. The CNC machines ensure that holes in tubesheets, baffles and supports plates are concentric and precise enough to allow them to be easily occupied by tubes. If tubesheets and baffles/support plates are stacked and drilled on conventional radial drilling machines, the drill can drift as it penetrates the stack.

During assembly, hole-to-hole positions may also be displaced if tubesheet main center lines are not maintained congruently. Additionally, major difficulties may also be created if tubesheets are not kept parallel with each other. For these reasons, it is important for a purchaser to review the manufacturer's equipment/tools and techniques used for drilling and assembly.

Guidelines for manufacturers to ensure proper assembly include:

- Tube-side and shell-side faces of a tubesheet should be machined flat and perpendicular to tube (and bolt) holes. Adjacent faces of tubesheets should also be machined in similar fashion from just outside of outside tube limit (OTL) to the tubesheet periphery.
- A suitable number of spacers (made from pipe, rod or plate) should be prepared and preciously machined to the specified gap distance between the tubesheets.
- The spacers must be placed equally on the periphery between the pair of tubesheets. These aligned tubesheet pairs should be clamped and kept in place until all tubing, tube-to-tubesheet joining, and tubesheet-to-shell/channel assembly have been completed.
- A Go gauge machined from a rod that is slightly longer than the distance between the outer faces of the tubesheets should be prepared. The Go gauge ensures free entry of tubes in the tube holes of both tubesheets. Before tubing the assembly, randomly check each quadrant of the tubesheet layout to ensure that the gauge is entering freely. Since non-concentric holes

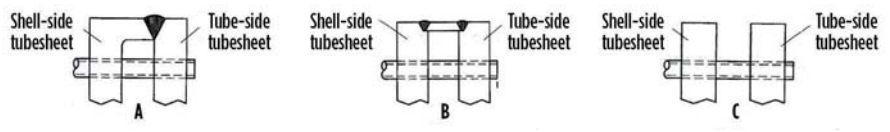

FIG. 3. Integral (A), connected (B) and separate (C) double-tubesheet type constructions.

in adjacent double-tubesheets induce bending and shear forces on tubes and tubesheet ligaments, their concentricity is ensured with this Go gauge.
- Tubesheet ligament tolerances should be strictly ensured, as per TEMA Table RCB 7.22 or RCB 7.22M.[1] With double-tubesheet constructions, these tolerances can be made tighter based on the manufacturer's capabilities and confidence.

Careful selection of the type of tube-to-tubesheet joint and the sequence of welding and expansion within the tubesheet are vital. Displaced holes and ligament distortions make it very difficult to produce tight expanded joints. The outer tubesheet joints can be made tight by welding. However, the challenge remains at the inner tubesheet, where joints can only be made by the process of expansion, as there is no access for welding.

In general, tube end rolling (expansion) within the tubesheet should always follow the welding of the tube-to-tubesheet joint. This is due to:
- Tube expansion (rolling) before welding may leave lubricant from the tube expander in the tube holes. Other fabrication impurities can also accumulate at the tube ends. Satisfactory welds are rarely possible without extreme cleanliness.
- During tube expansion and before welding, the expander pushes tubes against the inside surface of the tubesheet in the tube holes, creating uneven gaps between the outer periphery of the tube and tube hole within the tubesheet. Successful welding with an uneven weld gap is very difficult.
- Tube-to-tubesheet joint welding after expansion creates uneven tube movement within the tubesheet due to tube thermal expansion. This leads to non-uniform tube tightness with the tubesheet surface within the tube holes, which was already achieved by rolling operation.
- Tube-to-tubesheet joint welding after expansion will trap the welding gases in the space between the outer tube surface and the tubesheet hole.

During tube expansion, the expanded portion should never extend beyond the shell-side face of the tubesheet since the removal of such a tube is extremely difficult. Additionally, tube expansion for the inner tubesheets should happen before welding to the outer tubesheets.[2]

Consequently, the correct sequences of assembly and testing are very important while fabricating the double-tubesheet construction, particularly in a fixed tubesheet—such as TEMA L, M, N and outside-packed floating heads (P-type rear heads)—where the number of tubesheets become four considering a double-tubesheet arrangement. In such cases, insertion of tubes through all four tubesheets becomes critical and presents many challenges within the facility. U-tube, double-tubesheet constructions are relatively easy in assembly.

FABRICATION AND ASSEMBLY SEQUENCES

Fabrication and assembly sequences are presented here for a fixed double-tubesheet heat exchanger.

Method 1:

- In the case of small-diameter shells, the tubesheet/baffle/tie rod/spacer skeleton should be built outside the shell, considering the inaccessible shell inside area. The same can be made inside the shell (in the case of a larger-diameter shell) where the operator can enter inside and work.
- The first bundle skeleton should be made with a tie-rod end tubesheet pair in place, as well as spacers and clamping, as discussed previously (**FIG. 6A**).
- The skeleton is then inserted into the main shell. The non-tie rod end tubesheet pair (along with spacers

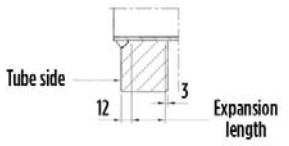

FIG. 4. A tube-to-tubesheet (tube side) joint.

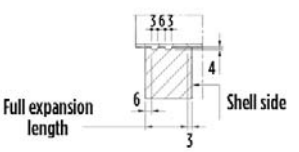

FIG. 5. A tube-to-tubesheet (shell side) joint.

and clamping) should also be kept in line. Tack welding of the shell with shell-side tubesheets should be carried out (FIG. 6B).

- Tubes should be inserted from the tie rod end tubesheet pair through the skeleton and guided through the holes of the non-tie rod end tubesheet pair. Typically, a guiding rod of very small diameter (less than the tube inside diameter) is used from the opposite end (non-tie rod end) to enable tube entry through the holes in the tubesheets and baffles/support plate (FIG. 6C).
- Welding from the tubesheets to the main shell and non-destructive examination (NDE) are carried out (FIG. 6C).
- Both ends of the shell-side tube-to-tubesheet joint expansion in grooves will be carried out. The length of mandrel must be suitable for tube expansion inside the tubesheet, shown in FIG. 6D. Both ends of the channel-side tube-to-tubesheet joint strength welding and light expansion are completed. Tube-to-shell side tubesheet joint leak testing (with helium or air) is done based on project specific requirements. The tube-to-tubesheet joint on the shell side is tested for shell-side hydrotest pressure. Any leakage can be seen from the free space between the pair of tubesheets (FIG. 6D).
- Channel assembly, which has been prepared in parallel, is connected and bolted with the main shell assembly (FIG. 6E). The tube-to-tubesheet joint, as well as other tubeside joints, are tested for tube-side hydrotest pressure and any leaks can be detected from the free space between the pair of tubesheets (FIG. 6E).
- The shroud shell is rolled separately in two pieces and match fitted to ensure perfect roundness.
- After completion of all the tests, the tubesheet spacers and clamping arrangement are removed. The shroud shell is inserted in the space between the pair of tubesheets in two different parts and is then welded along the length with a root run by tungsten inert gas (TIG). The shroud shell is welded with the tubesheets (FIG. 6F).
- A shroud shell hydrotest is not required.

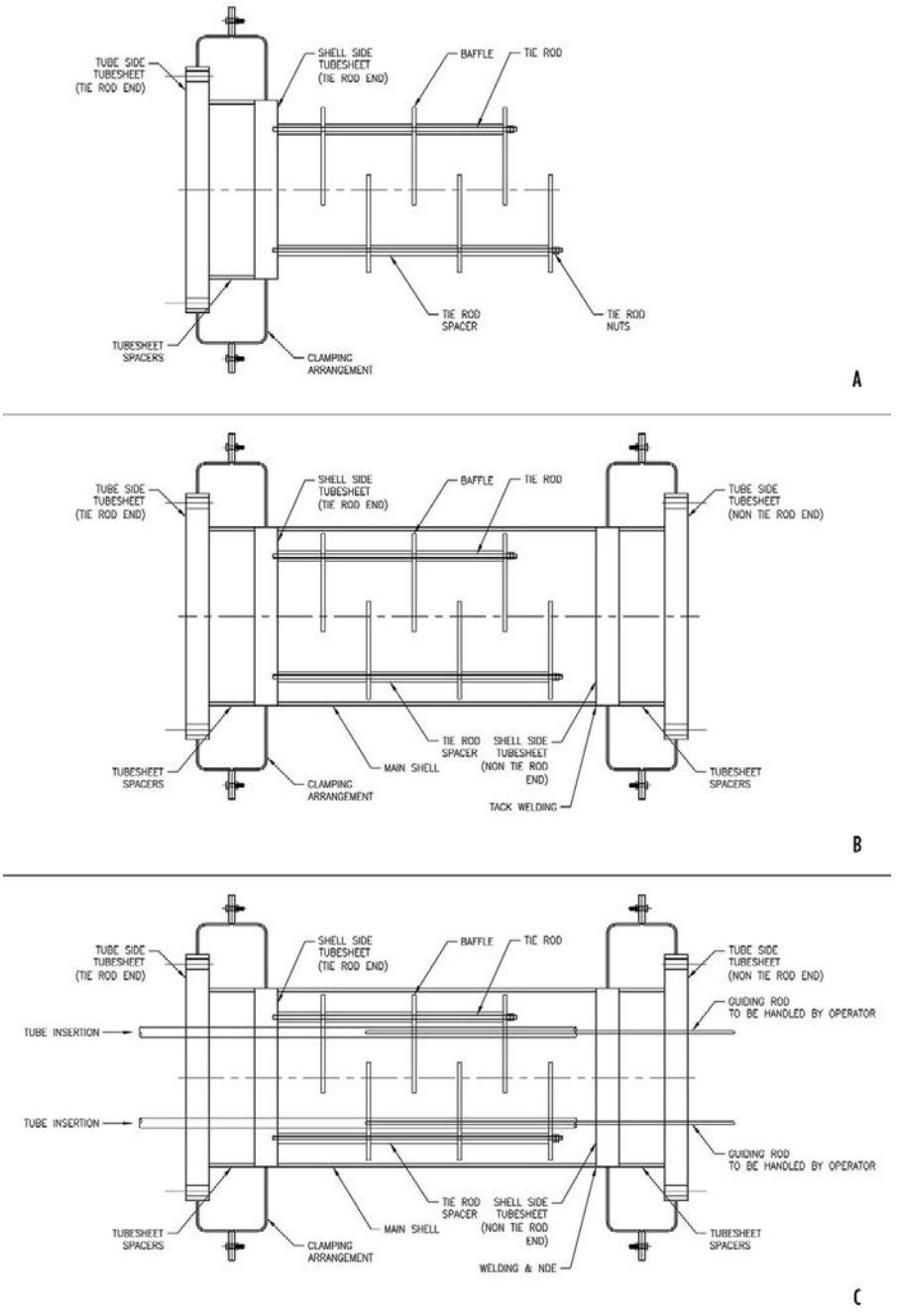

FIG. 6. (A-C) A fabrication and assembly sequence (A–F) has been presented for a fixed double-tubesheet heat exchanger.

In Method 1, the shroud shell is fitted at the very end. This allows visibility through the space between the pair of tubesheets, especially during hydrotest.[3]

Method 2. Method 1 may present difficulties in inserting the shroud shell in two parts—welding along the length and then with the tubesheet. To overcome this difficulty, an alternate method (Method 2) is presented here. All the steps in Method 1 should be followed except:

- The shroud shell is prepared and tack welded with one of the tubesheets on the tie-rod end side and the pair of tubesheets are prepared. In this arrangement, tubesheet clamping is still required; however, tubesheet spacers can be avoided as the shroud shell will now act as spacers. In similar fashion, the

non-tie rod end tubesheet pair is also prepared.
- The tube-to-tubesheet joint on the shell side is tested for shell-side hydrotest pressure. Any leakage must be detected with a drop in pressure because—with the presence of the shroud shell—there is no visibility in the space between the pair of tubesheets.

The manufacturer can alter the intermediate fabrication and testing sequences based on shop facilities, experience and individual technical capability.

Drawbacks of double-tubesheet heat exchangers. Although the total surface area of the exchanger is more, the effective surface area is reduced significantly because the effective tube length is measured between the inside faces of the shell-side tubesheet. The tube length surface area in the shroud area is not considered as a heat transfer area. This increases the required tube length and, in turn, the overall length of the exchanger, further increasing the cost of the heat exchanger.

The addition of two more tubesheets in double-tubesheet construction increases the cost further.

As discussed in previous sections, many criticalities and difficulties are involved in tubesheet/baffle/support plate drilling and machining, especially to achieve tube hole concentricity and tubesheet surface parallelism. Additionally, challenges exist in the correct sequence of assembly, making it difficult to produce quality product.

Maintenance of these heat exchangers can be very difficult, particularly tube removal and replacement since the tube has been fixed with tubesheets in four places. A better option is to plug the damaged tubes.

The arrangement is only possible in a fixed tubesheet, a U tube and outside-packed floating head. During the operation, the vents/drains of the shroud shell must be regularly monitored to avoid mixing of hazardous or carcinogenic fluid into the atmosphere.

Takeaway. Well-planned fabrication and assembly sequences can be useful while manufacturing double-tubesheet heat exchangers. These heat exchangers are also required in the pharmaceutical industry for sanitary applications and are designed to meet that industry's high-quality requirements and hygienic standards. These heat exchangers are also required in polysilicon manufacturing plants, as well as solar power plants. Distilled hexane reboilers, hexane heaters and titanium chloride heaters in the petrochemical industry are further examples.

This paper has presented reasons for selection of such types of heat exchangers, various types of stresses in tubes, tubesheets and shroud shell, fabrication, assembly sequences and testing methodologies. Either of the two proposed assembly sequence methods can be adopted by a manufacturer. HP

LITERATURE CITED

[1] *Standards of the Tubular Exchanger Manufacturers Association (TEMA),* 9th Ed., New York, January 2007.
[2] *Perry's Chemical Engineers Handbook,* 7th Ed., Mc-Graw Hill Publications, 1997.
[3] *A Working Guide to Shell and Tube Heat Exchangers,* Stanley Yokell, Mc-Graw Hill, 1990.

PURUSHOTTAM M. MISAL works for Fluor in New Delhi, India. The author can be reached at Purushottam.m.misal@fluor.com.

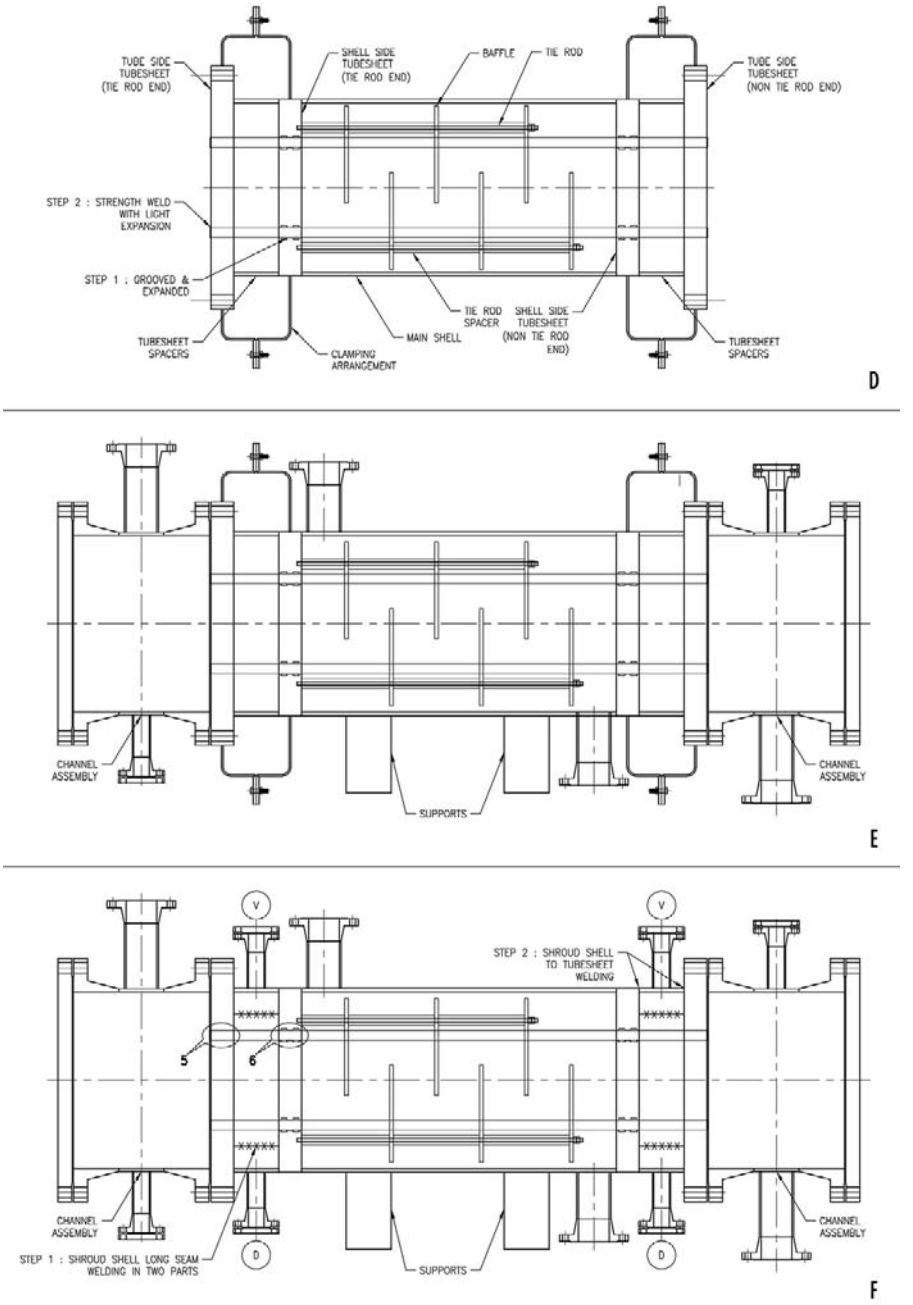

FIG. 6. (D-F) A fabrication and assembly sequence (A–F) has been presented for a fixed double-tubesheet heat exchanger.

A. GARZA, Endress+Hauser, Greenwood, Indiana; and **S. MILLER,** Endress+Hauser, Rancho Cucamonga, California

Improved measurement of water content in natural gas

Consumers likely imagine natural gas as a stream of pure methane. Those who are closer to the energy industry know that methane is the major component, but there can easily be dozens of other substances making up a sizeable portion of the total volume. Natural gas producers, pipeline operators and major industrial users—such as various types of petrochemical plants—have reason to be concerned about what is in the mix (FIG. 1).

Contaminants in natural gas can cause a variety of problems for pipeline operators and petrochemical plants, especially when combined with water. This makes accurate and reliable measurement of water content in natural gas streams critical, but traditional techniques often fall short. Fortunately, new analyzers offer much-improved performance.

Water exacerbates issues. Natural gas composition is controlled to some extent. Wherever natural gas is traded commercially, there are regulations as to its chemical content and attributes, such as calorific value. Local specifications and ranges vary, but, typically, there are limits for total sulfur, hydrogen sulfide (H_2S), carbon dioxide (CO_2), oxygen and water. This list is not exhaustive, as there are many other possible components, such as higher hydrocarbons and other diluent gases. The common element of these specific components is that they are contaminants and considered undesirable:

- Sulfur and its many compounds represent the most widely encountered contaminant in all fossil fuels, including natural gas—and they are known for their toxicity and pollutants produced during combustion.
- Oxygen degrades amine and some mercaptans, which are used in natural gas treatment.
- CO_2 dilutes the overall heat value.

The greater problem results when these contaminants combine with another contaminant: water. All of them work together with water to produce acids capable of attacking carbon-steel piping, valves and other equipment to cause internal corrosion and metal loss over time (FIG. 2). Natural gas pipelines can corrode from the outside and inside, but internal metal loss is more difficult to recognize and measure.

The Pipeline and Hazardous Materials Safety Administration's (PHMSA's) "Pipeline Corrosion" report summarizes the situation: "Typically, sales-quality dry gas will not corrode pipeline interior surfaces. However, natural gas, as it comes from the well, may contain small amounts of contaminants such as water, carbon dioxide and hydrogen sulfide. If the water condenses, it can react with the carbon dioxide or hydrogen sulfide to form an acid that might collect in a low spot and cause internal corrosion."

This leaves natural gas producers, pipeline companies and users understandably concerned about water content—both liquid and vapor—in the gas flow, since a pipeline leak or break caused by unchecked

FIG. 1. Since natural gas can come from a variety of sources (fossil and renewable), its composition and attributes vary.

corrosion can cause enormous damage.

As a given volume of gas makes its way from a source to its consumption point, it may experience variations in temperature, above and below the immediate dew point, causing water to change phase multiple times. If enough vapor condenses in a cold section of pipe, liquid water can accumulate in a low spot. If the temperature is cold enough, water accumulations can freeze, causing solid clogs. Even if the water remains a liquid, it may cause enough of a blockage to force the gas velocity to increase, entraining water droplets in the gas stream or pushing liquid slugs that accumulate somewhere else downstream. If a slug reaches the final use point (e.g., gas turbine), it can cause serious damage.

Water can be removed by chemical and physical mechanisms, but this adds processing costs. Consequently, there is little incentive to treat gas once it meets the standard for tariff gas. This amount varies between 50 ppmv–200 ppmv, depending on the location. Once water is below the limit, it is less of a problem—provided it stays there and continues to flow from a reliable source. The supply can and will change at various times, so there is no reason to assume that conditions at one time or location will invariably persist. Given all these considerations, knowing the specific moisture content of the gas flow in real time is critical.

Measuring water content. A small selection of measurement technologies can determine the amount of water in a natural gas pipeline, and, as is normally the case with instrumentation, each has its combination of practicality, accuracy and cost trade-offs. All typically involve extracting a sample for individual testing, rather than inserting a sensor for a continuous real-time reading. The following are several common electrochemical and electromechanical approaches:

- **Aluminum oxide:** Water content is determined by measuring the change of capacitance of water molecules captured in microscopic pores across the sensor surface. After an increase in water content, the pores must be dried. Problems occur when molecules are trapped inside, as this causes incomplete drying, or when surface contamination clogs pores, keeping molecules out. This technique can also misidentify glycol and methanol content as water. These characteristics make these types of instruments prone to drifting and, therefore, to being maintenance intensive.
- **Phosphorus pentoxide:** Gas passes through a cell containing electrodes coated with phosphorus pentoxide able to electrolyze water molecules. Current passing through the electrodes is proportional to the amount of water present. Combining the gas flowrate with the consumed current yields an absolute moisture content measurement. However, the reading can be distorted by changes in flowrate through the analyzer or methanol content in the gas, which is read as water. The sensor is also susceptible to contamination like aluminum oxide and must be replaced on a regular basis, thus increasing operational costs.
- **Quartz crystal microbalance:** Sample gas is fed into a chamber where water molecules condense on a chilled surface attached to a quartz crystal. The action assesses the change in mass of the microscopic amount of liquid that forms. This approach has high sensitivity, but it cannot differentiate between water and other liquids that condense, such as glycol. If the mechanism does not fully dry between samples, then readings will appear higher than actual. Corrosion inside the chamber is common when H_2S and CO_2 are present in the sample.
- **Chilled mirror:** This approach calculates water content by determining the dew point. A glass surface inside the sample chamber is chilled until the dew point is reached where condensation forms, which can be detected optically or by visual inspection. Again, this technique lacks the ability to identify water specifically apart from other liquids that may be in the stream.

A common drawback to these approaches is the potential for contamination (TABLE 1). Some contaminants—such as compressor oil, methanol and amine—can cause slow or inaccurate readings. Other contaminants can poison the sensor and require replacement. For example, chlorine and ammonia traces in enough quantities can damage all these technologies, except for phosphorus pentoxide.

The problem, ultimately resulting from a poorly performing electrochemical sensor, is a mistrust of the technology. Operators simply assume that the reading is incorrect, and act on whatever estimate they substitute for reliable data. This leaves two possibilities. First, they assume that the gas cannot possibly have as much water as the sensors indicate, so they take less action than is truly merited, thus allowing the corrosive conditions to get worse. Second, they assume that the gas must have more water than the sensors

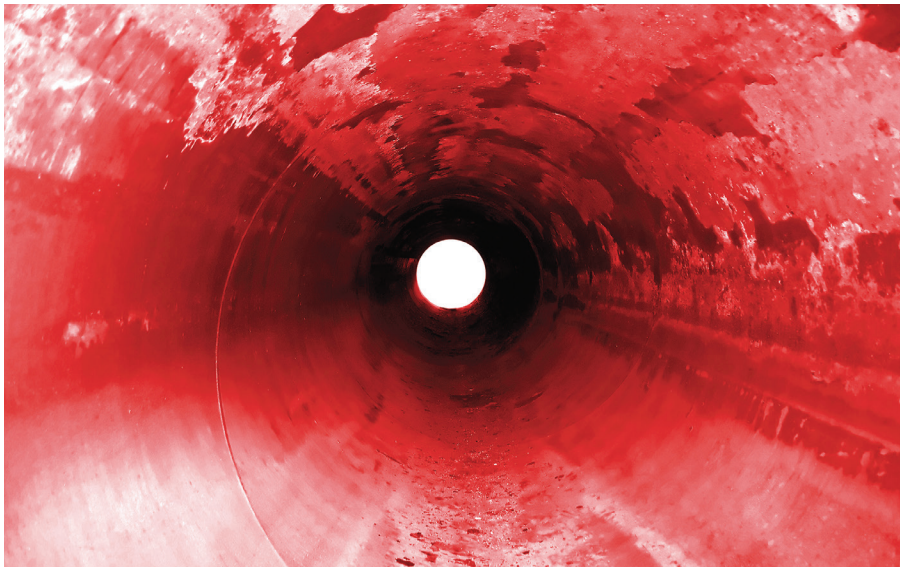

FIG. 2. When water mixes with other contaminants in natural gas, corrosive acids can form that can attack carbon-steel piping from the inside.

indicate and they overtreat it, adding cost. The first situation could contribute to a safety incident, whereas the second hurts profitability. The clear need to solve both challenges is a water content measurement that is correct and consistent.

Traditional tunable diode laser analyzers. From a theoretical standpoint, a tunable diode laser absorption spectroscopy (TDLAS) analyzer is arguably the most effective mechanism to measure water content in natural gas. Using an infrared wavelength laser, it is possible to isolate the very distinct peaks in the wavelength absorption spectrum that are indicating water and other components in the stream. This means that the analyzer can provide a water content measurement unaffected by glycol, methanol, amine or H_2S. While this underlying capability is a matter of physics, putting it to work in a way that is practical and usable in a typical operating environment is challenging for manufacturers.

TDLAS analyzers are, by nature, very stable and rarely need calibration. The sensor itself is not subject to drift or problems from chemical contamination. However, the supporting mechanisms can challenge effective operation. For example, a TDLAS analyzer is optical in nature, so designs employ mirrors and lenses to direct and focus the beam from the source to the detector (**FIG. 3**).

The sample gas flows through the measurement cell—the space where the beam passes. When the sample contains free liquids, there is an opportunity for flooding the cell. If the mirrors become coated, then the beam can be attenuated or blocked. When such problems eventually occur, the cell requires service; however, it may take operators some time to realize this type of problem.

These difficulties stem largely from the sample conditioning system. It must capture contaminants and deliver a clean sample to the measurement cell, but it must not affect the water content. The system must also control temperature and pressure of the sample gas to ensure accuracy and repeatability. When servicing is necessary, some analyzer designs can be very complex or impossible to disassemble, with extensive tweaking required as part of reassembly. Some analyzers call for matched sets of components, requiring expensive replacement-part kits, or the end user is forced to send the analyzer back to the factory for repair. This can detrimentally lower measurement uptime availability in critical custody-transfer points.

Fortunately, TDLAS analyzer designs have been evolving to provide operational simplicity, while delivering more sophisticated analysis.

Analyzer improvements. TDLAS analyzer improvements have concentrated on three main areas. These include:

- Transmitter electronics, including human-machine interface (HMI), data presentation, system connectivity and diagnostics
- Modular construction to simplify serviceability, including a sampling system, an optical enclosure, a sample cell and electronics
- Enclosure protection for mounting versatility.

A field-mounted analyzer depends on its transmitter to perform a very wide range of functions. It must support the basic metrology calculations to provide excellent accuracy, linearity and repeatability. It must also provide internal HMI support for its local display, along with connectivity to send its data to a larger supervisory control and data acquisition (SCADA) system or another automation host system. The ability to program functions easily and intuitively makes all the difference for ease of use and enables high measurement uptime, so this capability must be provided.

Desired connectivity options have expanded to include web server capabilities, extending the range of remote data access via the internet to any device capable of hosting a web browser, such as a laptop, smartphone or tablet. This capability is particularly critical when an analyzer is deployed in a location not easily accessible by technicians and operators. When remote access is combined with internal data storage, it is a simple matter for authorized users to upload gas analysis data from extended periods of time.

In many respects, the most important new capability that the transmitter supports is internal diagnostics to indicate how the unit is functioning (**FIG. 4**). This determines when problems are developing that can cause poor readings or a complete outage. When severe enough, these situations must trigger alarms to call for immediate maintenance attention. Continuous evaluation and reporting should

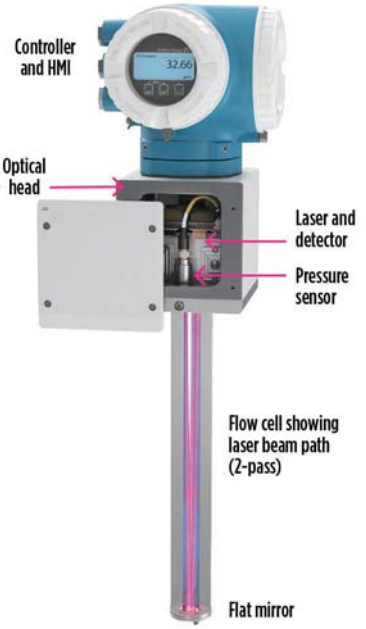

FIG. 3. A gas sample must be contained in the space where the beam passes through, so a dirty sample can coat optical surfaces.

TABLE 1. Compounds frequently found in natural gas streams that can damage electrochemical measurement methods or make them ineffective (but that do not affect a TDLAS analyzer)

Gas phase contaminant	Aluminum oxide	Phosphorus pentoxide	Quartz crystal	Chilled mirror	TDL sensor
Methanol	O	O	O	O	X
Glycol	O	O	O	O	X
Amine	O	O	O	O	X
Mercury	•	X	X	X	X
H_2S	•	O	O	•	X
Hydrogen chloride	•	O	O	•	X
Chlorine	•	O	•	•	X
Ammonia	•	O	•	•	X

X = Analyzer unaffected • = Can cause permanent damage to the sensor O = Can cause slow or inaccurate readings

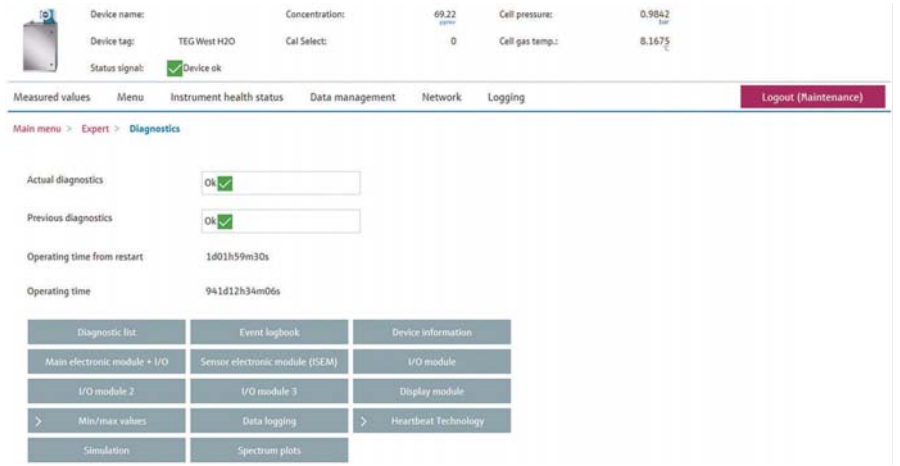

FIG. 4. Analyzer diagnostics include a range of functions related to the sensing cell and sampling system.

FIG. 5. Robust internals protected in solid enclosures avoid the need for analyzer shelters.

be done, which have been simplified for many types of instrumentation through the use of NAMUR 107 alarm categories for consistent data presentation.

Since analyzers need service work eventually, modular construction makes this task much easier and less expensive. Previous designs tended to be difficult to access and reassemble, calling for challenging adjustments before returning to full operation. These requirements could cause lengthy outages, leaving users with no analysis data.

However, at present, major functional components can be extracted as a unit and serviced quickly—or a substitute assembly, standing by, can be inserted to resume operation with minimal delay. When supported by detailed diagnostic information, a technician knows exactly what needs to happen and can have the necessary parts in hand before the unit is serviced.

Analyzers traditionally have a reputation for requiring specialized enclosures to protect their delicate mechanisms from the harsh surrounding environment. Improvements in construction with more robust internals (FIG. 5) allow them to be mounted in more environments with a broader range of environmental temperatures. Upgraded enclosures, combined with better insulation and enclosure heating, permit outside installation, even in wet and cold climates.

Solution to a clear need. Given the unsettled nature of energy markets caused by the COVID-19 pandemic, the importance of monitoring critical attributes of pipeline gas is very high. With changes in gas fields and the growth of renewables, there is every reason to take nothing for granted. Keeping pipelines and other equipment in reliable and safe operation calls for knowing when corrosion might be happening internally, and this is driven to a large extent by condensation combining with other contaminants.

Pipeline natural gas is routinely monitored for a range of attributes and composition at sources and transfer points, but the reliability of these measurements is no better than the technologies applied and their operators. Where water content is critical, operators have depended on electrochemical techniques, often with hit-or-miss results from poorly performing sensors. In other cases, operators struggle to keep finicky analyzers working properly and are often forced to return them to the factory for repair.

Both of these challenging situations can be solved through improved TDLAS analyzers, which can deliver a high degree of accuracy combined with an easy-to-use operator interface and reliable construction. On a continuous basis, with readings only seconds apart, operators can tell if gas quality specifications are met or if remedial actions need to be taken. They can also continuously monitor the analyzer by watching diagnostic data.

If a problem is developing due to highly contaminated gas, operators will know if the reading data is impaired in any way, and they will understand exactly what actions are necessary to correct the situation. Operators do not need to be close by, as improved connectivity means that they can access the analyzer from virtually anywhere. While gas supplies are in question, it is important to know that the analysis is reliable. HP

ALAN GARZA is the Product Marketing Manager for the advanced analysis product lines at Endress+Hauser. He began his career at Endress+Hauser as a rotational engineer, working with multiple instrumentation technologies. Mr. Garza was also part of the inside sales team, where he championed gas analytics and developed his skills as an applications engineer. His background also includes business development and operations management. Mr. Garza earned a BS degree in mechanical engineering technology from the University of Houston.

SAM MILLER is responsible for product marketing at SpectraSensors, an Endress+Hauser company. He has more than 20 yr of experience in oil and gas markets and in the development of laser-based products. He is a member of the ASTM D03 standards committee and participates in numerous natural gas conferences and symposiums, including those of the American Gas Association (AGA), the ISA Analysis Division, and various international hydrocarbon measurement organizations. Mr. Miller earned a BS degree from California Polytechnic University, Pomona, and an MBA degree from the University of California, Irvine.

G. GOUS and **P. DE VAAL,** The University of Pretoria, Pretoria, South Africa; and
G. VAN COLLER, Sasol, Secunda, South Africa

Implementation of averaging level control using native DCS functions

When applying averaging level control in a process plant, engineers can typically choose between proportional integral derivative (PID)-based control, such as p-only, gap and non-linear, or a model-based control like optimal averaging level control. PID controllers allow the level to go outside of limits when disturbances are larger than the assumed maximum disturbance used during tuning. Model-based controllers will be more successful in keeping the level between limits, as no assumed maximum disturbance is used during tuning. However, model-based control requires additional hardware and software and typically runs at a slower execution interval of approximately 1 min.

Two simplifications of model-based averaging level controllers are proposed here. They ensure that levels stay within limits in the same way as model-based controllers. They can run at fast execution intervals, as they can be directly implemented on a standard distributed control system (DCS).

The first method is a simplification of the control of imbalanced ramps in standard advanced process control (APC) software, called the ramp horizon controller. Here, the process model is also simplified to use a gain only. The controller uses a pre-defined time, called the ramp horizon, during which the limits may not be exceeded. If no limits are exceeded within the ramp horizon, then no controller moves are implemented. If a limit violation is predicted, a move is implemented that is large enough to prevent the calculated violation only.

The second method is a simplification of the optimal averaging level controller, called the simplified optimal averaging level controller (SOALC). By simplifying the process model to a gain only, the calculations required by the controller are decreased enough to enable implementation on a standard DCS. The SOALC then calculates the minimum controller moves that must be made continuously to reduce the rate-of-change of the level to zero at the time it reaches the approached limit.

Averaging level control. Many plants have feed drums with tightly tuned level controllers that essentially reduce a drum to nothing more than a pipe, wasting the initial capital outlay of installing the drum. Averaging level control will allow the level to move away from setpoint to allow the controller to reduce movement of the output, which should stabilize downstream processes.

Averaging level control is typically done by using properly tuned PID-based controllers[1,2] or by using model-based controllers[3,4,5,6] designed to minimize controller output (OP) movement. The PID controllers include p-only,[7] proportional-integral (PI), gap and non-linear techniques,[2] typically implemented as standard algorithms on modern DCSs[8] and programmable logic controllers (PLCs) and running at execution cycles of 1 sec or faster.

A shortcoming of PID-based controllers is that they are typically tuned to accommodate an assumed maximum size disturbance.[2,9,10] If a larger disturbance is encountered, the desired upper or lower limits for the level will be exceeded. This often leads control engineers to make conservative estimates for the maximum size disturbance that may be encountered. If smaller disturbances than these occur, these controllers will not make full use of the buffer capacity.

Model-based control is performed using APC software that will normally operate on dedicated control servers that communicate via a network connection to the DCS or PLC. These controllers typically run at 1-min execution cycles.

Model-based controllers will make full use of the buffer capacity by letting the level move between the high and low limits. Disadvantages of model-based control include:

- Additional hardware and software are required.
- A network connection is used to link the controller to the DCS or PLC.
- Once the controllers have allowed the level to move up to a limit, consecutive disturbances in the same direction will cause the level to exceed the limit, albeit not by a large amount.

Two new control methods are proposed that are simplifications of model-based averaging level control techniques. Benefits include:

- They run on a modern DCS using its standard control functionality.
- They run at ≤ 1-sec execution cycles.
- They take full advantage of the available buffer capacity.

- They do not exceed limits if larger than expected disturbances occur.

Ramp horizon controller. Ramp horizon control is a simplification of the way level buffering is done by an APC.[5] A timespan or ramp horizon is selected during which the high and low limits imposed on the level may not be exceeded. The trajectory of the level is estimated, based on the current position and current rate-of-change. OP moves are only made if the estimated trajectory will violate a limit within the ramp horizon. If no violation is predicted, no OP moves are made.

The algorithm is initiated by calculating the current ramp rate (Eq. 1):

$$RR = (L_n - L_{n-i})/\, i \quad (1)$$

where:

RR = Current ramp rate, % per execution cycle
L_n = Level at current execution cycle, n (%)
L_{n-i} = Level at execution cycle, $n–i$ (%)
i = Number of execution cycles used to calculate ramp rate.

Consider the example shown in **FIG. 1.** The ramp rate is calculated by subtracting the current process value (PV) of the level (which is 50) from a previous value of 45 at Time 2 and dividing that by the time difference of two intervals to obtain the current rate-of-change of the level of 2.5% per interval. The value of i should be large enough to minimize noise and small enough to limit the amount of lag introduced.

Next, the change in level over the ramp horizon is calculated by Eq. 2:

$$\Delta L = RR \times RH \quad (2)$$

where:

ΔL = Amount that the level is predicted to change over the ramp horizon
RH = Ramp horizon.

In the example, the ramp rate of 2.5%/cycle is multiplied by the ramp horizon of 10 execution cycles. This calculates the change in level over the ramp horizon to be 25% (Eq. 3):

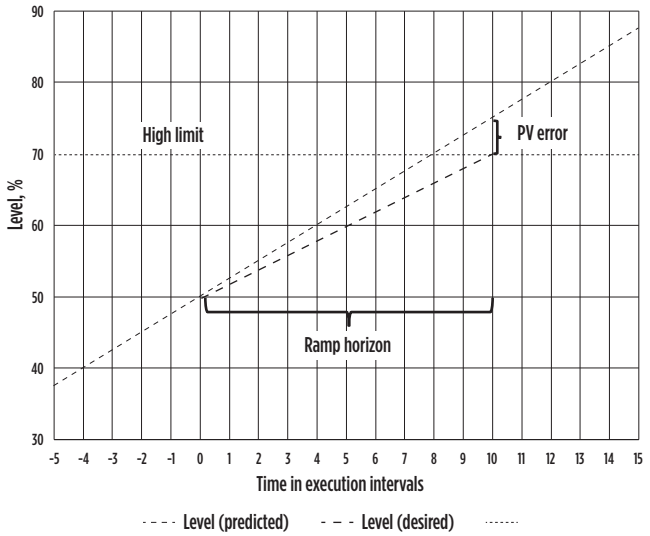

FIG. 1. Ramp horizon controller.

$$L_{n+RH} = L_n + \Delta L \quad (3)$$

where:

L_{n+RH} = Predicted value of level at ramp horizon.

In the example, 25% is added to the current value of the level of 50% to calculate the predicted value of the level at the ramp horizon to be 75%. If this predicted value does not violate the high or low limit, no OP moves are made. However, the predicted value violates the high limit of 70%, so an OP move will be calculated and implemented.

A controller gain is calculated initially by either using step test data or calculating the volume of liquid between the high and low limits on the drum. The gain is the change in the level rate-of-change that will result when the OP is moved up by one engineering unit (Eq. 4):

$$Gain = (RR_{SS} - RR_{initial})/\Delta OP \quad (4)$$

where:

$Gain$ = Ramp horizon controller gain, % level/execution cycle/% OP
RR_{SS} = Ramp rate when steady state is reached after step was made
$RR_{initial}$ = Ramp rate at steady state before step change was made
ΔOP = Step change in OP that was made.

For this example, a step test was conducted with the ramp rate of the level at -2 initially. The OP was stepped up by 4 and the ramp rate reached steady state at 6. The gain is calculated as 2 using Eq. 4. This indicates a 2%/execution cycle change in the rate-of-change of the level for every 1% change in OP.

Using the controller gain, it was possible to calculate how much the OP must be changed to prevent the limit being exceeded (Eq. 5):

$$\Delta OP = (L_{n+RH} - Limit)/\, RH \,/\, Gain \quad (5)$$

where:

$Limit$ = Limit towards which the level is moving.

In the example, the PV error is calculated by taking the difference between the predicted value of the level at the ramp horizon and the exceeded limit—this is 5% in the example. We now need to calculate how much the OP should be moved so that the level will be at 70% at the ramp horizon. Dividing the error by the ramp horizon calculates the desired change in the rate-of-change for the level to be 0.5%/interval. Dividing this value by the controller gain shows that the OP must be moved up by 0.25% to change the trajectory of the level just enough so it will be on the limit at the ramp horizon.

This will prevent the level from exceeding the limit at the ramp horizon. However, as the level will still be approaching the limit, the controller during the next execution cycle will once again predict that the limit will be exceeded. It will implement another controller move to ensure that at the ramp horizon, the level will still be inside the limit. If no other process influences the trajectory of the level, this process will be repeated until the rate-of-change of the level reaches 0 as it reaches the high limit.

When a relatively small disturbance causes a change on a level that is controlled by using the ramp horizon method, the prediction will initially not show that a limit will be exceeded within the ramp horizon. As the level then goes towards a limit, no OP

moves will be made. As time passes, the level will approach the limit and at some stage a small violation will be predicted. An OP move will be calculated to change the rate-of-change of the level such that the level will be on the limit at the ramp horizon.

At the next execution cycle, the prediction will show a small violation again, as the level is still moving in the direction of the limit. Once again, a small OP movement will be calculated to bring the level to the limit at the ramp horizon. This will be repeated until the cumulative OP moves will bring the rate-of-change of the level to zero when the level reaches the limit. No attempt is made to return the level to a setpoint (SP) value or to move away from limits.

Because this method will allow the level to achieve limits while making small OP moves to ensure the limits are not exceeded, the risk remains that continuous or consecutive disturbances in the same direction may occur once the level has reached the limit. When this happens, the controller will not be able to keep the level between the imposed limits. If this occurs and the level moves outside a limit, the ramp horizon controller will return the level to the limit that was exceeded using the same algorithm.

Because the method simplifies the response of the level by calculating a gain only, it ignores any dynamic behavior. Combining this with measurement noise, unmeasured disturbances and the possibility of an incorrect gain being used may lead to imprecise control action. However, in a short execution cycle, the level measurement that is taken as input and the rate-of-change of the level that is calculated at every execution cycle continuously update the controller error. This compensates for the possible inaccuracies in measurement and control.

SOALC. Optimal averaging level control[3,11,12] is accomplished using model-based control software to calculate the smallest moves that can be made continuously to allow the level to attain a zero rate-of-change when it reaches the limit. While optimal averaging level control requires model predictive control software running on a dedicated server, the approach may be simplified in the same way as the ramp horizon controller to allow running the algorithm natively on a standard DCS at a higher frequency.

If the dynamics of the level are ignored and only the absolute value of the level and its current rate-of-change are used to calculate the future trajectory of the level, an approach like the optimal averaging level controller may be developed. If the current rate-of-change of the level is extrapolated from the current value of the level, limit violations can be predicted. The OP move required during every execution cycle until the level is balanced at the limit can then be calculated.

Because dynamics are ignored, this approach will not be as accurate as a model-based controller. Like the ramp horizon controller, a short execution cycle, the level measurement that is taken as input and the rate-of-change of the level that is calculated at every execution cycle will continuously update the controller error and will ensure adherence to limits.

If a level is currently at PV_0, with a positive rate-of-change of ROC_0, and a high limit of H that will be exceeded based on an extrapolation of ROC_0, then a sequence of n OP moves of size x must be calculated to balance the level at H. The total move of the OP over the control horizon must be (Eq. 6):

$$dOP = x.n \tag{6}$$

If a controller gain (G) is defined as the change per execution cycle in the rate-of-change of the level brought about by increasing the OP by 1%, then (Eq. 7):

$$dOP = ROC_0 / G \tag{7}$$

Combining Eqs. 1 and 2 yields Eq. 8:

$$x = ROC_0 / (G.n) \tag{8}$$

If the level begins at the current PV with the current rate-of-change and ends at the high limit with the rate-of-change at 0, the initial and final conditions must be as shown in TABLE 1.

If a step of size x is made every execution cycle, then the rate-of-change of the level will be decreased by $x.G$ every execution cycle. The level will also increase by the current rate-of-change per execution cycle. Therefore, TABLE 2 can be calculated.

In TABLE 2, the first column shows the Execution cycle. The second column shows the Level measurement, calculated as the previous value of the level plus the change in the level. The change in the level will be the Rate-of-change in the level during the previous Execution cycle, as shown in Column 4.

For example, during Execution cycle 3, the previous value of the level was calculated as $PV_0 + ROC_0 + ROC_0 - x.G$. If the change in level seen in Column 4 $(ROC_0 - 2.x.G)$ is added, the value for the level at Cycle 3 is calculated as $PV_0 + ROC_0 + ROC_0 - x.G + ROC_0 - 2.x.G$. This is simplified in Column 3 to $PV_0 + 3.ROC_0 - 3.x.G$.

TABLE 1. Initial and final conditions for SOALC

Variable	Initial value	Final value
Level	PV_0	H
Rate-of-change	ROC_0	Zero

TABLE 2. Change in level and rate-of-change over control horizon

Execution cycle	Level, showing changes per cycle	Level, changes added	Rate-of-change of level	Change in OP
0	PV_0	PV_0	ROC_0	x
1	$PV_0 + ROC_0$	$PV_0 + ROC_0$	$ROC_0 - x.G$	x
2	$PV_0 + ROC_0 + ROC_0 - x.G$	$PV_0 + 2.ROC_0 - x.G$	$ROC_0 - 2.x.G$	x
3	$PV_0 + ROC_0 + ROC_0 - x.G + ROC_0 - 2.x.G$	$PV_0 + 3.ROC_0 - 3.x.G$	$ROC_0 - 3.x.G$	x
4	$PV_0 + ROC_0 + ROC_0 - x.G + ROC_0 - 2.x.G + ROC_0 - 3.x.G$	$PV_0 + 4.ROC_0 - 6.x.G$	$ROC_0 - 4.x.G$	x
5	$PV_0 + ROC_0 + ROC_0 - x.G + ROC_0 - 2.x.G + ROC_0 - 3.x.G + ROC_0 - 4.x.G$	$PV_0 + 5.ROC_0 - 10.x.G$	$ROC_0 - 5.x.G$	x
n	H	$PV_0 + n.ROC_0 - (0.5.n^2 - 0.5n)x.G$	$ROC_0 - n.x.G$	0

At the Execution cycle n, the controller has made the last move of size x, which will cause the rate-of-change of the level to become 0 at the high limit. Therefore, at Row n in TABLE 2, the value of the level is H and the rate-of-change is 0.

To calculate the level at Execution cycle n in terms of x, PV_0 and ROC_0, Column 3 of TABLE 2 is set equal to H. In calculating the equation in Column 3, Row n, the coefficient of PV_0 should be 1 and the coefficient of ROC_0 should be n. The series of coefficients for the term $x.G$ (0, 1, 3, 6, 10 ...) shown in Column 3 can be calculated as $0.5n^2 - 0.5n$. Therefore, the value of the level at Cycle n can be expressed as $PV_0 + n.ROC_0 - (0.5.n^2 - 0.5n)x.G$, as shown in the last row of Column 3 in TABLE 2.

Combining $H = PV_0 + n.ROC_0 - (0.5.n^2 - 0.5n)x.G$ and Eq. 8 yields Eq. 9:

$$x = 0.5 \times ROC_0 \times ROC_0 / [G \times (H - PV_0 - 0.5 \times ROC_0)] \quad (9)$$

Eq. 9 calculates by how much the OP must be changed during every execution cycle to balance the level at the high limit. As stated before, dynamics on the level model may cause inaccuracies, but as the value and rate-of-change of the level are measured every execution cycle, the inaccuracies are remedied.

In the same way, it can be calculated in Eq. 10 that:

$$x = 0.5 \times ROC_0 \times ROC_0 / [G \times (L - PV_0 - 0.5 \times ROC_0)] \quad (10)$$

will balance the level at the low limit (L) if the level is moving downward.

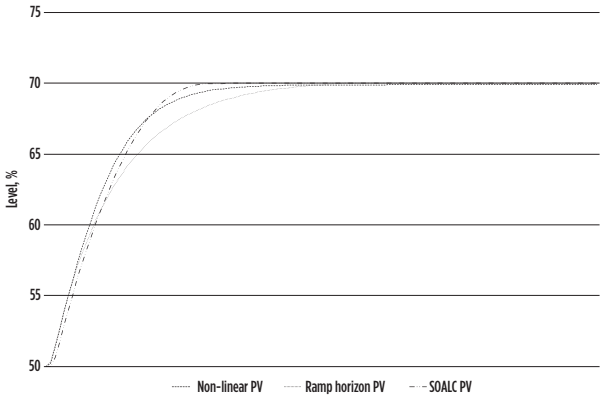

FIG. 2. Level response to a step disturbance of 5 m³/hr.

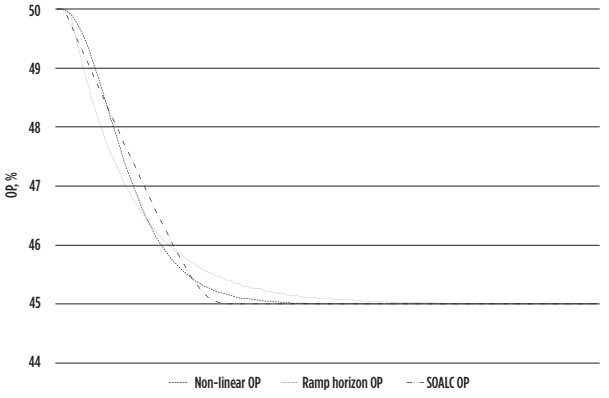

FIG. 3. OP response to a step disturbance of 5 m³/hr.

SIMULATION RESULTS

To test the ramp horizon and SOALC, a level was simulated and subjected to step disturbances of different sizes. A standard non-linear or error-squared PID controller[2] was used as comparison and tuned to handle a maximum disturbance of 5 m³/hr.

To measure the success of the control, the variance of the OP derivative (VOD) was measured.[2,12,13,14]

If a control method can minimize total OP movement over time or prevent the OP from moving in one direction initially and then moving back later when the limits would not have been exceeded if no moves were made, this would be a big advantage in improving plant stability. There were no performance metrics in literature that highlighted this behavior. To test to what extent this occurs, the average of the absolute moves (AAM) of the OP of a controller, as shown in Eq. 11, was developed as an additional performance indicator:

$$AAM = [\Sigma_i^N abs(OP_i - OP_{i-1})] / N \quad (11)$$

Positive step disturbance of 5 m³/hr. When responding to a positive step of 5 m³/hr in the feed to the drum, FIG. 2 shows how the controllers all managed to keep the level below the high limit of 70%. FIG. 3 shows how all the controllers moved their OPs by the same total amount. This is as expected, because the volume balance must be restored to bring the rate-of-change of the different levels to zero.

TABLE 3 shows that the controllers performed similarly when considering the VOD and the same on the AAM. This is because all the controllers moved their OPs by exactly 5% over the time horizon considered.

Positive step disturbance of 6.25 m³/hr. If the disturbance size is increased by 25%, FIG. 4 shows how the non-linear controller was unable to keep its level below the high limit of 70%. This is because it was tuned to accommodate an assumed maximum disturbance of 5 m³/hr. Both the ramp horizon controller and the SOALC managed to keep the level within the limit. TABLE 4 indicates how the VOD showed slightly poorer performance from the SOALC and ramp horizon controllers, while the AAM is the same as before. FIG. 5 also shows how the ramp horizon controller and SOALC initially moved their OP faster to prevent the level from exceeding the limit. The VOD shows slightly poorer performance from the SOALC, while the AAM is the same as before.[15,16,17]

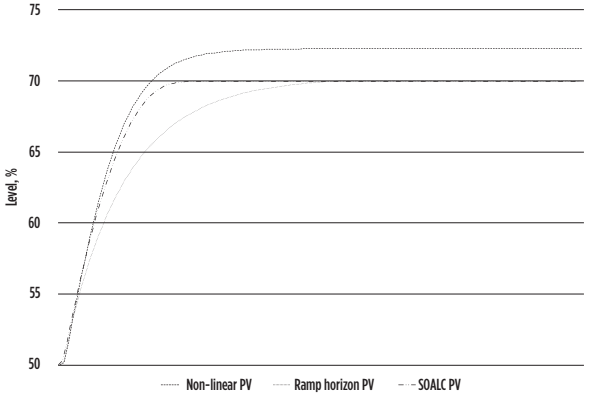

FIG. 4. Level response to a step disturbance of 6.25 m³/hr.

Positive step disturbance of 3.75 m³/hr. If the magnitude of the disturbance is decreased by 25%, FIG. 6 shows how the non-linear controller did not use the full range allowed for level buffering. FIG. 7 shows how the ramp horizon controller initially did not move its OP because a limit violation was not predicted within the defined time horizon. Later, the controller then had to move the OP faster to prevent a limit violation, which increased its VOD (TABLE 5).

Plant test. A ramp horizon control was deployed on a feed drum to a reactor in an industrial plant. The feed to the drum varies and the existing PI gap controller was tuned to keep the OP as steady as possible while maintaining the level within limits of 30%–70%. If the low level is exceeded, the reactor feed pumps will cavitate; if the high level is exceeded, a high-level protection controller will send reactor feed material to another process where the feed material would be converted to a lower value product.

The ramp horizon controller results were compared to the original PI gap controller and analyzed using the VOD and AAM, as well as visual inspection of the PV and OP trajectories.

Data of the feed to the drum were collected and used as disturbance data to a simulated level controlled by a ramp horizon controller. Tuning was then refined to minimize the standard deviation of the OP.

The controller was commissioned, and data was collected for a period of 1 mos. This was compared to data collected during the same month of the previous year to eliminate seasonal influences, as far as possible. The data sets show that the ramp horizon controller managed to maintain the level between 30% and 70%, while the PI gap controller allowed the level to vary between 36.7% and 84.7%.

Data where the controllers were switched to MAN were excluded. This accounted for 11.9% of the data for the ramp horizon controller and 19.7% for the PI gap controller.

TABLE 3. Performance metrics for a step disturbance of 5 m³/hr

	Non-linear	Ramp horizon	SOALC
VOD	0.073	0.074	0.067
AAM	0.041	0.041	0.041

TABLE 4. Performance metrics for a step disturbance of 6.25 m³/hr

	Non-linear	Ramp horizon	SOALC
VOD	0.098	0.115	0.097
AAM	0.051	0.051	0.051

TABLE 5. Performance metrics for a step disturbance of 3.75 m³/hr

	Non-linear	Ramp horizon	SOALC
VOD	0.05	0.056	0.041
AAM	0.031	0.031	0.031

TABLE 6. Performance metrics comparing ramp horizon controller and PI gap controller

	Ramp horizon	PI gap
VOD	0.09	0.11
AAM	0.013	0.018

FIG. 8 shows one day's data while the ramp horizon controller was used. When comparing this with one day's data from the PI gap controller in FIG. 9, the ramp horizon controller moved the OP less than the PI gap controller, but it had to move it faster when it was required to remain between limits.

All metrics shown in TABLE 6 indicate that the ramp horizon controller outperformed the PI gap controller. The simulation results show how the non-linear PI controller will perform similarly to the ramp horizon and SOALC when a disturbance of the exact size that was used to tune the non-linear PI controller occurs.

When a disturbance occurs that is larger than was assumed to tune the controllers, the non-linear PI controller will allow the level to move outside the limits. As the ramp horizon and SOALC calculate a response that is not based on an assumed maximum disturbance, they will maintain the level within limits.

When a smaller disturbance occurs, the ramp horizon may make no changes initially and the SOALC will make small changes throughout. They both allow the level to reach the limit. In this case, the non-linear PI controller will prevent the level from going to the limit, using only part of the available buffer capacity offered by the drum. Consequently, the non-linear PI controller will move the OP more aggressively than the ramp horizon and SOALC controllers.

The plant test shows how the ramp horizon controller outperformed the non-linear PI controller by:

- Keeping the level within limits
- Implementing smaller and fewer moves.

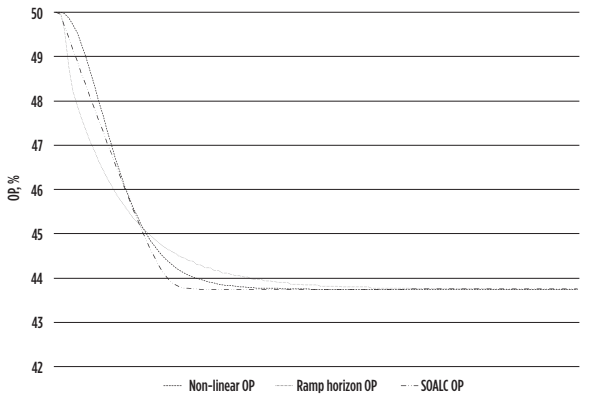

FIG. 5. OP response to a step disturbance of 6.25 m³/hr.

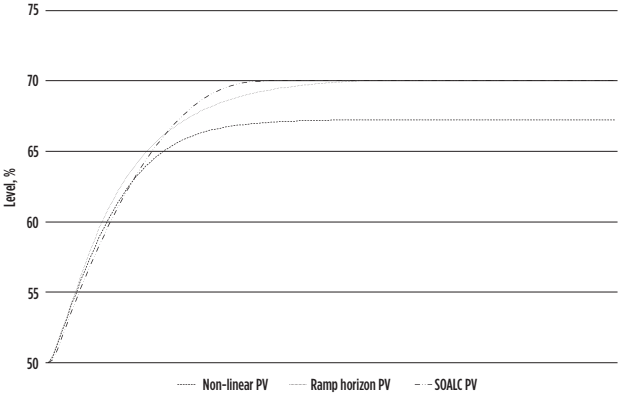

FIG. 6. Level response to a step disturbance of 3.75 m³/hr.

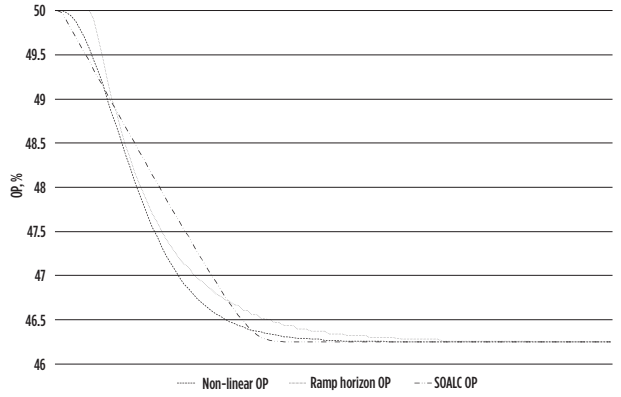

FIG. 7. OP response to a step disturbance of 3.75 m^3/hr.

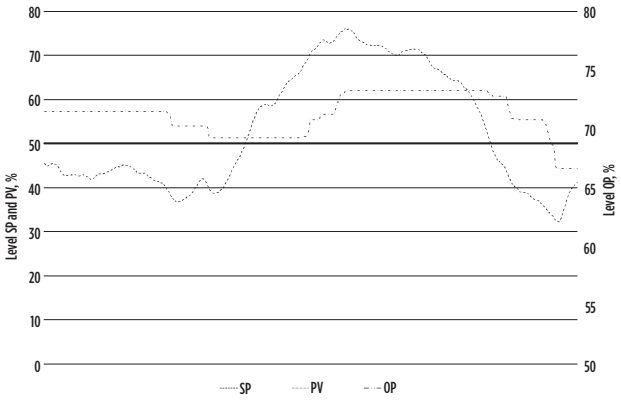

FIG. 8. Drum level controlled with ramp horizon controller.

Takeaway. The proposed SOALC and ramp horizon controllers will maintain levels within limits when disturbances occur that are larger than what was assumed during tuning and commissioning. Both controllers will outperform a traditional PI controller in minimizing OP movement. Additional control hardware and software will not be required to implement them if the plant is controlled by a modern DCS.

Because the level and rate-of-change of the level are calculated at every cycle, and they run at a high execution rate, noise and tuning errors can be accommodated.

As these controllers do not attempt to return the level to SP, consecutive disturbances in the same direction will allow the level to move outside the set limits. When this happens, the ramp horizon controller will return the level to within limits while the SOALC will have to revert to PID control until the level is within limits again.

When attempting averaging level control on a plant with disturbances of varying sizes, ramp horizon control or SOALC can be used. This will ensure that levels remain within desired limits while moving the OP less than traditional PID-based methods, while minimizing OP movement.

However, some challenges exist in the implementation of RH and SOALC. Since both the ramp horizon and SOALC will allow the level to reach limits while making the smallest OP moves to ensure the limits are not exceeded, the risk remains that disturbances that push the level in the same direction as before may occur once the level has reached the limit. If this occurs, the

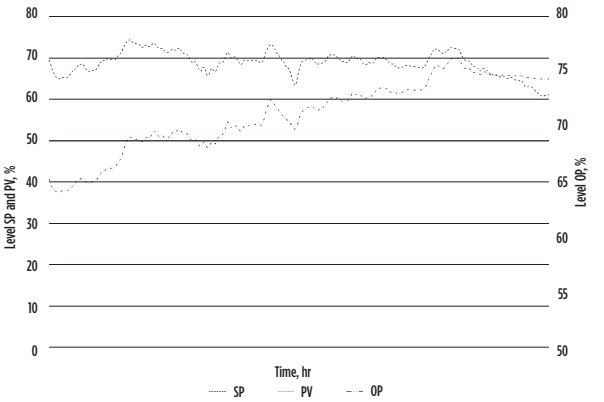

FIG. 9. Drum level controlled with PI gap controller.

SOALC will not return the level to the limit that was exceeded using the same algorithm. Eqs. 9 or 10 will move the OP in the wrong direction, aiding the disturbance that pushed the level outside its limits. When this happens, the error will grow and the SOALC will accelerate the OP movement in the wrong direction. While this might occur infrequently, reverting to PID control when the PV is outside limits is recommended. HP

LITERATURE CITED

[1] Lindholm, A., "Buffer management strategies for improving plant availability," MSc Thesis, Department of Automatic Control, Lund University, 2009.
[2] King, M., *Process control: A practical approach,* Wiley, December 2010.
[3] McDonald, K. A., T. J. McAvoy and A. Tits, "Optimal averaging level control," *AIChe Journal,* Vol. 32, No. 1, 1986.
[4] Kotze, G. and F. Pieterse, "ROC level control," Honeywell internal document, 2011.
[5] AspenTech DMCplus Advanced Concepts Course, MA305.06.10, 2007.
[6] Reyes-L´ua, A., C. F. Backi and S. Skogestad, "Improved PI control for a surge tank satisfying level constraints," 3rd IFAC Conference on Advances in Proportional-integral-derivative control, Ghent, Belgium, May 9–11, 2018.
[7] Taylor, A. J. and T. G. la Grange, "Optimize surge vessel control," *Hydrocarbon Processing,* May 2002.
[8] "Experion control builder components theory," Vol. 1, Honeywell 2005.
[9] Shinskey, F.G., "Special rules for tuning level controllers," 2005, online: www.controlglobal.com/articles
[10] Friedman, Y. Z., "Tuning of averaging level controllers," Petrocontrol, 1994, online: http://www.petrocontrol.com/papers/1994
[11] Ogawa, S., B. Allison, G. Dumont and M. Davies, "A new approach to optimal averaging level control with state constraints," 41st IEEE Conference on Decision and Control, Las Vegas, Nevada, U.S., December 2002.
[12] Rosander, P., A. J. Isaksson, J. Löfberg and K. Forsman, "Robust averaging level control," AIChe Annual Meeting, Minneapolis, Minnesota, U.S., 2011.
[13] Sidhu, M., "Multivariable averaging level control," BSc Thesis, University of British Columbia, Canada, 2001.
[14] Ye, N., T. J. McAvoy, K. A. Kosanovich and M. J. Piovosv, "Optimal averaging level control for the Tennessee Eastman problem," *The Canadian Journal of Chemical Engineering,* Vol. 73, 1995.

Complete Litature Cited available online at www.HydrocarbonProcessing.com.

GUSTAF GOUS works as Senior Manager Electrical and Instrumentation at Sasol's Secunda Chemical Operations. He graduated from the University of Pretoria in South Africa with a BS degree in chemical engineering in 1987, followed by a BA degree in English (honors) and an MS degree.

PHILIP DE VAAL is an Emeritus professor of chemical engineering at the University of Pretoria in South Africa. He was Head of the Department of Chemical Engineering from 2004–2020. He earned a BS degree in chemical engineering, followed by an MS degree and PhD.

GERT VAN COLLER graduated from the Department of Chemical Engineering at the University of Pretoria with a BS degree in chemical engineering. He completed his engineer in training course at Sasol in 2018 and now works as a process control engineer at the Solvent Units at Sasol's Secunda Chemical Operations.

A. MURUGAN, Fitiri, Houston, Texas; and
V. PATTABATHULA, SVP Chemical Plant Services, Brisbane, Australia

Quantum leap in chemical plant safety and reliability through mobile technology

The human factor has played a significant role in chemical plant accidents and production loss incidents over the past 60 yr. Process equipment design, fabrication, metallurgy and control systems have improved significantly within this time frame. The human factor might be the most critical element in safe chemical plant operations.

The authors have identified certain critical plant activities where mobile technologies can advance human-machine interaction, thus improving plant safety and productivity. Activities dependent on human factors (such as operator rounds, routine and non-routine tasks, and plant emergencies) can be handled effectively with mobile technology.

A proprietary plant management software solution[a] helps operators safely run plant operations through data and documents, rather than from memory and experience. Equipping plant personnel with the right procedures and documents reduces stress and errors and supports better decision making during emergencies. This system also enforces discipline and streamlines the plant's operational functions, such as compelling an operator to be physically present near the equipment at the time of operator rounds. Making technical documents intelligent and accessing them anywhere on demand through mobile tablets raises an entry-level operator's knowledge level to mimic that of a highly experienced operator. Implementation of the system has empowered plant personnel to perform efficiently, thus reducing plant accidents and production loss incidents.

This comprehensive plant management software solution interacts with plant machinery, plant resources and plant personnel to improve productivity and safety. It automates the shift activity log process and enhances communication and transparency of plant operational activities. It ensures a fail-proof, timely completion of critical work orders and shift activities.

Operators spend most of the time with plant equipment (i.e., assets). They are the first to sense if something is wrong or abnormal about the equipment's operation or condition. If operators are empowered, they can correct many problems at the incipient stages, or work closely with the maintenance team to tackle significant problems, which leads to operator-driven reliability.

The three main areas in plant operation where the human factor plays a critical role are:

1. **Routine operations:** Daily operator rounds and routine tasks
2. **Effective communication:** Between the operators, supervisors and management, using shift descriptive logs
3. **Non-routine operations:** Startups and shutdowns.

Routine operations. As a part of routine operations, the supervisor manages and coordinates a shift, while panel operators control the plant by distributed control systems (DCSs) and human-machine interfaces, and the field operators make inspection rounds to ensure that equipment is functioning properly. The current system does not fully use the field operators when plants are running normally. When the plants have upsets or shutdowns, they receive instructions from the control room and the supervisor to open and/or close manual valves and restart equipment. During normal operation, the proprietary system can mold the field operator into a precious resource.

Field operator rounds. Field operator rounds are critical tasks carried out by plant personnel to ensure that every piece of equipment in the plant area is functioning properly. The system provides an intuitive interface for the operator to smoothly collect data, and assists to make meaning out of the data collection process. The system automatically feeds the log sheets that are required to be completed at a particular time for a particular area. Within the proprietary system, order and tag names are identical to ones used in paper log sheets (FIG. 1). This method enables familiarity with the system, thus reducing the learning curve.

An option to view historical data is helpful when a reading is not within operating parameters and past data is required for verification. When physically near equipment, electronic tags placed on equipment provide relevant log sheets. If, for instance, a reading cannot be taken due to a faulty gauge, then a standard message can be chosen that raises a report of all the faulty gauges in the plant for the supervisor to follow up on. The system is menu-driven and effortless to follow, and requires the operator's physical presence near the equipment to open the log sheets to input the equipment's readings. The readings are all stamped as to date, time and name, which helps to preserve the authentication, authorization and accountability aspects of plant safety.

Continuous monitoring of key performance indexes. Traditionally, equipment and catalyst performances are evaluated quarterly, biannually or annually. However, due to new digital software, performance calculations can now be completed as frequently as a reading set is taken. Compressor performance, exchanger heat duties and heat transfer coefficients can be tracked as frequently as operators take readings. At any time, operators are able to pull up trends on polytrophic efficiencies of rotating equipment, catalyst approaches to equilibrium and poisoning rates, and exchanger heat transfer coefficients. This provides personnel the ability to make meaningful decisions about equipment performance based on calculated parameters rather than on implied process parameters. With live field readings, precursors to equipment failures and safety incidents are able to be determined ahead of time.

Along with DCS readings, field equipment readings are integrated to monitor and generate an automated reporting system for the following:

1. Key performance indicators (KPIs) of plant operability
2. Real-time operation reports geared to provide operating personnel key information on plant performance
3. Energy monitoring on a real-time basis and shift basis
4. Daily and/or monthly production reports on plants or sites
5. Equipment/asset performance on a real-time basis
6. Catalyst performance.

These reports help identify any deteriorating equipment conditions, even those that do not generally come back to the DCS. Real-time data, along with historical data, is readily made available, which is critical for troubleshooting.

Follow-ups on routine work. The system follows up on pending work orders and tracks them, along with additional items, such as:

- Ensuring that operators prepare chemicals to maintain levels
- Tracking standby equipment for changeovers
- Providing forms to fill field vibration and skin temperature readings
- Aiding lube oil top-ups and scheduled oil analyses
- Sending reminders to operators regarding routine tasks, along with those tasks that are still pending to be completed
- Ensuring that plant reliability elements are effectively managed

Plant management software helps operators run their plant safely with reliable data and documents, rather than from memory and/or experience.

List: AN-NA Prill Tower DCS (AN-NA Prill Tower DCS)
Name/Date: 12/8/20 - 12/8/2020 Printed: 12/8/2020

Asset	Vibration Monitor				Motor	Ammonia				Air	NH3/Air Mixer		Ammonia Converter	Weak Acid Sep	Tail Gas Combuster				Condensate	Bleach Air Flow
Group																				
Data Point	K-700 Vibration Monitor 311X	K-700 Vibration Monitor 310X	K-700 Vibration Monitor 301X	K-700 Vibration Monitor 300X	K-700 MOTOR AMPS	Vaporizer Pressure	NH3 Press to NH3/Air Mixer	NH3 Flow to NH3/Air Mixer	NH3 Temp to NH3/Air Mixer	Air Temp to NH3/Air Mixer	NH3/Air Mixer Temp	%NH3 to Gauze	Gauze Temp Recorder	Weak Acid Sep Temp	Tail Gas Preheater Temp	Combustor Inlet Temp	Combustor Outlet Temp	% O2 in Tail Gas to Combuster	Condensate Flow to Absorber	Bleach Air Flow to Absorber
Instr	F3-T Graphic 311x	F3-T Graphic 310x	F3-T Graphic 301x	F3-T Graphic 300x	AY-700	PICY-3170	PITY-3158	FIY-3113	TI-3291.5 -PV	3291-7 -PV	TI-3291-3 -PV	RIY-3113 PV	TI-3183	TI-3281	TI-3291-8 -PV	TI-3286-A	TI-3286-B	ARY-3202	FIC-3212	FIY-3111
UOM	MILS	MILS	MILS	MILS	A	PSIG	PSIG	SCFM	oF	oF	oF	%Ratio	oF	oF	oF	oF	oF	%	GPM	SCFM
Hi Trip Hi Alarm Normal Lo Alarm Lo Trip	2.50	3.00	2.50	3.00												450.00	1050.00	1.80 1.0		
0400	.60	2.12	1.02	1.73	193	171	125	732	309	494	465	11.9	1686	126	125	866	963	.97	3.60	273
0800																				

FIG. 1. The proprietary plant management software solution[a] provides an identical look to paper log sheets, enabling familiarity with operations and reducing the learning curve.

and tracked, thus significantly reducing plant shutdowns due to reliability issues.

Checklists. Apart from regular operator readings, checklists that are used for data collection should be given equal importance. Prestartup checklists, safety checklists, preventive and corrective checklists, field inspection checklists, personal protective equipment checklists, hazard analysis checklists, fugitive emission checklists and flare monitoring checklists are some of the critical checklists that are automated, and the data collected can be archived and tracked to check for issues. This also helps in the effective implementation of process safety management (PSM) elements. Making checklists digital saves unnecessary trips to the control room or file cabinets.

Lockout/tagout (LOTO). Improper LOTO procedures are one of the major causes of accidents and fatalities. During a shutdown, the supervisor and operators manage several activities—and errors with manual work permits and logout procedures can prove fatal. The proprietary system logically groups isolation points by task or trade and creates automated packages. These prebuilt packages can then be retrieved when required. Documents can be linked to equipment. The LOTO process associated with equipment isolation or confined space entry is greatly enhanced by automatically instructing the necessary lockout points. The system prints all the necessary tags for hot work and cold work permits and shows where to display them. The supervisor can perform a LOTO field verification with the click of a button.

Effective communication. Effective communication is very critical in chemical plant operations, and this is why plants invest in expensive radio systems to provide interference-free, real-time communication. While voice communication is essential, many traditional communications occur through a physical operator logbook and whiteboards. This leads to inefficiencies in proper tracking and follow-ups. Therefore, to optimize operations, it is necessary to have a digital operator log that tracks all of the communication.

Communication of operation. Effective communication and timely follow-up among plant personnel are vital to plant

safety and reliability. The proprietary system enables real-time communication from field operators to the panel operator, supervisor and management through mobile devices. Work permits in progress, LOTOs performed and equipment isolation are all adequately communicated across shifts. Through a context-aware system, when the operator physically approaches the problem area, personnel are automatically notified. Many accidents and production loss incidents occur not because the operational personnel did not know there was a problem in the plant, but because they failed to act promptly. A problem faced 6 mos prior, which was not remedied due to any reason, can become a significant incident in the future. The proprietary system tracks all reported problems by the field operators to the supervisor, along with instructions from the supervisor, and keeps active reminders in place until the problem is fixed. It sends reminders and follow-ups on tasks such as pending work orders and unclosed instructions from the supervisor. When a critical task is not carried out, the system sends texts and alerts to both the operator and supervisor (FIG. 2).

Shift supervisor log. The proprietary software helps the shift supervisor prepare a comprehensive shift report (i.e., a descriptive log) by automatically populating shift activities. The system tracks the activities performed during the shift, such as work orders, chemical preparations, scheduled activities, safety toolbox and training, equipment changeovers, observations, notes and completed tasks. The system helps in effective coordination between maintenance and operations. Tracking these shift activities at the field level, along with their completion, also improves plant performance. Scheduling and tracking the makeup of chemicals for shift consumption, and tracking timely completion of equipment changeovers, are essential to plant reliability.

The system tracks shift instructions given to operators, along with notes written by operators and information regarding the status of shift activities. Alerts regarding incomplete activities are provided during the shift so that appropriate remedial actions can be taken. Such alerts are escalated to plant management if these remedial actions are not completed within the allocated time and priority.

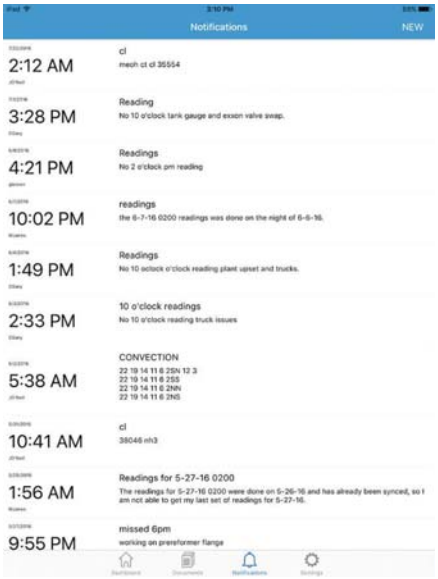

FIG. 2. Notifications on plant activities provide an effective means of communication, increasing plant reliability and safety.

Web-enabled shift supervisor descriptive logs promote increased communication about shift activity and transparency. Temporary fixes performed to an issue or a malfunction that requires follow-up and/or similar scenarios are appropriately communicated, documented and tracked within the system.

Non-routine operations. From 1970–1989, 60%–75% of major accidents in continuous processes occurred during non-routine modes (principally startup and online maintenance modes). This trend has continued unabated for most of the process industry to the present day. Therefore, a greater emphasis must be given to non-routine operations in the plant. Although routine operations are of high priority for the operator, personnel are responsible for taking care of all activities that pertain to their area. The following are several critical, non-routine jobs that an operator handles:

1. Performing non-routine inspections, such as reformer tube metal temperature monitoring, electrical systems and infrared thermography, surface vibration monitoring, relief valve leak testing, fugitive emissions testing and checks on rupture disk integrity
2. Attending hazard and operability (HAZOP) study meetings
3. Attending meetings regarding plant modifications and standard operating procedure (SOP) change reviews
4. Conducting plant tours for visitors and contractors
5. Reviewing plant piping and instrumentation diagrams.

Effectively following up on non-routine jobs improves plant reliability. The proprietary software helps operators streamline their daily activities, along with non-routine and case-based tasks. This software addresses the following critical parameters that enhance the safety and efficiency of non-routine operations:

- **Procedure accuracy and clarity (the most cited root cause of accidents):**
  - A procedure typically needs to be 95% accurate to help reduce human error; humans tend to compensate for the remaining 5% of errors in a written procedure.
  - A procedure must convey the information (there are approximately 25 rules for structuring procedures to accomplish this) and be convenient to use.
  - Checklist features should be used and enforced, either in the procedure or in a supplemental document. All the SOPs and checklists are made available in a digital format through the proprietary software.
- **Training, knowledge and skills:**
  - Initial training must be useful. Demonstration-based training should be conducted on each proactive and reactive (e.g., alarm response) task. Making the training materials accessible (such as taking quizzes through integration with learning management systems) greatly enhances the learning experience during operator training.
  - Ongoing human action validation is required and usually must be repeated (in either actual performance or drills/practice) at least once per year. For human factors, the action must also be demonstrated to be quick enough to be effective. This is completed by offering recertifications and by providing safety videos and other multimedia materials that are designed to refresh the operator's memory.
  - The human performance must be documented and retained to demonstrate that the error rates chosen are valid. Since every action is documented electronically, the operator can be evaluated quickly and then efficiently trained on how to prevent the errors in the future.
- **Communication:** Miscommunication—included in instructions, a set of instructions or the status of a process—is one of the most common causes of human error in the workplace. Proper documentation through electronic operator logbooks helps maintain better communication across all parties of management and shifts.
- **Human system interface:** Factors to control include layout of equipment, displays, controls and their integration to displays, alarm nature, control of alarm overload, labeling, color coding, and fool-proofing measures, among others. Operators are provided with digital documents that are critical for performing their job. These digital documents are available at the touch of a finger, saving a trip to the control room or administration building.

Takeaway. We live in a digital era where, every day, decision-making processes are influenced by data and information systems, which has helped to increase efficiency by avoiding mistakes and unwanted delays. The process of offering a similar workplace approach and empowering people to have the right data and documents relieves personnel of handling stressful situations not with just memory and experience, but also with tools and technology. This, in turn, improves the quality of the people and significantly reduces preventable failures and downtime attributed to human error, resulting in millions of dollars in potential savings. HP

NOTE

[a] Fitiri's Plant*MS* software

ARUNKUMAR MURUGAN is the Director of Software Engineering at Fitiri. He has an extensive background in software engineering and in developing solutions to automate and augment personnel at their work environment. After joining Fitiri, he has been involved in interacting with ammonia plant operators, supervisors and managers, as well as in the development of Plant*MS*, a comprehensive plant operations management solution. Mr. Murugan earned a Bch degree in information technology from Anna University in India.

VENKAT PATTABATHULA is the Principal Consultant at SVP Chemical Plant Services. Prior to this position, he was the global ammonia technology manager for Incitec Pivot Ltd., where he supported manufacturing facilities in Australia and North America. His specialties include process design, project development, commissioning, plant operation, process safety management and manufacturing excellence programs. Mr. Pattabathula has been a member of AIChE since 1989, and has been an elected member of the Ammonia Safety Committee of AIChE since 2005. He is a chartered professional engineer of Engineers Australia and a registered professional engineer of Queensland. Mr. Pattabathula earned an MTech degree in chemical engineering from the Indian Institute of Technology.

LEE NICHOLS, Editor-in-Chief/
Associate Publisher

IRPC Process Technology: The latest advancements in process technologies

The impact of COVID-19 has not changed the need for information on innovative, developing technologies that can revolutionize business, improve efficiencies and streamline processes.

Each year, *Hydrocarbon Processing* hosts technical events to provide the latest technologies and services that are optimizing the refining and petrochemical industries. The International Refining and Petrochemical Conference (IRPC) brings together leaders in the downstream processing industries to discuss best practices and advancements in processing technologies.

IRPC Process Technology will showcase world-leading technologies in conventional and energy transition processes within the refining and petrochemical industries. The innovative virtual conference will be held June 2–3 and will provide a platform for knowledge-sharing, networking and making business connections with downstream leaders.

The two-day event will be highlighted by timely keynote presentations. These include:

- **Transforming refineries to minimize carbon footprint and maximize handprint:** Petri Lehmus, *Vice President,* Research and Development, Neste
- **The future role of the technology licensor:** Leon de Bruyn, *Chief Executive Officer,* Lummus Technology
- **Market drivers impacting demand for biofuels and alternative refinery feedstocks:** Mark Schmalfeld, *Global Marketing Manager,* BASF
- **What does the energy transition mean for the oil and gas industry?** Cees de Regt, *Senior Principal Consultant,* DNV.

The keynote presentations will be followed by a three-track agenda that will focus on dozens of technologies advancing the processing industries into a sustainable world (**TABLE 1**).

These sessions will feature processing technologies from companies such as Axens, BASF, Braskem, Clariant, Dow Chemical, DuPont Clean Technologies, Eni, Haldor Topsoe, Honeywell UOP, Invista Performance Technologies, Johnson Matthey, KBR, Linde, Lummus Technology, MyRechemical, Reliance Industries Ltd., Shell, Sinopec, Sulzer, Technip Energies, W. R. Grace and Worley.

IRPC Process Technology is a free online event; however, you must register to attend. More information can be found by visiting www.HydrocarbonProcessing.com/Events. Individuals can register for the event, view the latest agenda, learn more about sponsorship opportunities and the benefits of IPRC Process Technology's digital platform. The full agenda will also be available in this month's digital edition, which is open access for all readers of the magazine: https://www.nxtbook.com/nxtbooks/gulfpub/hp_202105.

Additional benefits of attending *Hydrocarbon Processing's* IRPC Process Technology digital event include:

- No travel—All presentations can be viewed from anywhere with an internet connection
- Engaged participation—An enhanced chat function enables viewers to speak and ask questions of various presenters
- Enhanced archives—Registrants can access event presentations, whitepapers, marketing collateral, etc., for one year
- Networking—The digital platform contains an enhanced virtual networking system to enable attendees to "meet" and chat with speakers and other attendees.

IRPC Process Technology will be followed by IRPC Operations, to be held virtually September 21–22. HP

TABLE 1. Technologies featured at IRPC Process Technology

Refining	Petrochemicals
Conventional processing technologies	
Distillation	Ethylene
Fluid catalytic cracking/hydrocracking	Propylene
Alkylation	Refinery-petrochemicals integration
Coking	
Sulfur/treating	
Energy transition technologies	
The green refiner	Emissions reduction
Alternative fuels, biofuels and clean fuels	Plastics recycling
Sustainability	Sustainability
Emissions reduction	Circular economy

MIKE RHODES, MANAGING EDITOR
Mike.Rhodes@HydrocarbonProcessing.com

Extended digital transmission portfolio with edge-enabled transformers and switchgear

Siemens Energy has extended its switchgear and transformer portfolio with Edgeformer™ and Edgegear™, presenting the first high-voltage devices with edge computing. The new generation of digitally enabled transmission products and systems opens new possibilities for grid operators to benefit from data-driven applications by deploying them within the local substation network.

The shift to an increasingly decarbonized energy landscape poses tremendous challenges to grid operators that require a new way of managing the energy system. The digitalization of power transmission assets in the substation, the heart of any electrical power distribution system, plays an important role to manage the increased feed-ins of renewable energy and the exponential increase of complexity. While most digital solutions for substation assets rely solely on equipment with cloud connectivity, edge-enabled transmission products like Edgegear and Edgeformer offer new possibilities to connect equipment directly within the substation without having to forego the benefits of cloud-based solutions like app-based data analytics. Edge computing technology enables faster computing capabilities for quicker decision-making as well as data storage and processing onsite.

With edge computing, the data is kept offline in the substation without compromising a seamless, secure and easy integration into the existing customer IT-landscape. The result is a highly cybersecure system. Siemens Energy's edge-enabled transformers and switchgear will come with app-based data analytics and asset management.

With Edgeformer and Edgegear, every transmission system operator will have access to value-added applications, enabling them to respond faster to changes in the system and increase asset transparency, productivity and reliability. Edgegear, for example, provides operators with real-time partial discharge analyses as well as gas and oil leakage prediction supported by artificial intelligence and machine learning, allowing grid operators to manage their networks more effectively.

Ultra-compact flowmeter for utilities and industrial automation

KROHNE has introduced the AF-E 400 ultra-compact electromagnetic flowmeter (FIG. 1) for utilities and industrial automation applications. It is specially designed to fit in applications with little installation space available (e.g., in cooling lines of welding equipment, bending machines and robots, or on chemical dosing skids). AF-E 400 matches the requirements of application areas in heating and cooling/temperature control, machine building of washing or dosing equipment, HVAC, and utilities and industrial automation applications in all process industries.

KROHNE has examined issues with products in this segment and developed the cost-effective, ultra-compact flowmeter to be best-in-class in terms of temperature range, accuracy, pressure drop and flow range: AF-E 400 features a stainless-steel housing and is suitable for continuous use at > 90°C (> 194°F) liquid temperature, allowing for operation in very demanding cooling and hot water applications. The round bore reduction of the sensor makes the flowmeter more resilient in terms of increased pressure, ensuring high accuracy over a wide pressure and temperature range, and a high turndown ratio without risk of cavitation. The integrated temperature measurement eliminates the need for an additional sensor, minimizing the intrusion points in the pipe and providing more data from the process.

AF-E 400 also features extensive self-diagnostics: the meter continuously monitors several critical aspects, including low supply voltage, incorrect parametrization, flow range exceedance, or short circuit on any of its outputs. Warning messages—according to NAMUR NE107—alert the user via the rotatable full-color display or the communication outputs.

FIG. 1. The KROHNE AF-E 400 ultra-compact electromagnetic flowmeter.

Due to the special design of its magnetic circuit, field strength and electronics, AF-E 400 is immune to crosstalk caused by magnetic field overlap of adjacent devices, and can be installed in series or in parallel up to a distance of 2 mm/0.08 in. from device to device without interference.

Nominal sensor sizes reach from DN6...25/ ¼...1 in. for flowrates up to 150 l/min/40 gpm as standard, and up to 500 l/min/132 gpm on request. Output options include 4...20 mA, pulse, frequency, switch, IO–link or Modbus to provide operators with multiple sensor and application data for smarter factory automation. AF-E 400 is sold from stock and shipped within 48 hr.

Maintain critical temperature in multi-fuel boilers

Ensuring that steam turbines run at maximum efficiency is directly dependent on the steam's temperature entering the turbine. Higher steam temperatures mean higher efficiency and lower emissions. With a highly controlled temperature, the turbine can produce more power with the same amount of fuel.

For ultra-super critical (USC) multi-fuel boiler technology, accurate temperature measurement from 550°C–700°C

FIG. 2. JOFRA RTC Series reference temperature calibrators from AMETEK STC.

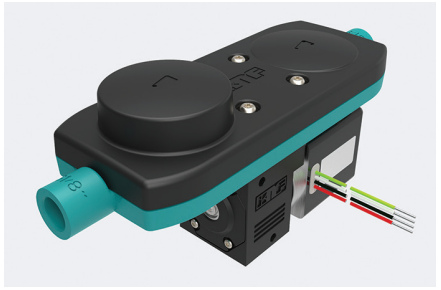

FIG. 3. KNF expands its series of smooth flow liquid pumps with its FP 70.

(1,022°F–1,292°F) is essential. Any deviation in temperature can result in increased maintenance, higher risk of a shutdown and a reduced lifetime.

Turbines use temperature sensors to monitor the inlet steam to avoid these temperature deviations. However, these sensors may drift over time, so regular calibration is required. Because the temperature and demand for accuracy are exceptionally high, finding the right piece of equipment to calibrate these sensors is challenging.

AMETEK STC has the solution with its JOFRA RTC Series Reference Temperature Calibrators (FIG. 2). The RTC temperature calibrator series includes seven models covering a total range from –100°C–700°C (–148°F–1,292°F). The RTC-700 model features a temperature range from 33°C–700°C (91°F–1,272°F), allowing it to calibrate steam turbine sensors. In addition to its highly accurate internal sensors, the RTC temperature calibrator can be combined with the patented DLC system to provide perfect temperature uniformity inside the insert. It also features an advanced simplicity interface, so learning how to use the calibrator takes just minutes.

With an accuracy of ± 0.29°C, stability to ± 0.02°C, and perfect temperature homogeneity in the insert, the RTC-700 temperature calibrator with the DLC sensor is the ideal solution to ensure these critical turbine temperature sensors are working as intended.

Diaphragm liquid pump

With the introduction of FP 70, KNF further expands its series of smooth flow liquid pumps (FIG. 3). This product line combines the low pulsation of a gear or centrifugal pump with the strengths and advantages of diaphragm pumps.

The KNF FP 70 delivers up to 850 ml/min while producing up to 29.4 psig (2 bar) pressure under continuous operation. Thanks to the patented four-point valves, the KNF FP 70 is reliably self-priming, even at very low motor speeds. It also can safely run dry, handles liquid transfer gently and cleanly, and is available with chemically resistant flow path materials. The integration of the pulsation dampening technology eliminates the need for additional pulsation dampening elements and tubing when using the KNF FP 70, thus reducing space requirements vs. a pump-plus-damper approach.

The versatile FP 70 is available with a selection of motors to match the functionality and lifetime requirements of the application: from high-end BLDC to lower-end DC motors. Depending on the operating parameters, the high-end BLDC motor achieves a lifetime of more than 20,000 hr. Furthermore, the parameters of these motors can be customized at KNF to dial in the desired control behavior, performance characteristics and pump accuracy. Additional options include a selection of hydraulic connections and a variety of flow path materials, including an NSF food-grade version. Combined with all these options is KNF's ability to further optimize pumps to customer needs at any lot size.

The FP 70 is well suited for a wide range of applications, including medical technology, inkjet, 3D printing and analytical instruments. It joins a growing line of KNF smooth flow liquid diaphragm pumps that now boasts a flowrate range spanning from 120 ml/min–12.4 l/min.

Membrane for carbon capture

Compact Membrane Systems (CMS), a pioneer in separations technology, has developed a new membrane for capturing carbon dioxide (CO_2) out of flue gas. This is the third addition to CMS's Optiperm™ product portfolio (after separating olefins from paraffins and upgrading biogas) and is aimed at reducing greenhouse gas emissions.

Early results show promise, with the high-flow membrane consistent with a $20/t cost of carbon capture. These results position Optiperm *carbon* as more cost-effective than many alternative CO_2 capture methods and in an economically attractive range for current projects and incentives. Optiperm *carbon* will scale up on CMS' existing Optiperm technology and manufacturing platform.

With the sustainable energy transition in motion, it is vital to reduce greenhouse gas emissions from existing processes in the short term to continue to produce reliable and affordable power. A majority of the world still relies on fossil fuel technology for power and coal-fired power plants account for 30% of global CO_2 emissions. Carbon capture technology allows users to filter and sequester the CO_2 at the source and reduce emissions by up to 90%. Fouling resistant membranes hold promise for carbon capture because they can be scaled to the size of the application and require lower energy usage and operational cost than existing carbon capture technologies.

Optiperm *carbon* is a fluoropolymer facilitated transport membrane with anti-fouling properties. The initial lab results show a permeability of 4000 GPU–6000 GPU, a 3x improvement over the industry standard. The high GPU and resistance to fouling are expected to significantly decrease the cost of carbon capture. Work is continuing to scale up the membrane on the same spiral wound platform as existing Optiperm products. HP